NAT'L INST. OF STAND & TECH
A11106 395924
NBS
PUBLICATIONS

NBSIR 81-2235

1980 Annual Report: Technical Contributions to the Development of Incipient Fault Detection/ Location Instrumentation

W. E. Anderson and J. D. Ramboz

Electrosystems Division
U.S. Department of Commerce
National Bureau of Standards
Washington, DC 20234

January 1981

Issued March 1981

sored by:
e of Electric Energy Systems
artment of Energy

QC
100
.U56
81-2235
1981
c. 2

NATIONAL BUREAU
OF STANDARDS
LIBRARY
APR 15 1981
Not circ - Circ
QC100
.U56
110.81-2235
1981
C.2

NBSIR 81-2235

1980 ANNUAL REPORT: TECHNICAL CONTRIBUTIONS TO THE DEVELOPMENT OF INCIPIENT FAULT DETECTION/ LOCATION INSTRUMENTATION

W. E. Anderson and J. D. Ramboz

Electrosystems Division
U.S. Department of Commerce
National Bureau of Standards
Washington, DC 20234

January 1981

Issued March 1981

Sponsored by:
Office of Electric Energy Systems
Department of Energy

U.S. DEPARTMENT OF COMMERCE, Malcolm Baldrige, *Secretary*
NATIONAL BUREAU OF STANDARDS, Ernest Ambler, *Director*

TABLE OF CONTENTS

Summary i

Abstract iii

I. Introduction 1

II. Technical Progress 3

II.1 Measurement System 3

II.2 Experimental Results 7

II.3 Software Development 39

III. Conclusion 46

IV. References 47

Appendix A 49

Appendix B 59

Appendix C 68

Appendix D 76

Appendix E 84

Summary

The objective of this NBS program is to identify and, insofar as practical, remove technical barriers to the development of instrumentation for use in detecting and locating incipient faults in underground power transmission systems.

Underground transmission of electrical energy has economic and environmental advantages compared to overhead transmission. A major concern, however, is reliability. Failures are more costly to locate and repair.

The Department of Energy has a program to develop instrumentation for the detection and location of incipient faults (the condition within a cable n which insulation degradation is occurring at a significantly higher than normal rate which, if not corrected, will cause the cable to fail prematurely). If this program is successful, cables about to fail can be repaired during scheduled outages minimizing perturbation to the transmission system.

Three contracts were awarded by DoE to develop such instrumentation. Besides monitoring the technical progress under these contracts, NBS has provided technical support where needed. Technical barriers include lack of knowledge of (1) the physical, chemical, and electromagnetic behavior of cable insulation immediately preceding breakdown; (2) the manner in which characteristic information concerning this behavior is propagated through the power system; and (3) appropriate methods of coupling detection systems to operating transmission cables.

A measurement system has been developed at NBS to enable studies of the rf properties of cables, and of the spectral content of discharges at incipient fault sites, and to perform time and frequency domain reflectometry and other related measurements.

Preliminary measurements were aimed at determining the sensitivity of cable sounding techniques (frequency or time domain) in detecting impedance changes in the cable. Changes of the order of a few parts per million (ppm) were detectable in some cases. A sharp needle was inserted into the cable dielectric and voltage applied. After several breakdowns the resulting breakdown channels were not detectable. The high frequency signals necessary to interact with small damage sites were apparently not reaching the breakdown region. Substantia effort was applied to improving the coupling between the TDR (Time Domain Reflectometry) unit and the cable under test. While this improved matters, the intrinsic attenuation in the dielectric was shown to rule out sounding approaches in the cable selected for these measurements. Such techniques might still be useful in other types of cables and for fault location in general.

Future measurements will characterize the rf properties of underground transmission cables. Extensive software has been developed to permit these measurements in the time domain and analysis in the frequency domain.

Abstract

Technical barriers exist in the development of instrumentation to detect and locate incipient faults in underground transmission cables. Knowledge is required of the physical, chemical, and electromagnetic properties of cables which precede breakdown, of the manner in which characteristic rf signals propagate in cables, and of appropriate methods of coupling detection systems to operating transmission cables. A measurement program has been initiated that will provide data on the rf properties of cables and on the characteristics of some forms of incipient faults. Preliminary measurements demonstrate the limitations of frequency- and time-domain-reflectometry techniques in the detection of incipient faults. Software is presented which permits the Fourier transform of step-like waveforms.

I. Introduction

The objective of this NBS program is to identify and, insofar as practical, remove technical barriers to the development of instrumentation for use in detecting and locating incipient faults in underground power transmission systems.

In many situations underground power transmission cables have economic (and environmental) advantages over overhead transmission lines resulting in an increase in underground installations. Underground transmission does have a major disadvantage in the area of reliability. Faults can be extremely difficult to locate accurately and repair with the results that either long unscheduled outages or extensive redundant cables are necessary.

To alleviate this problem, the Department of Energy has a program area entitled "Research and Development of Fault Detection/Location Techniques and/or Equipment for Underground Power Transmission Cable Systems." The output of this program is expected to be instrumentation and techniques for the detection and location of incipient faults in different types of underground cables; viz. pipe-type (high or medium pressure oil or gas impregnated), extruded solid dielectric, compressed gas, and possibly cryogenic. An "incipient fault" is defined to be the condition within a cable system in which local insulation degradation is occurring at a significantly higher than normal rate which, if not corrected, will cause the cable system to fail prematurely. A reliable incipient fault detector/locator would allow the defective area to be repaired during a scheduled outage, minimizing the perturbation to the transmission system.

The Department of Energy in the summer of 1978 awarded contracts to Purdue University, SRI International, and Westinghouse Corporation to develop (or determine the feasibility of) instrumentation for the detection/location of incipient faults. The School of Electrical Engineering, Purdue University proposed to develop instrumentation that would correlate, using variable time delay, the noise signal received at both ends of the cable emanating from partial discharges at incipient fault sites. The Remote Measurements Laboratory of SRI International proposed instrumentation based on swept-frequency reflectometry. A two-frequency mixing (resulting from the nonlinear incipient fault region) approach was proposed by the Electromagnetics Sciences Laboratory of SRI International. The Chemical Sciences Division of the Westinghouse R&D Center proposed to do a feasibility study on the use of acoustic waveguides for sensing incipient faults. As their work evolved this also included acousto-optic techniques using fiber optics.

The NBS contribution to this program, besides monitoring the technical progress of the three contractors for DoE, was to provide technical support to the research, development, and testing of incipient fault detection/location instrumentation. In general, the NBS research program was directed towards providing knowledge of the physical, chemical, and electromagnetic behavior which immediately precede breakdown of cables, of the manner in which characteristic information concerning these events is propagated through the power system, and of appropriate methods of coupling detection systems to operating transmission cables.

II. Technical Progress

II.1 Measurement System

During this year a measurement system has been developed at NBS to enable studies of the rf properties of cables and of the spectral content of discharges at incipient fault sites, to perform time- and frequency-domain reflectometry and to conduct other related measurements. Time-domain-reflectometry (TDR) measurements were performed on cables with induced defects to determine the sensitivity of TDR techniques for incipient fault detection. Software was developed that will permit the determination of the velocity and attenuation of rf signals in cables as a function of frequency (or equivalently the transfer function) in the time domain.

Figure 1 shows a block diagram of the measurement system for generating signals, capturing signals, and providing signal analysis capabilities in both the time and frequency domains.[1] The heart of the system is the Tektronix[1] 4051 intelligent terminal with its peripherals. The intelligent terminal is connected to both the RS-232 and general purpose interface bus (GPIB). This provided direct communication between other system components shown. Also through the modem the terminal can communicate with other intelligent sources such as the NBS Univac[1] 1108 computer or with a minicomputer at relatively high data transfer rates. The terminal outputs can go to the Univac[1] 1108, via the RS-232 bus, the printer via the RS-232 bus, the plotter via the GPIB bus, or to a hard copy unit. Directly attached to this system is the floppy disc file manager system capable of storing approximately 1900 kilobytes of information for direct access. Both data files and programs can be accessed rapidly. The ROM (read-only-memory)

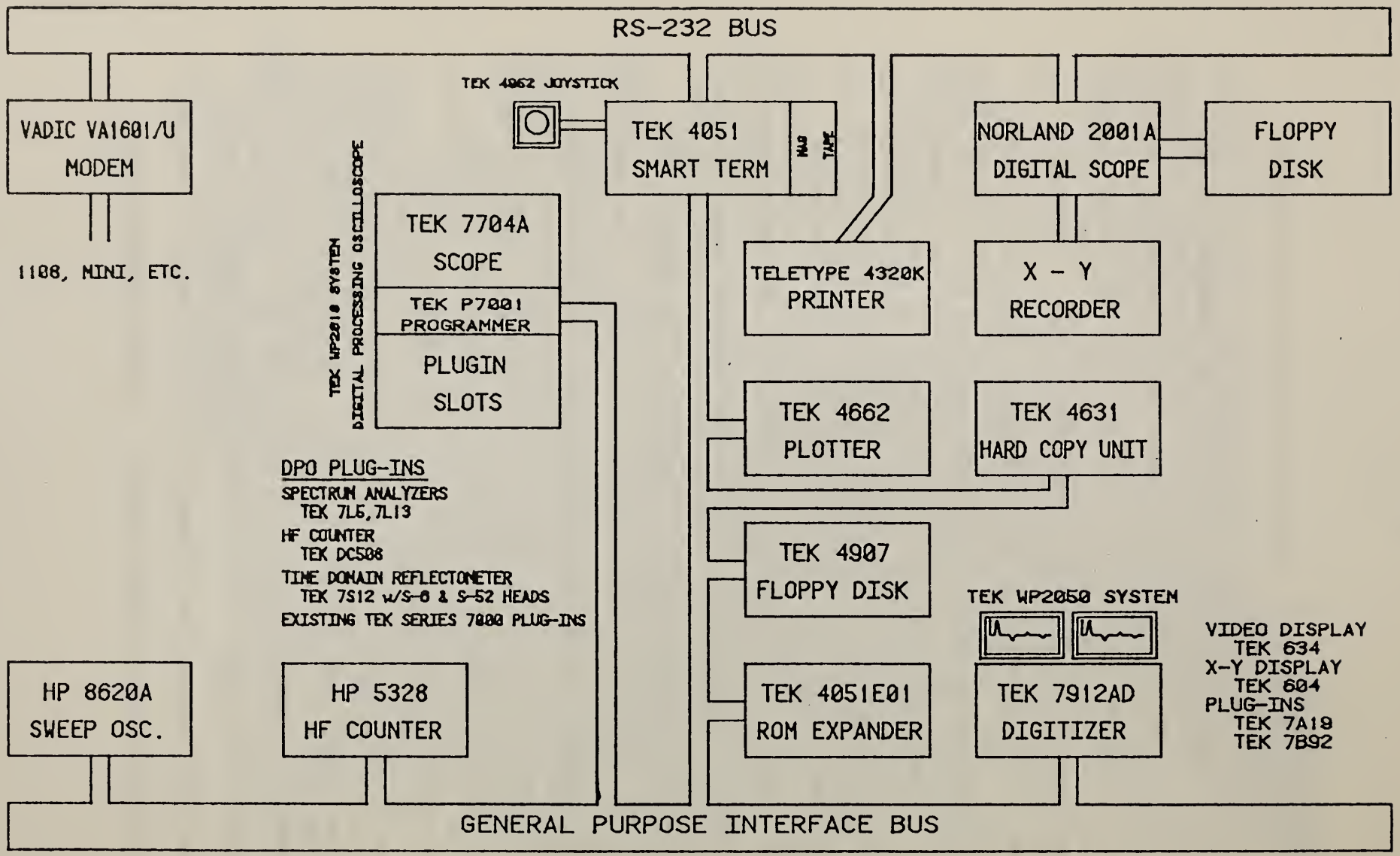

INCIPIENT FAULT PROGRAM EQUIPMENT

Figure 1. Incipient fault program equipment.

expander provides eight slots for specially designed and programmed "ROM packs" for editing, matrix functions, binary conversions and loading, special signal processing routines, etc. This adds a quick utility to the system without using memory overhead or requiring additional programming time. Having 32 kilobytes of memory, the 4051 system possesses substantial "stand alone" analysis and processing power. Large jobs are more efficiently managed by batch processing by the Univac[1] 1108 or other large system. A Tektronix[1] 4054 intelligent terminal is also available which is an order of magnitude faster than the 4051.

The Norland[1] 2001A digital oscilloscope is a digitizing oscilloscope with sample times as short as 2 μs/point for a 10-bit word to 1 μs/point for an 8-bit word. It can digitize simultaneously up to 4 input channels each of 1024 points, 2 simultaneous channels of 2048 points each, or 1 large continuous array of 4096 points. It has signal processing intelligence that can do, among other things, FFT (fast Fourier transform) and correlations with single keystroke commands. Programs and data can be stored and retrieved from its floppy disc system. It currently communicates with the remaining system over the RS-232 bus but can be adapted to use the GPIB structure through an interface.

The Tektronix[1] 7704A oscilloscope coupled with the Tektronix[1] P7001 Programmer forms a versatile digital processing oscilloscope (DPO) which can accept spectrum analyzer plug-ins, time-domain reflectometer plug-ins as well as numerous Tektronix[1] series 7000 plug-ins. Using on-hand spectrum analyzers, capability exists for spectral analysis over a frequency range

from 20 Hz to 1.8 GHz. Because the DPO is interfaced onto the GPIB structure, the digitized output from any of the plug-ins can be "captured" and processed by the intelligent terminal. The digitized waveform consist of 512 10-bit words. A high-speed-average option is included which permits up to 4096 different waveform samples to be averaged before transmission to the intelligent terminal. In principle these 4096 waveforms could be transmitted sequentially to the terminal which could do the averaging, but because the transfer time is relatively long, the latter method is not normally practical.

The Tektronix[1] 7912AD is a very high speed state-of-the-art digitizer capable of digitizing rates up to 1 GHz. Fast transients can be sampled every nanosecond for an array of 512 points and with a resolution of 9-bits. Using a special direct access plug-in, rise-times as fast as 350 ps can be digitized. Data can be output over the GPIB to the intelligent terminal.

The time-domain reflectometry equipment consists of the Tektronix[1] 7S12 plug-in and associated sampling, pulse generator, and trigger recognizer heads. Used for TDR, the 7S12 can measure reflection coefficients, ρ, from 2×10^{-3}/division to 500×10^{-3}/division. (When $\rho = \pm 1$, there is total reflection, when $\rho = 0$, there is no reflection). Used as a general-purpose sampler, repetitive waveforms up to 18 GHz can be displayed. This TDR/sampler can be used as a plug-in in the DPO permitting digitizing and transmitting of waveforms to the intelligent terminal.

Three spectrum analyzers are available. Two of them (Tektronix[1] 7L5 and 7L13) can be used in the DPO. The 7L5 has a frequency range of 20 Hz to

5 MHz and the 7L13 has a 1 kHz to 1.8 GHz range. A third spectrum analyzer (Tektronix[1] 5L4N) is available for low frequency measurements (20 Hz to 100 kHz).

Besides the above-described instrumentation the measurement system consists of various pulse generators, counters, and sweep-frequency oscillators most of which can communicate with the intelligent terminal over the GPIB.

II.2 Experimental Results

Time-domain-reflectometry measurements were made on cable samples containing known defects in order to determine the limitations of TDR methods for incipient fault detection. The TDR unit was used as a plug-in in the digital processing oscilloscope permitting communication with the intelligent terminal. Software (see Appendix A) was written to process this data. The software permits automatic acquisition of waveforms, high-speed averaging, proper scaling, plotting, and filtering. Portions of the waveforms can even be enlarged for more detailed plots.

A series of TDR measurements was performed on a short length of distribution cable. The cable studied was a 6.2 m long, 2 cm diameter, 15-kV, extruded-polyethelene distribution cable with semiconducting screen layers. The cable had three skid wires helically wound around the outer surface of the dielectric. Preliminary measurements indicated that the cable could not be treated as a coaxial cable with the skid wires serving as the return conductor. The calculated characteristic impedance of a coaxial cable, of the same dimensions is about 40 ohms. The measured impedance varied between 50 and 75 ohms. The reduced capacitance between the skid wires (as opposed to a solid coaxial sheath) and the center conductor results in a higher characteristic impedance, Z_0, since

$$Z_0 = \sqrt{L/C} \quad . \tag{1}$$

Another indication of the non-coaxial cable behavior was the unstable TDR results obtained on measurements of the coiled cable. The skid wires did not provide adequate shielding between adjacent loops of the cable. In order to overcome these problems an improved outer conductor was needed and a copper braid sheath was used. With the improved coaxial-like behavior, the characteristic impedance was measured to be about 37 ohms -- near the predicted value of 40 ohms.

In a TDR measurement a pulse with a fast risetime is sent down a cable and is reflected back by variations in the cable impedance. The output of a TDR measurement is the reflection coefficient, ρ. A positive reflection referenced from the peak of the incident pulse indicates the impedance is greater than the TDR output impedance. The reflection coefficient varies from -1 to 1. The reflection coefficient is related to the load impedance (R_L) by the equation

$$R_L = Z_0(1 + \rho)/(1 - \rho) \quad . \tag{2}$$

This relation with Z_0 equal to 50 ohms is used in the following discussion in order to permit the approximate calculation of the impedance along the cable length from the TDR response.

Figure 2 shows the measured impedance (average over 50 runs) along the entire cable length. The response over the first 17 ns shows an impedance of 50 ohms. This represents the impedance of the connector and RG-58/U cable from the TDR output to the distribution cable input. The response from about 17 ns to 80 ns shows the impedance of the distribution cable. Since the cable

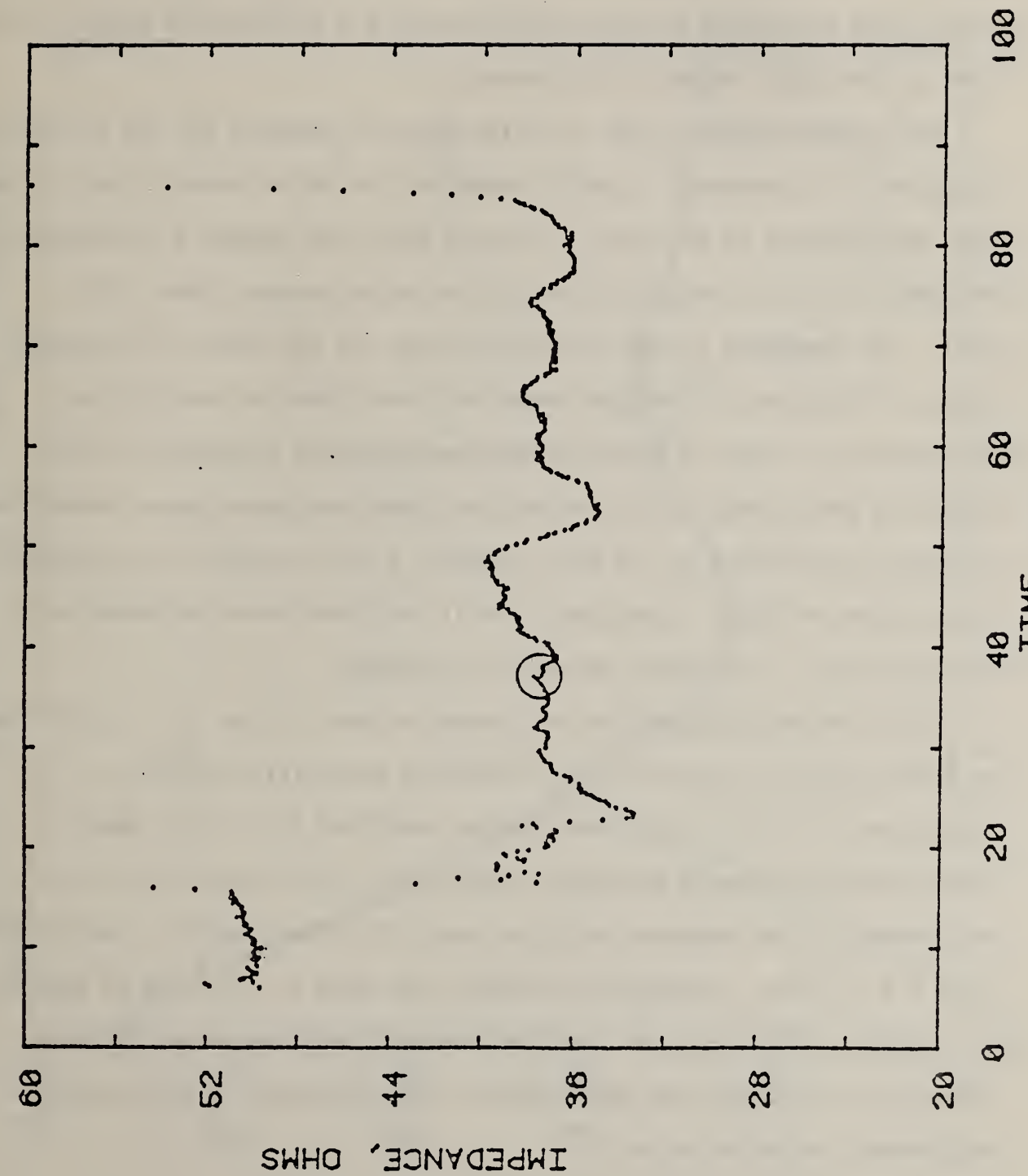

FIGURE 2. TDR response of full cable length.

was unterminated, the impedance rapidly increases at the cable end. The times shown are times for the signal to reach a point and return. Therefore, the time for the TDR signal to propagate the length of the cable is actually about 31.5 ns. Assuming a dielectric constant of 2.26, the length of the cable can be calculated to be $(3 \times 10^8 \text{ m/s})(31.5 \times 10^{-9}\text{s})/\sqrt{2.26}$ or 6.3 meters, close to the actual length of 6.2 meters.

The circled region of Fig. 2 is the point of interest for the following discussion. It represents a small segment of the cable located about 1.9 meters from the input end of the cable. Figure 3 shows the impedance (average over 200 runs) of a 0.5 m length (2.5 ns) of the cable centered about this point. The impedance is seen to vary by about 0.1 ohm along this distance. A mass of 120 grams (1.2 newton force) had been placed on the cable at this location. Figure 4 shows the measured impedance (average over 200 runs) with and without this force applied (lower and upper trace, respectively). Apparently application of the force produces a net decrease in the separation of the outer and inner conductors, a localized capacitance increase, and a consequent (Eq. 1) localized decrease in impedance.

The difference between the two traces is shown in Fig. 5. The difference has been scaled by a factor of 10 to show the sensitivity available. The circled region in Fig. 5 has been further amplified (Fig. 6) in order to demonstrate the ultimate meaningful sensitivity of this particular set of measurements. The impedance variation over this 10 cm length is seen to be about 3×10^{-3} ohm. Impedance variations less than 2×10^{-4} ohm (5 ppm) can be resolved. With increased sampling frequency and improved experimental techniques an ultimate TDR resolution of 1 ppm or better in such impedance measurements may be expected.

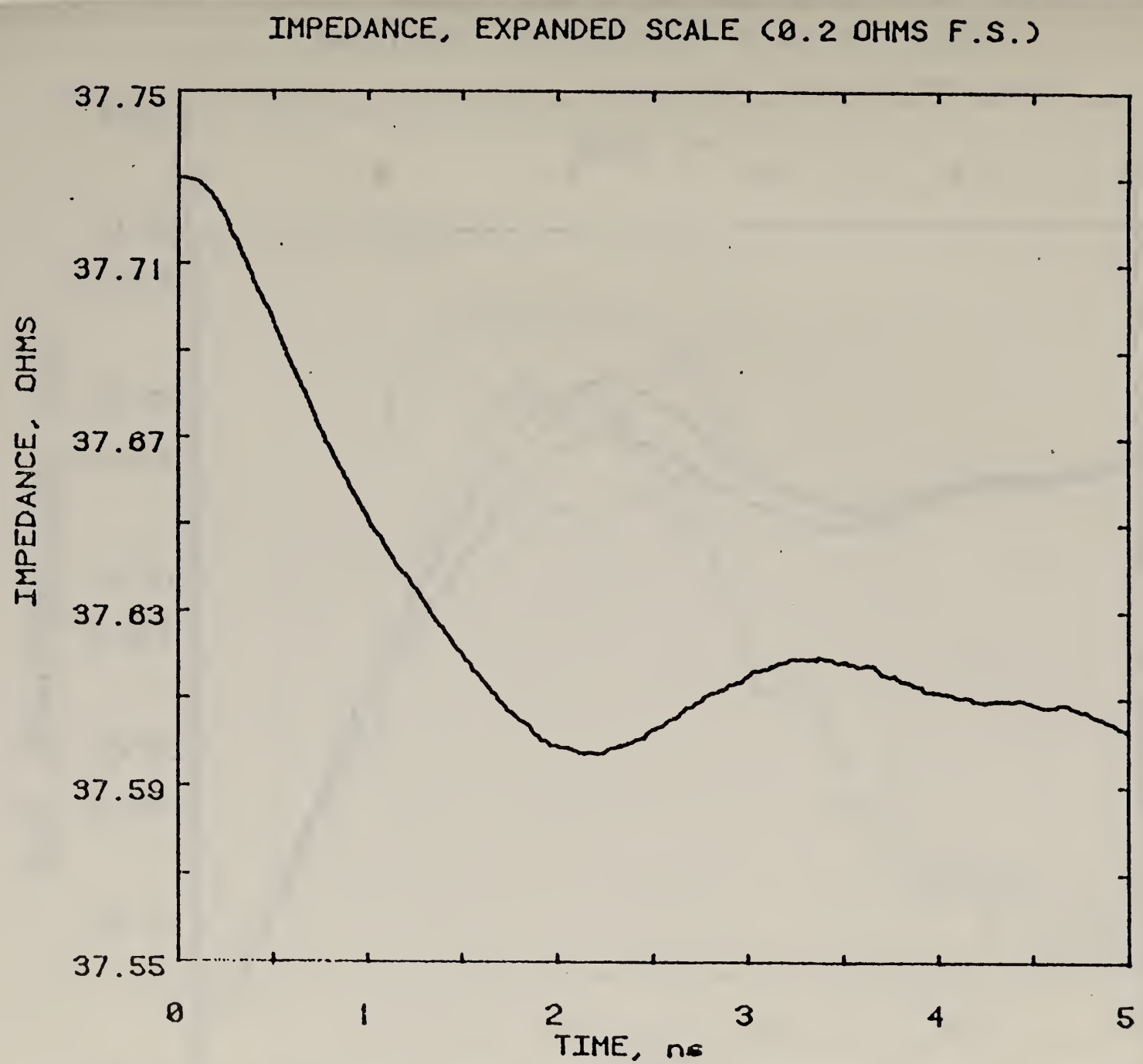

Figure 3. TDR response of 0.5 m length cable segment.

FIGURE 4 TDR response with and without external force (lower and upper trace).

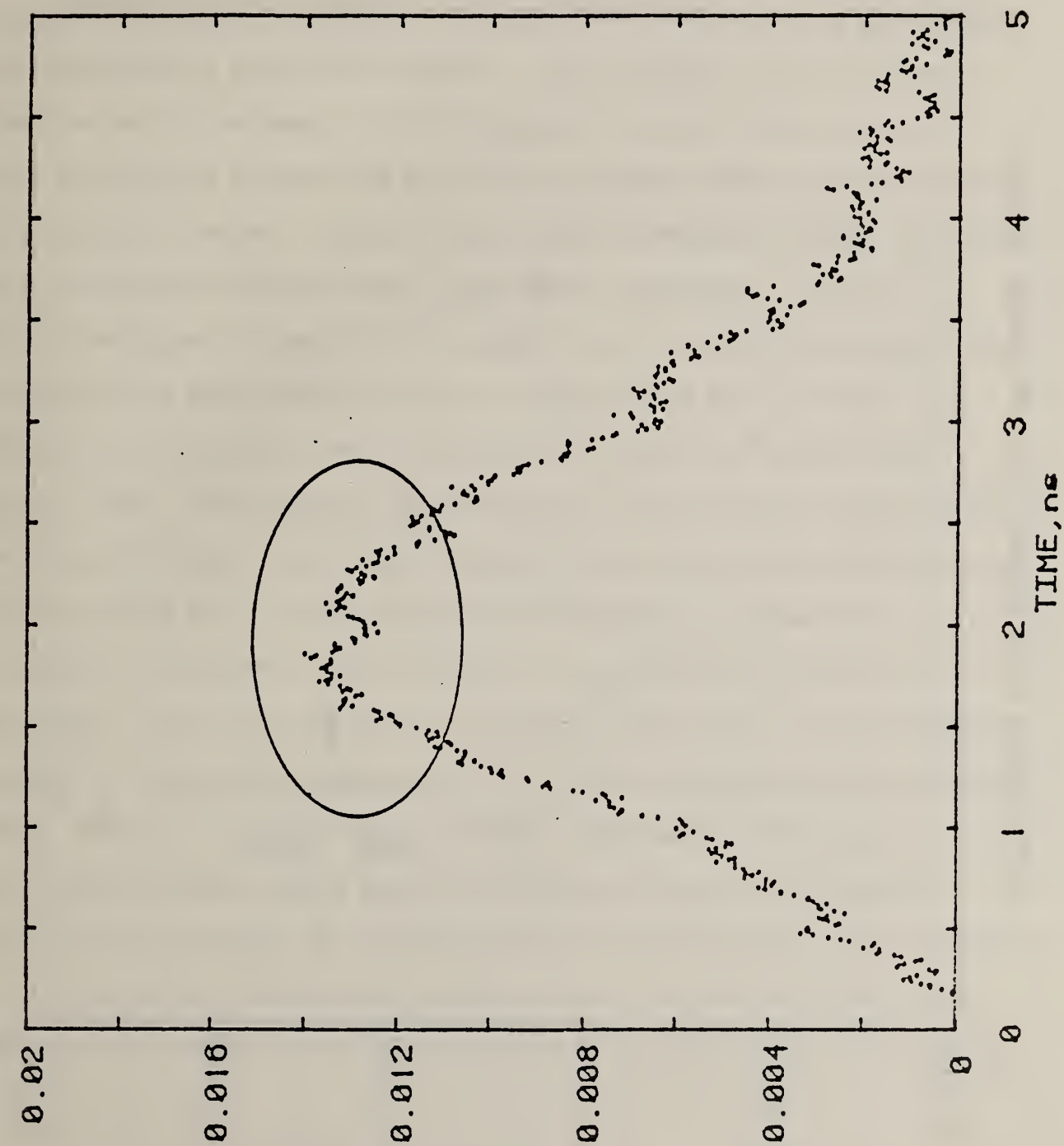

Figure 5. Impedance difference from Fig. 4.

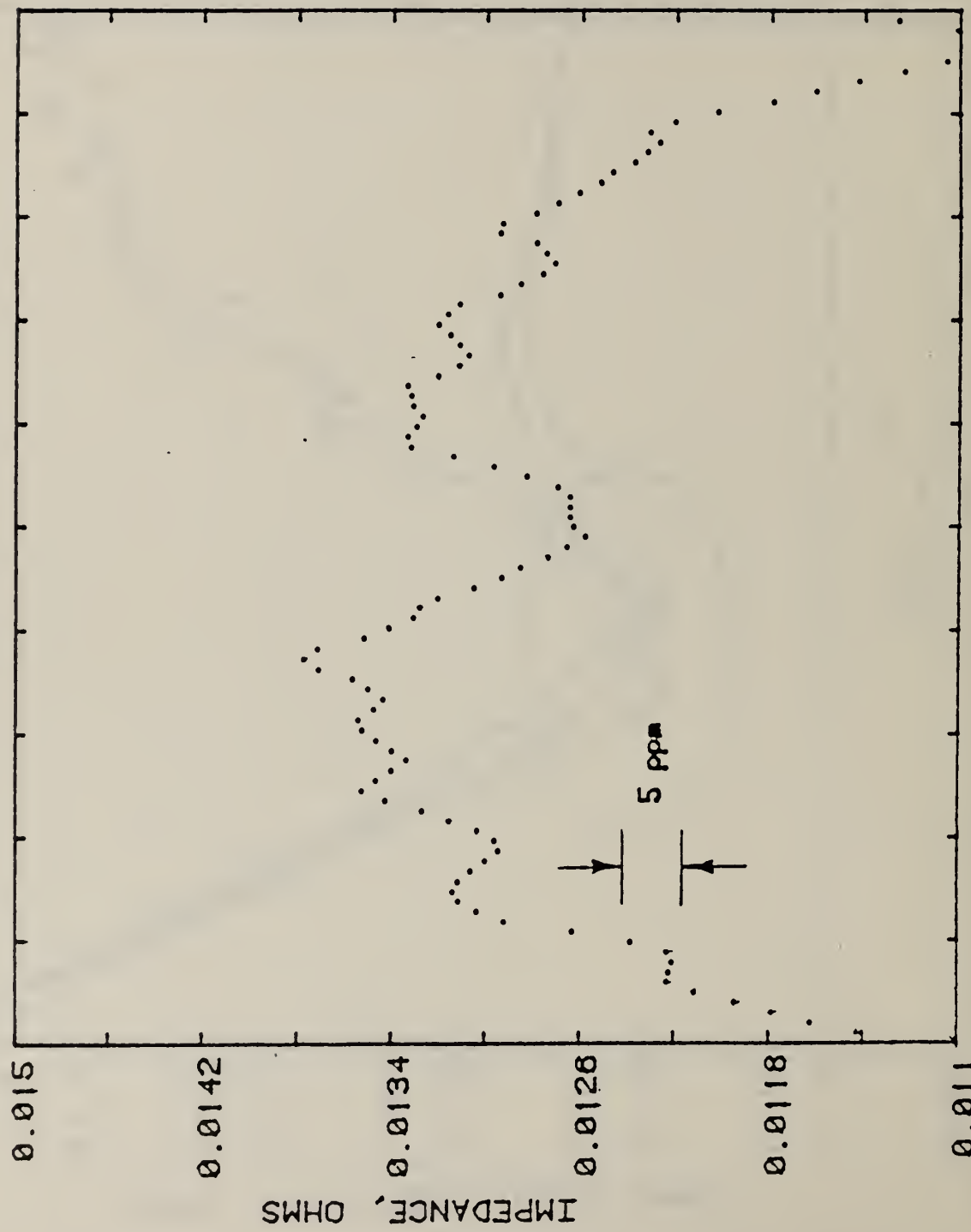

FIGURE 6. TDR response of 10 cm segment showing ultimate resolution.

This series of measurements suggests that if the dielectric constant changes by a part per million over a few millimeters length, the TDR technique should resolve it.

The cable dielectric was purposely altered in order to see if such changes were indeed detectable. A hole was drilled through the cable sheath and dielectric to the center conductor. The resulting hole was 2.3 mm in diameter and 4.6 mm deep. The TDR response of the cable with the empty hole was obtained and then the hole was filled with either isopropyl alcohol (2-propanol) or water. Figures 7 and 8 show the impedance change resulting from filling the hole with water and alcohol respectively. In Fig. 9 the TDR response of a portion of the cable with the empty hole (upper-trace), alcohol-filled hole (middle-trace), and water-filled hole is shown. The length of cable shown in Figs. 7-9 is $(5 \times 10^{-9}\text{s})(3 \times 10^{8}\ \text{m/s})/\sqrt{2.26}$ or about 1 meter. The volume of the dielectric in this cable is about 240 cm^3 per meter of length. The volume of the hole drilled through the dielectric is about 0.020 cm^3. The resulting defect represents a change in the dielectric volume in a length of 1 meter of 80 ppm. The dielectric properties of the hole are a function of the fluid it contains. Water has a static dielectric constant of about 80 and 2-propanol, 18. This is consistent with the trend shown in Fig. 9. One difficulty with this experiment is that the purity of the liquids is questionable within this hole drilled in the dielectric. Particularly of concern is the resistivity of the fluid under these conditions.

This series of measurements seems to imply that TDR techniques would be effective in detecting at least one type of incipient fault. In extruded

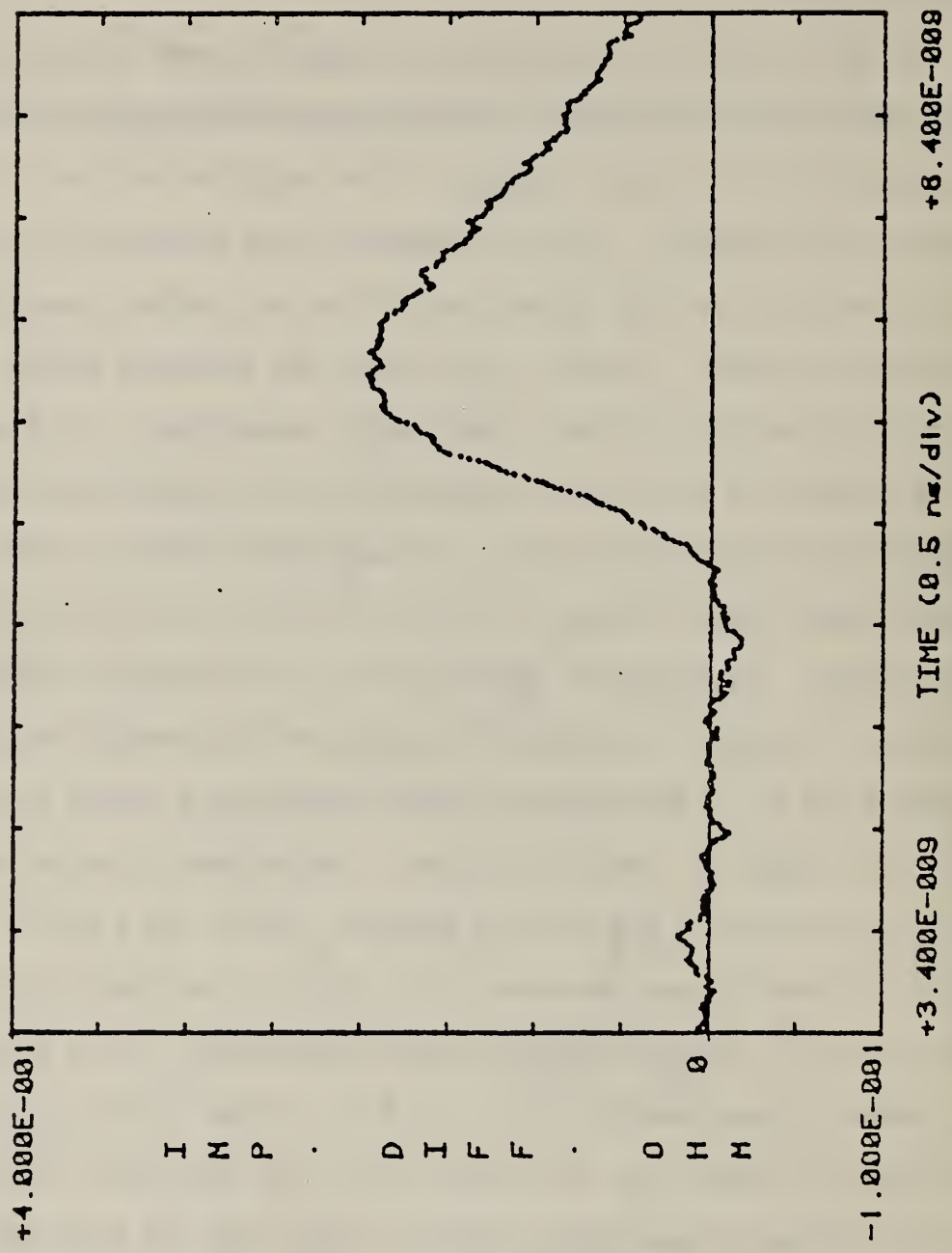

FIGURE 7. Impedance change caused by filling a 2.3 mm hole in cable dielectric with tap water.

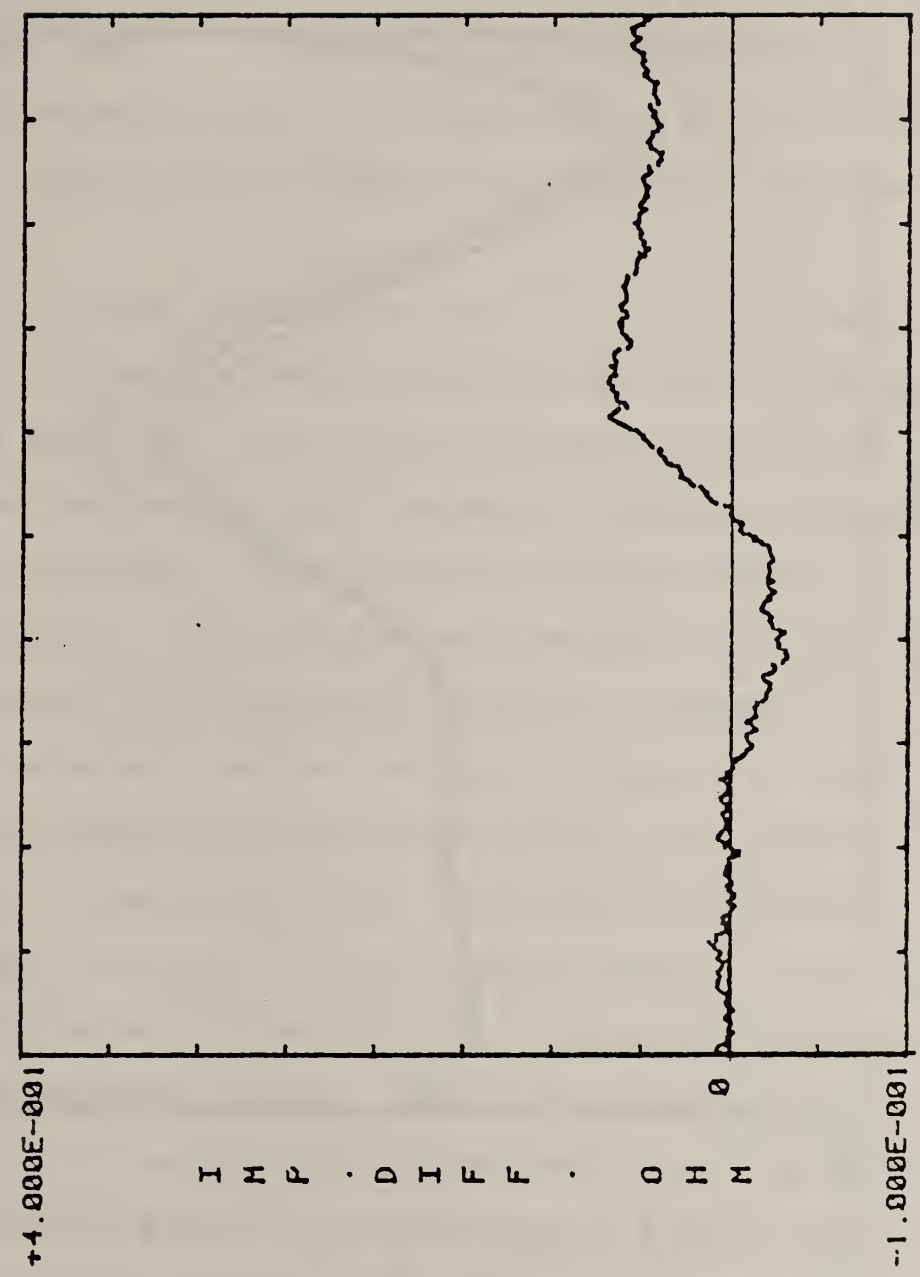

FIGURE 8. Impedance change caused by filling a 2.3 mm hole in cable dielectric with alcohol.

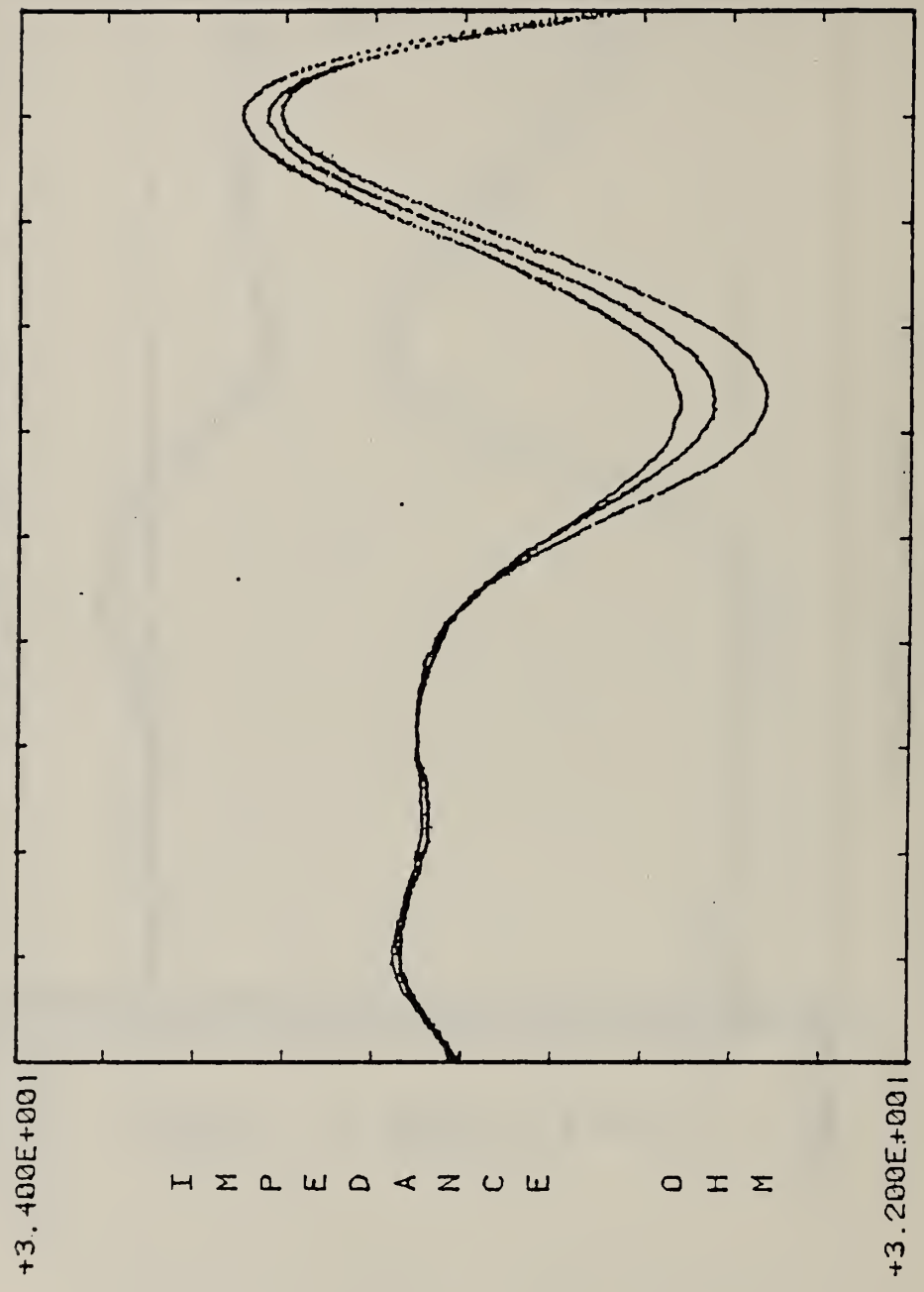

FIGURE 9. TDR response of air-filled (upper trace), alcohol-filled (middle trace), and water-filled (lower trace) 2.3 mm diameter hole in cable dielectric.

polyethylene cables partial discharge activity promotes the growth of hollow channels in the dielectric. These channels branch out forming a tree-like structure. Cables in service for several years have been found to contain many of these "trees".[3] If these "trees" extend from the inner to outer conductor, breakdown does occur. The inner walls of the "trees" are conductive[4] suggesting from the above experiment that TDR techniques could detect them.

There is a further difficulty with this series of measurements. It appears in Fig. 9 that the length of the disturbed area is 2 nanoseconds or about 0.4 meter long. The actual hole diameter is only 2.3 mm. The water and alcohol either must be diffusing a considerable distance outside the constraints of the hole, probably along the stranded wires that constitute the inner conductor, or the high-frequency components of the TDR signal are being attenuated so much that spatial resolution is hampered.

Further experiments were next initiated to determine if "trees" or localized sites damaged by partial discharges would be discernible by time-domain reflectometry techniques. Measurements were performed on the same cable described above. A fine steel sewing needle 1.3 mm in diameter was carefully inserted into the dielectric of the cable to within about one millimeter of the center conductor. (The outer semiconducting layer was previously removed from the vicinity of the needle site). Negative pulses having a duration of 500 μs were applied between the needle and the center conductor. At first, 10 pulses of 500 volts amplitude were applied and the TDR response obtained. Then the voltage was increased in 500 volt increments and more data were obtained. The maximum voltage applied (the limit of the power supply) was 2500 volts. The field at the tip of the needle under these

conditions is estimated to be of order 500 kV/mm. That is certainly high enough to cause damage to the dielectric. However, after applying these impulses even at the maximum voltage level, no change was seen in the TDR response.

While the voltage levels appeared to be high enough to cause some damage, the lack of change in the TDR response suggested that the dielectric was not being significantly altered. In order to test that hypothesis, dc voltage was applied to the needle. At 7 kV a breakdown was observed. The TDR response showed no change. After an additional 10 breakdowns another TDR response was taken. The results are shown in Fig. 10. The portion of cable over which the impedence is being measured is $(3 \times 10^{10}$ cm/s) x $(2 \times 10^{-9}$ s/2)/$\sqrt{2.26}$ or about 20 centimeters long. The reflection coefficient is negative because of the cable's impedance of 37 ohms compared to the output impedance of the TDR unit of 50 ohms. The data shown in Fig. 10 are the average of 512 runs. Any change in the TDR response is lost in the noise.

The result was initially surprising. Previous work had shown this technique to be quite sensitive. We assumed that the partially conducting surfaces of the breakdown channels or "trees" would be readily discernible using TDR. To further test the system, a hole 1.5 mm in diameter was drilled in the cable dielectric to the center conductor. The hole was then filled with graphite (pencil lead). The results are shown in Fig. 11. The TDR technique can readily detect the change in impedance. The graphite effectively is forming a resistive shunt between the outer and inner conductors. This is similar to the case of a "tree" extending across the dielectric.

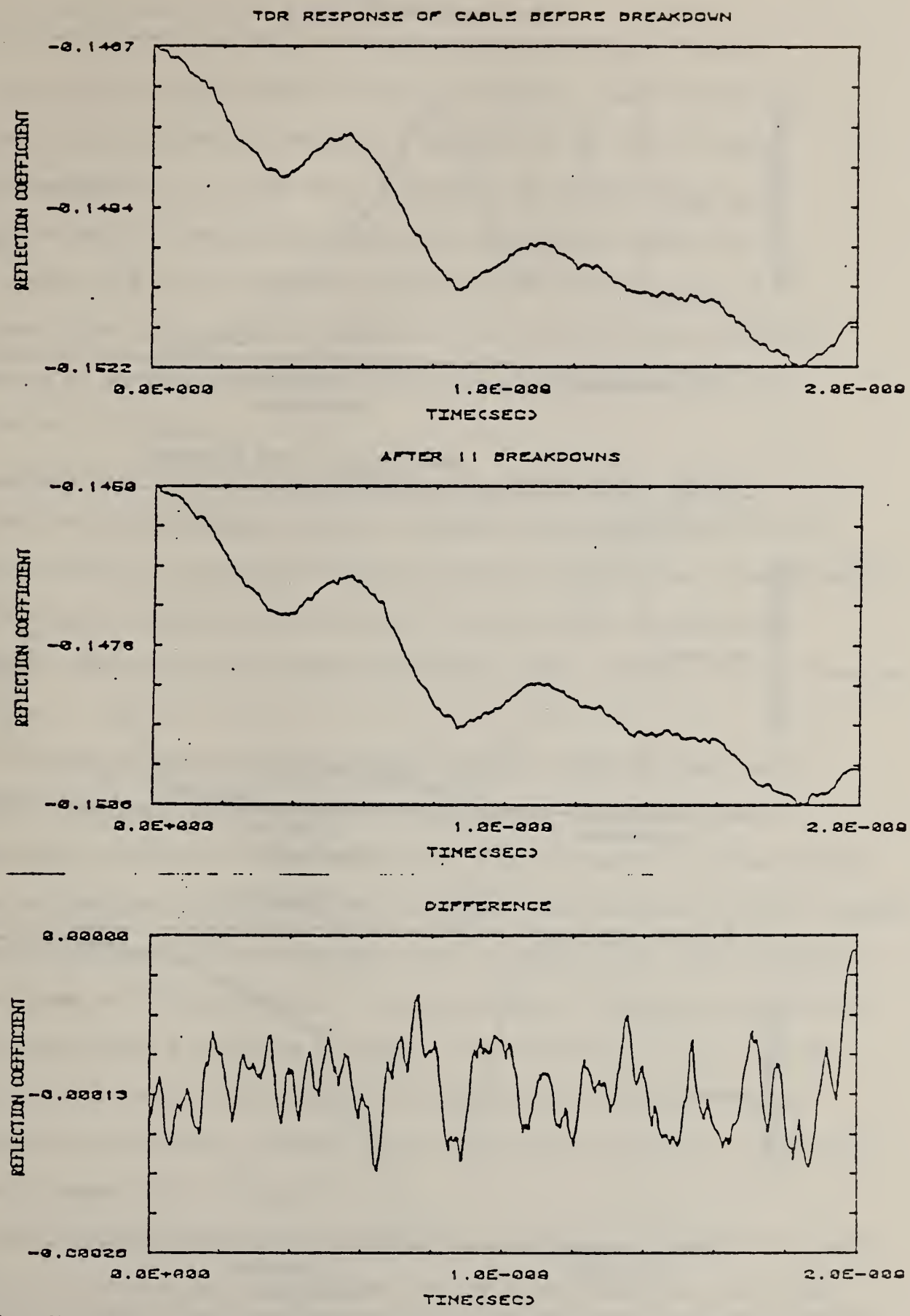

FIGURE 10. Change in TDR response of cable resulting from 11 breakdowns at 7 kV dc. Breakdown channel is estimated to be 1 mm long and is undetectable in the noise.

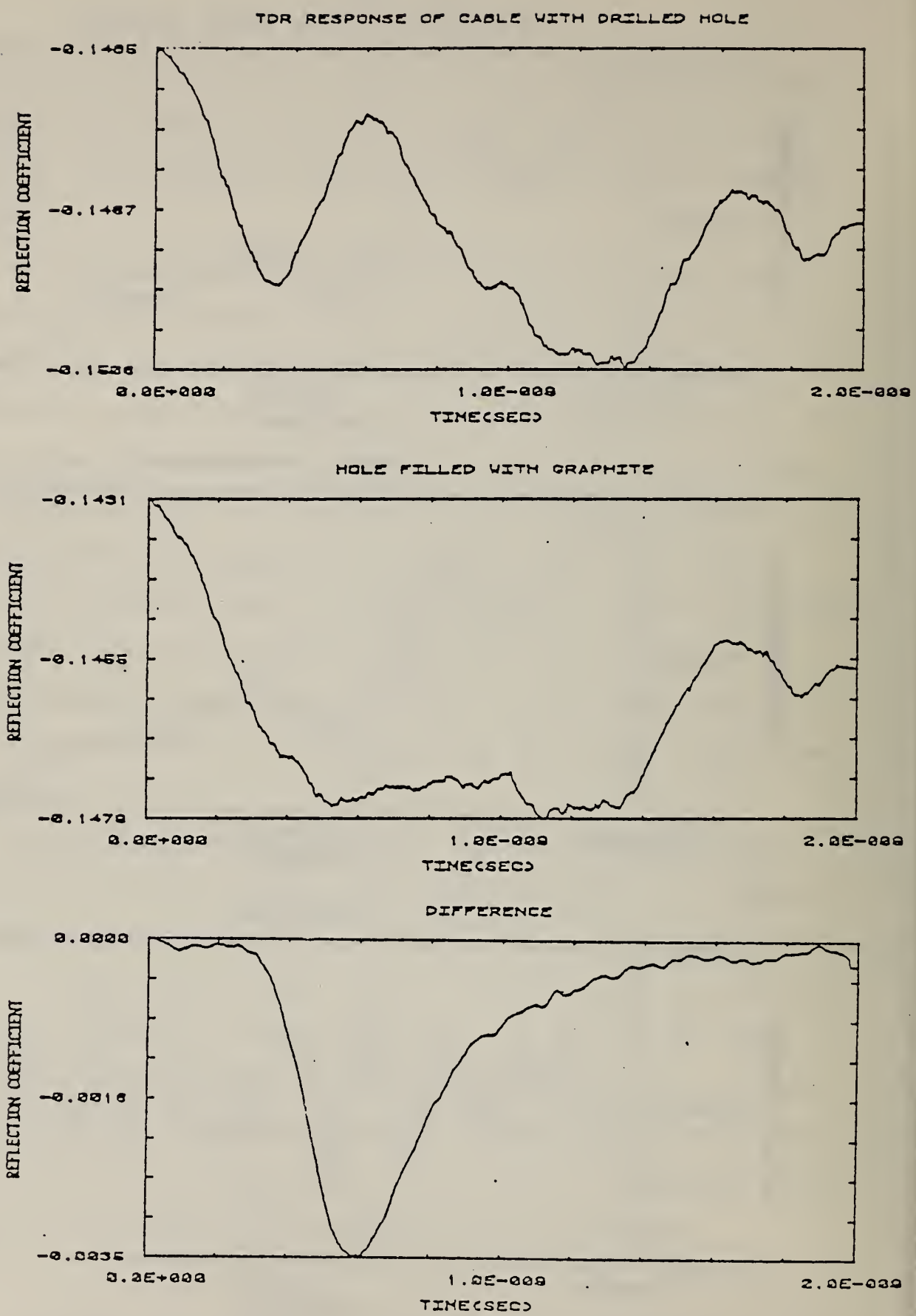

FIGURE 11. Change in TDR response of cable resulting from filling a drilled hole in the cable with graphite. The hole is 1.5 mm in diameter and 4 mm deep.

The negative results shown in Fig. 10 prompted a study to determine whether they arise from a fundamental limitation of the TDR or swept-frequency approach. In order for a reflection (or interaction) to occur from a region of inhomogeniety within a dielectric, the minimum size of that region must be the same order of magnitude as the wavelength of the incident signal (e.g., an electromagnetic signal with a minimum wavelength component of one meter would have little interaction with a defect one millimeter in length).

In the case of our TDR measurements, the incident pulse has a risetime of less than 30 picoseconds implying a maximum frequency component of the order of 30 GHz or a wavelength in the dielectric of about 6 mm. The estimated length of the breakdown channel in Fig. 10 is 1 mm. Assuming the high frequency components actually get to the damage site, detection should indeed be possible.

In order to determine if the higher frequency components were being severely attenuated making detection of small sites impossible, further measurements were made. Figure 12 shows the TDR response of a shorted RG-58/U cable and the power cable shorted at the damage site previously studied. Whereas the effect of the short in the RG-58/U cable is evident over a time interval of the order of 100 ps (length of 1 cm), the effect of the short in the power cable extends over 2 ns (20 cm in length). The difficulty in resolving the location of the short in the power cable demonstrates that high frequency attenuation is occurring. Without these high frequency components, resolution of small damage sites is impossible.

Two solutions to this problem have been considered: (1) better impedance matching to increase the high frequency content within the power cable; and

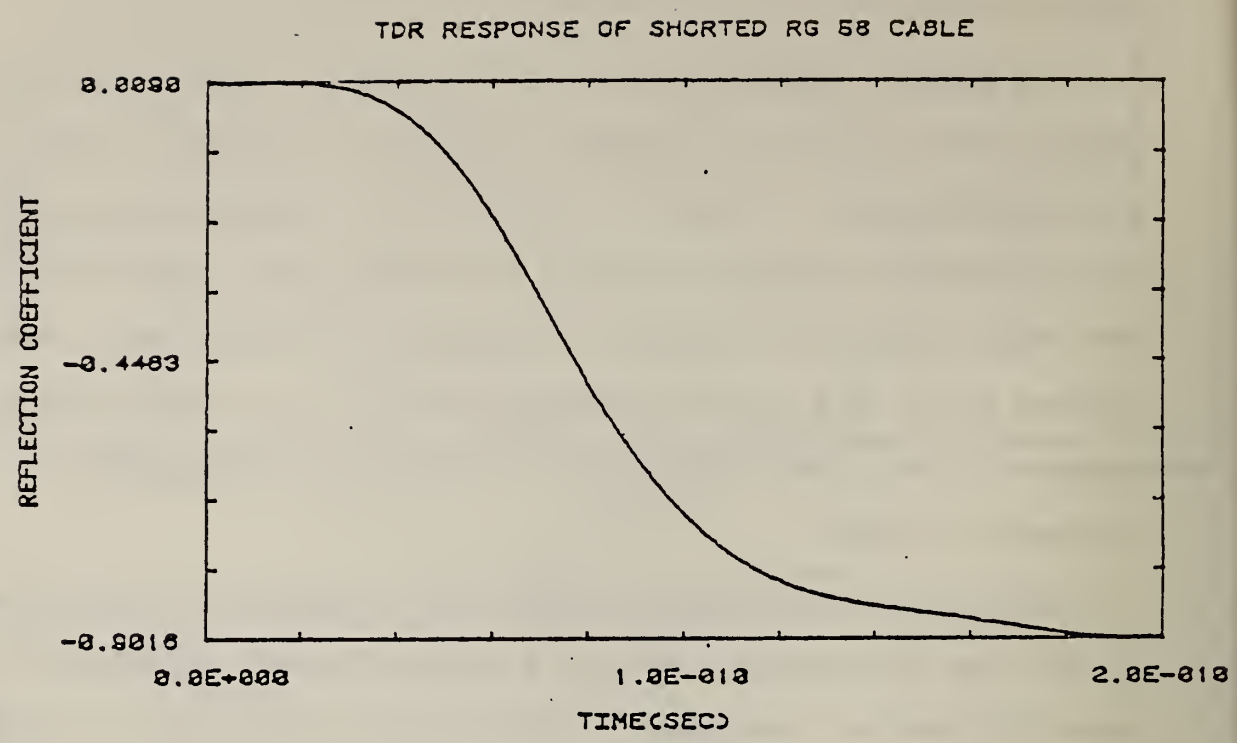

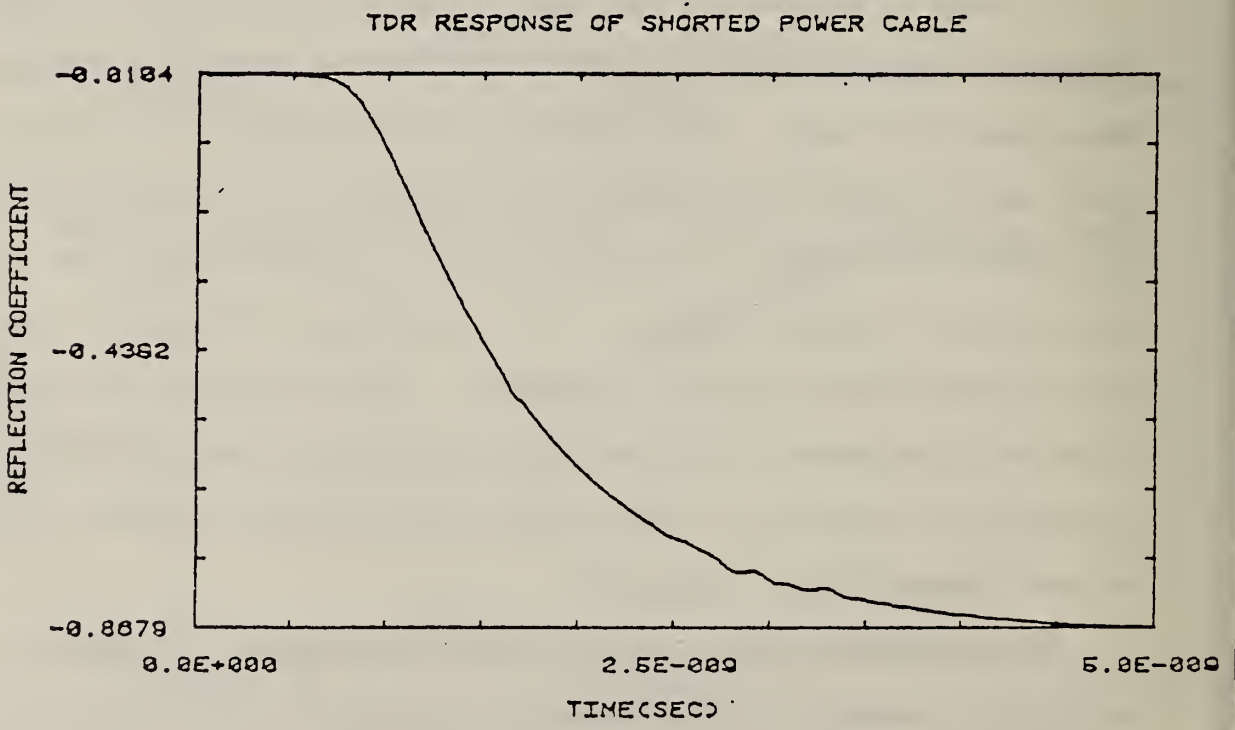

FIGURE 12. TDR response of RG-58/U cable and power terminated by zero impedance.

(2) after careful measurements, compensation for the attenuation in software.

As seen in Fig. 12 and discussed above, there is a serious attenuation of the high frequency components of the step input. A large fraction of this "loss" may be the result of the impedance mismatch between the 50 ohm TDR system and the 37 ohm high voltage cable. Additionally at or near the connection to the cable other mismatches are evident from the reflections present in that region. These results suggested the need for an impedance matching device to improve coupling of the high frequency components into the high voltage cable.

Impedance transforming baluns were considered, but the idea discarded since pulse risetimes of 25 ns or shorter are being considered. An investigation into other impedance matching schemes led to the use of tapered sections of coaxial transmission lines to achieve an impedance transformation. A design having minimal reflections over a wide bandwidth employing a gradual exponential taper was examined. A linear conical tapered line was also investigated. Although the exponential taper is theoretically better, the difference is so little so as to make the difficult exponential taper not worth the extra machine time and costs.[5] This is especially true if the taper is long and gradual in comparison to the wavelength of the lowest frequency of interest. The tapered section will act as a high pass filter so long as the phase constant does not contain an imaginary term. At lower frequencies the phase constant is complex and the signal is attenuated. Practically, impedance changes of 2 to 1 can be made if the tapered section is one wavelength long or longer. A good impedance match will result for higher frequencies.

Figure 13 shows details of the tapered line. The outer conductor of the line is made from a thick-walled section of brass tubing which clamps over the braided shield of the high voltage cable. In the right end of the "tube", a machined adaptor is inserted. This couples to a General Radio[1] type 874-BP58A flanged panel connector. This type of connector is known to have a constant 50-ohm impedance throughout its length and to provide for a good electrical connection with low series and shunt losses. The stepped portion of the center conductor shown in Fig. 13 fits inside the adaptor. The dimensions have been selected to maintain a 50-ohm characteristic impedance throughout its entire length. The susceptances at each "step" should be low enough even at the highest frequencies to provide a constant 50-ohm match in this region of the line.

The center conductor of the line is tapered. The tapered length is 30.18 cm which is one wavelength at a frequency of 993 MHz. It would be desirable to have a longer line so the lower cutoff frequency would be less, but this becomes mechanically difficult and cumbersome.

The left end of the tapered center conductor fits directly over the center conductor of the high voltage cable. Because of possible end effects of the tapered section and the abrupt discontinuity of the polyethylene dielectric at the end of the cable, impedance mismatch reflections can be expected. The influence of these remaining reflections has been experimentally determined.

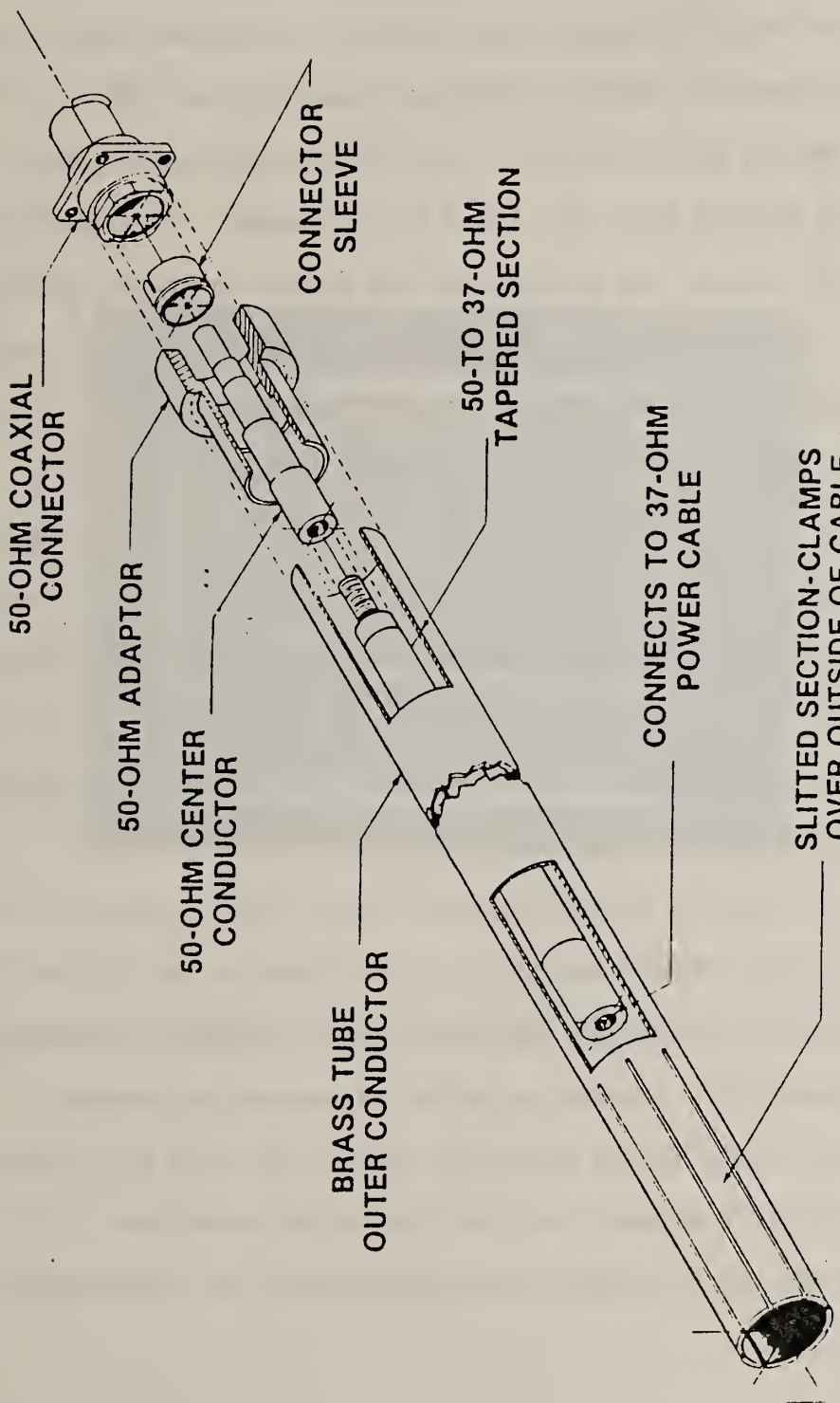

Figure 13. Tapered transition section

The performance of the transition section is shown in Figs. 14 to 17. Figure 14 shows the TDR response at the end of the 50-ohm coaxial cable and at the beginning of the 37-ohm distribution cable without the transition section. The output of the TDR analyzer was adapted to BNC-type coaxial connectors. A one meter length of RG-58/U cable was connected to a GR[1] type 874 BNC-to-GR adaptor. The six outer strands of the distribution cable center conductor were removed leaving only one strand at the center. The female portion of the BNC-to-GR adaptor was placed over the single remaining center strand of the cable's inner conductor. The braided sheath of the cable was then dressed over the adaptor and the whole assemblage taped into place. Using this arrangement, two major impedance mismatches occurred. The first was due to the short length of small diameter single-strand center conductor. This length was about 9 mm and caused the impedance to increase to about 90 ohms, the first major peak in Fig. 14. The second mismatch is due to the lower characteristic impedance of the distribution cable. (The small variations of impedance seen in the 37-ohm portion of the cable are caused principally by the unevenness of the braided sheath).

Figure 15 shows a cross-sectional view of the 50-ohm end of the transition. (The GR874BP connector is not shown on the left end). The steps of the center conductor were designed to coincide with the steps of the outer conductor. However, an error on the design drawing of 0.2 cm shifted the two larger diameters on the right towards the left end resulting in a lack of coincidence between the inner and outer conductors. This was discovered after the piece was fabricated and assembled and the TDR response obtained.

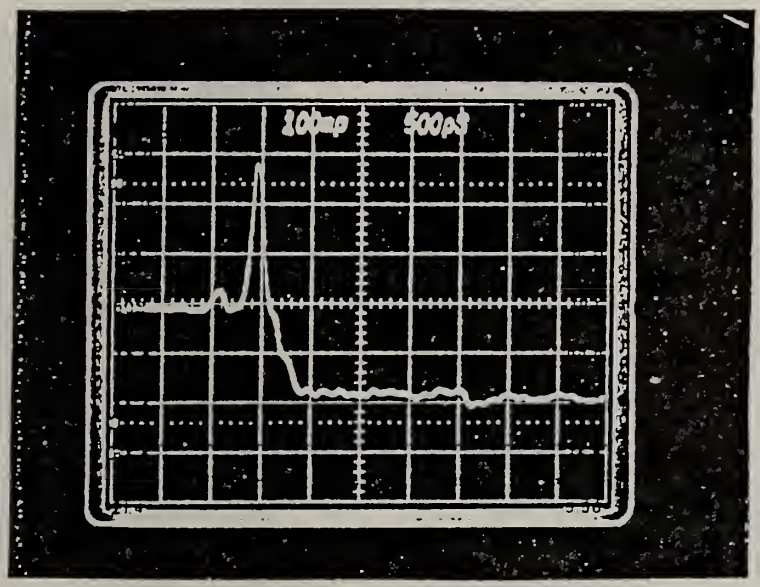

gure 14. TDR response of RG-58/U cable connection onto 37-ohm distribution cable.

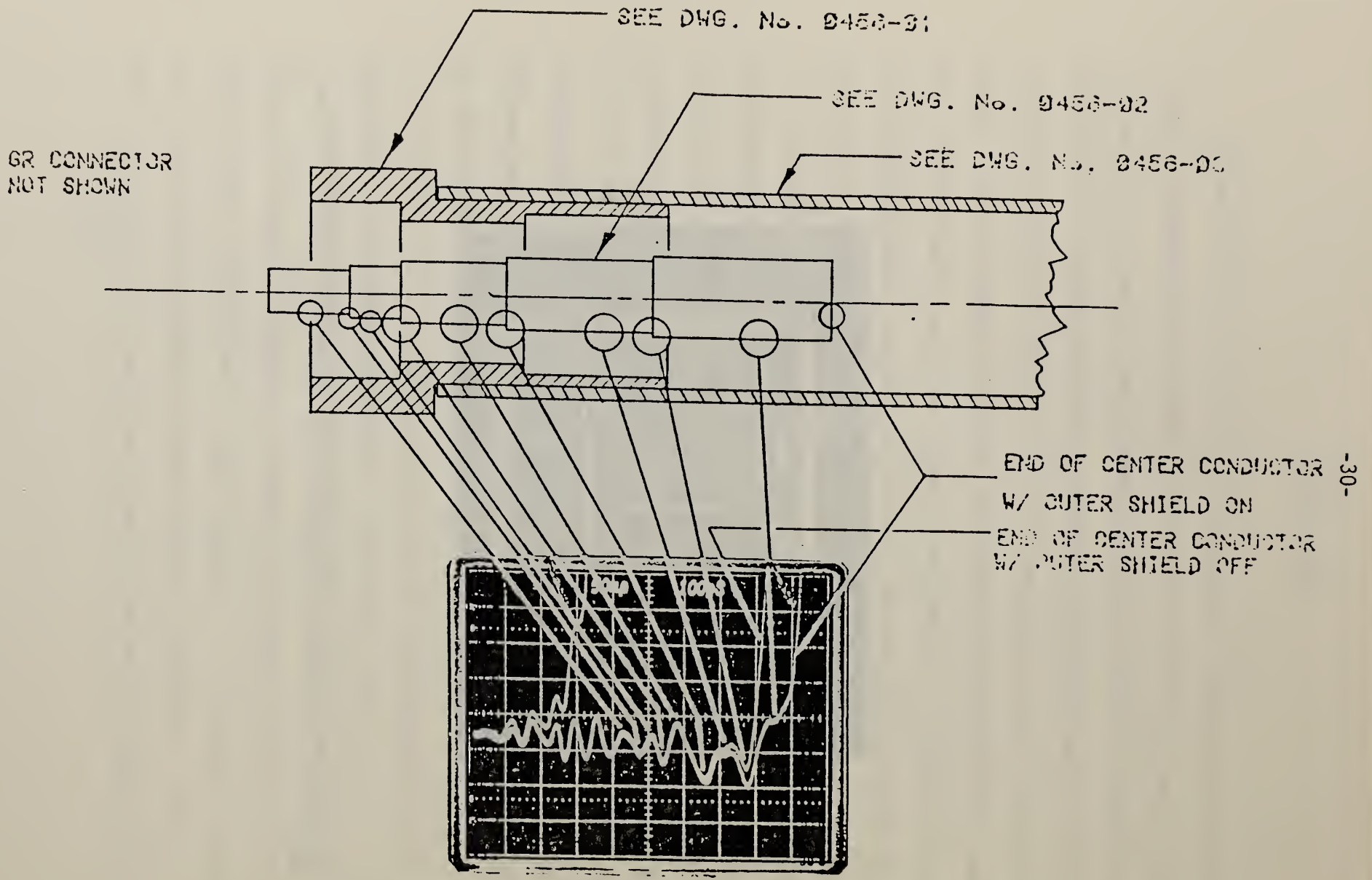

Figure 15. 50-ohm end of the transition section as per first design specifications.

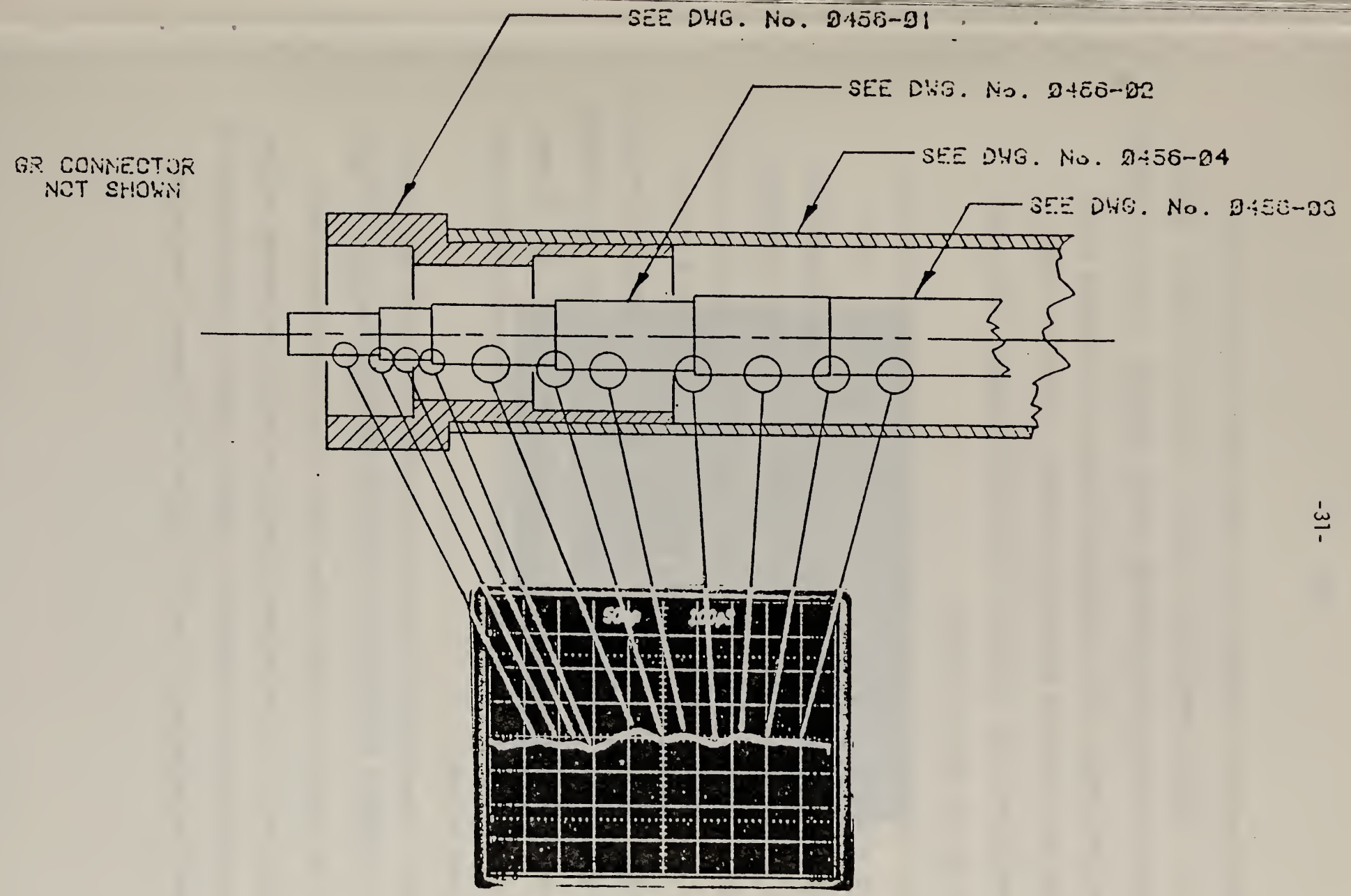

Figure 16. 50 ohm end of the transition section per second design.

The TDR response is keyed to the stepped center conductor as shown in Fig. 15. (Vertical sensitivity is about 5 ohms per division). Several problems were evident upon examination of this response. First the impedance variations were greater than expected and second, the impedance of the fourth step was lower than design specifications. From the latter, a second drawing error was discovered: the inside diameter of the outer conductor was too small by 0.09 cm.

It was obvious that even though the steps in diameter were each only 0.12 cm, a 3-to 5-ohm impedance change occurred at each step. Because the impedance decreased in the vicinity of each step, this indicated that the shunt susceptance at the steps was too great. In order to compensate for and to reduce this susceptance, each of the steps of the center conductor piece was shifted to the right by an amount equal to D/8 where D is the inside diameter of the outer conductor. Also the inside diameter of the last step of the outer conductor was increased by 0.09 cm to increase the impedance in that region of the transition section. The TDR response in Fig. 16 shows a significant improvement over that of Fig. 15. The impedance does not vary by more than two ohms.

Figure 17 shows the TDR response for the entire length of the tapered transition section. At the left is the 50-ohm TDR system impedance; in the center is the tapered line; and on the right is the 37-ohm high voltage distribution cable. As can be seen at the right end of the tapered section, impedance variatiations are apparent. These are caused by the end effects of the tapered line attaching to the distribution cable center conductor and

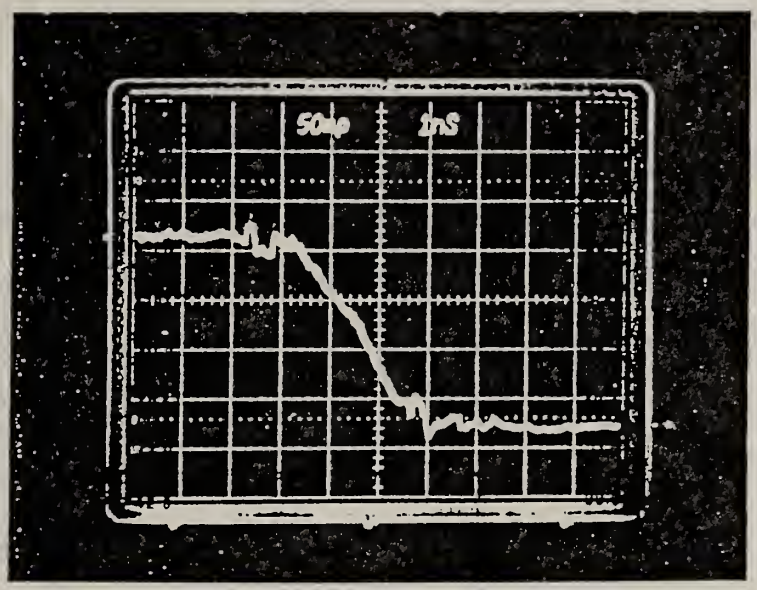

Figure 17. TDR response of tapered line transition section.

imperfections in the shield geometry at and near the beginning of the distribution cable.

Comparing Figs. 14 and 17 we see that the transition section has fulfilled its intended purpose -- a smooth impedance transition from the 50-ohm output impedance of the TDR analyzer to the 37-ohm characteristic impedance of the cable. The next step was to determine if this transition section permitted significantly more high frequency signal to enter the cable and, if so, would this enable resolution of incipient faults or would attenuation within the cable still be a problem.

With the transition section in place the outer and inner conductors were shorted together at a distance of 61 cm from the cable end (and the TDR analyzer). The TDR display was averaged 512 times and sent to the intelligent terminal for display. The results are shown in Fig. 18. The ordinate has not been normalized as on the previous figures (i.e., a constant has not been added to the reflection coefficient in order to force it to be zero for the power cable's characteristic impedance of 37 ohms). The important parameter, reflection coefficient variation, is not affected. The upper graph is from Fig. 12 and is taken without benefit of the transition section. The lower graph demonstrates the effect of the transition section. For the sake of simplicity we will define the decay time as the time it takes the signal to decrease from 7/8 to 1/8 of the difference of the average maximum and minimum values. The decay time, thus defined, is 1750 ps without and 800 ps with the transition section. This means the additional high frequency components entering the cable with the transition section have permitted better spatial resolution of the short. The 800 ps decay time corresponds to a length of 8 cm which is much longer than the shorted hole's

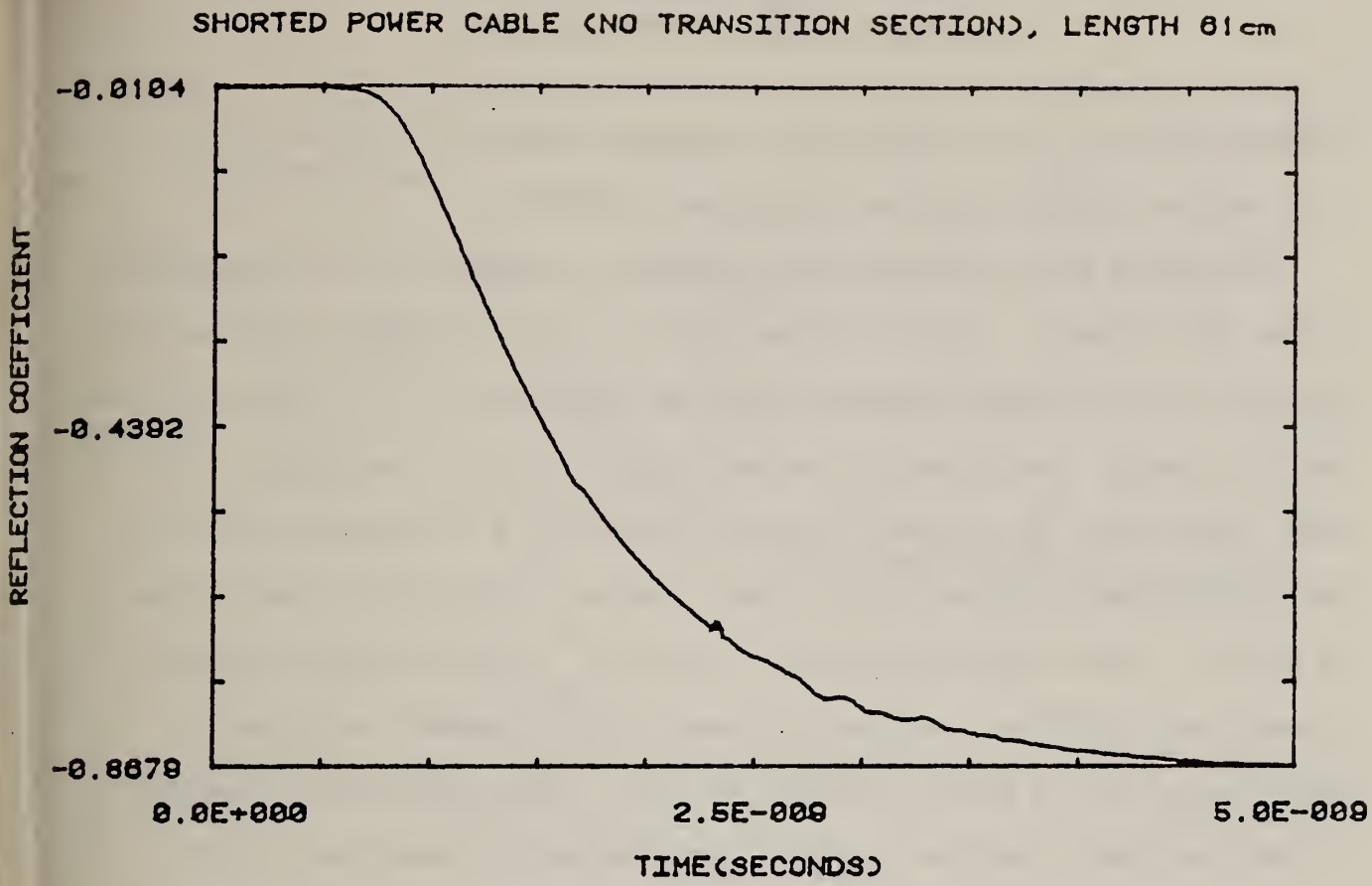

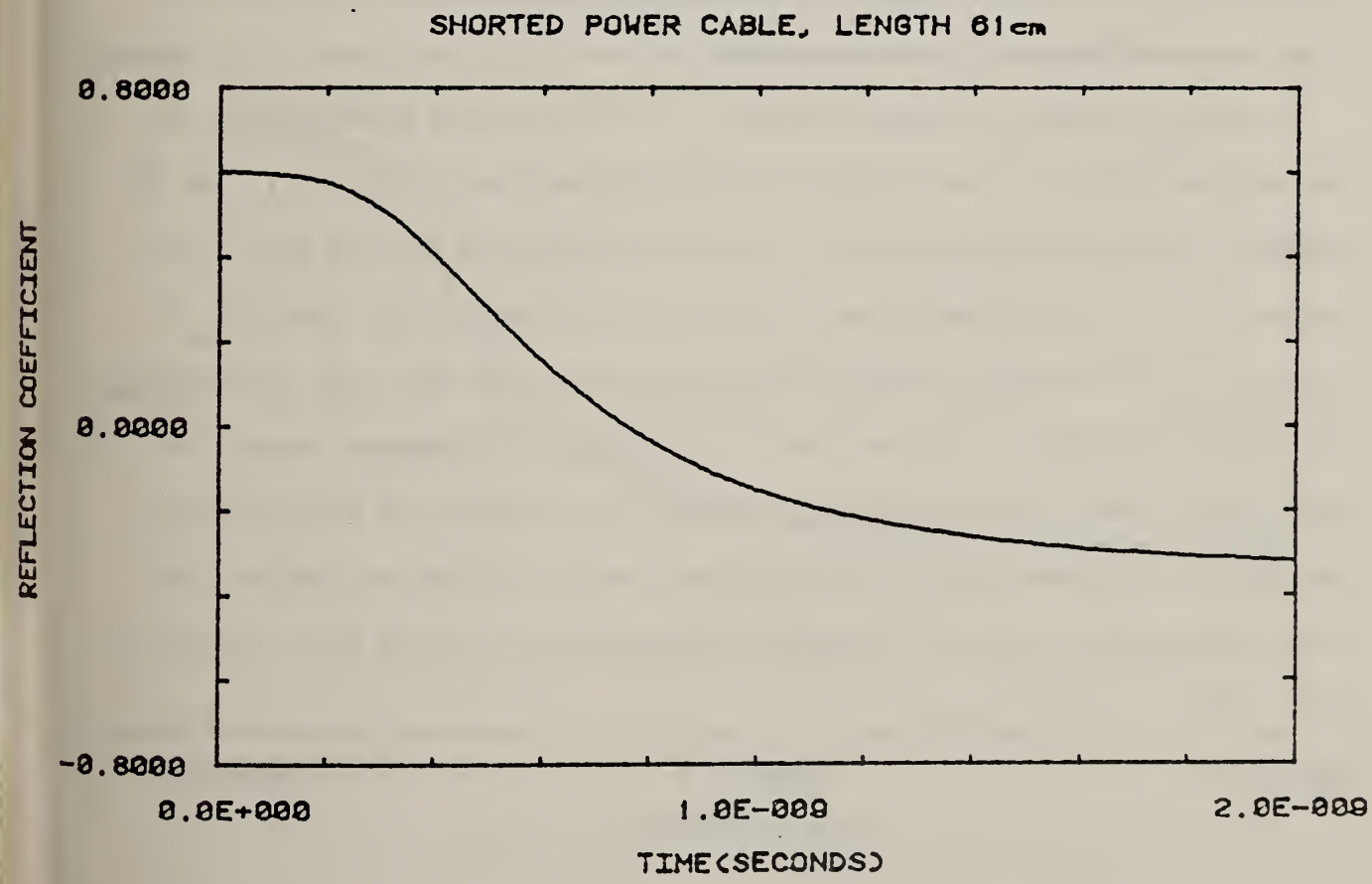

Figure 18. TDR response of power cable terminated by zero impedance with and without transition section.

diameter (0.13 cm). Sufficient high frequency content, therefore, is still not available to resolve this region adequately.

The second factor affecting high frequency propagation is the attenuation in the cable itself. Figure 19 shows results, taken as before, with the short located at two different distances from the TDR analyzer. The figure indicates that the greater the distance of propagation in the cable the greater the decay time of the TDR response. A short located at 4 cm from the cable end has a decay time of 340 ps while a short located at 163 cm has a decay time of 1050 ps. From above we found that a short 61 cm from the cable end has a decay time of 800 ps. At 4 cm the decay time corresponds to a spatial resolution of 3.4 cm and at 163 cm to 10.5 cm. These results are troubling in that they imply that the intrinsic high frequency attenuation in this type of cable makes the detection at large distances of small-size damage sites very difficult, if not impossible.

Figure 20 shows this quite clearly. In the previous measurements, we had not been able to detect a hole drilled through the dielectric 1.3 mm in diameter. We again attempted this with holes drilled 4 cm from the cable end and 61 cm from the cable end. At 61 cm the response with the hole (light trace) and without (heavy trace) are nearly the same, any differences not being repeatable. At 4 cm, there is a definite difference between the two traces. New minima and maxima have been introduced with the drilling of the hole. From these data, it is inferred that, at distances greater than a few centimeters, the high frequency attenuation has caused this information to be lost.

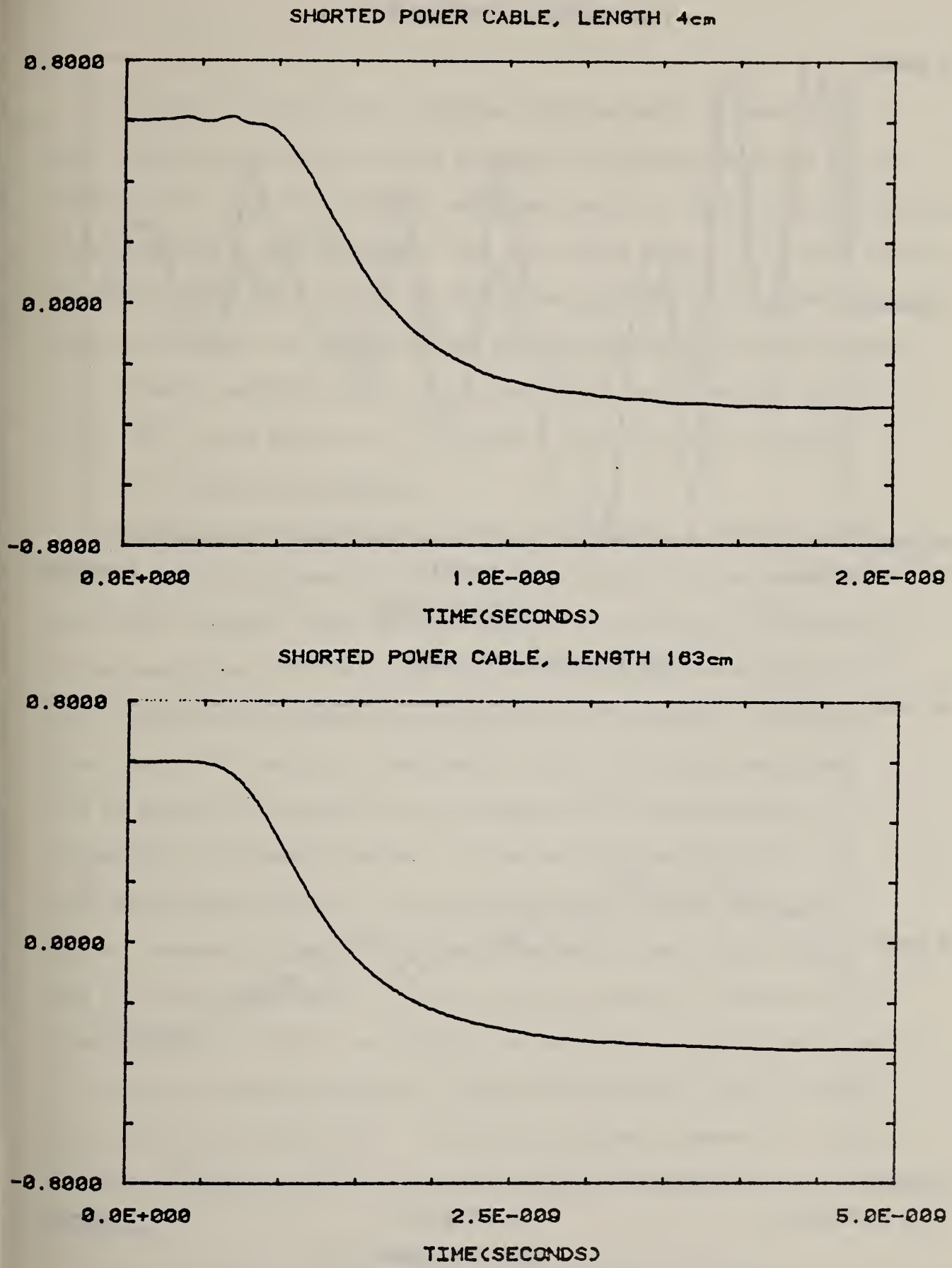

Figure 19. TDR response of power cable terminated by zero impedance; the location of short is 4 cm and 163 cm from cable end; measurements made using transition section.

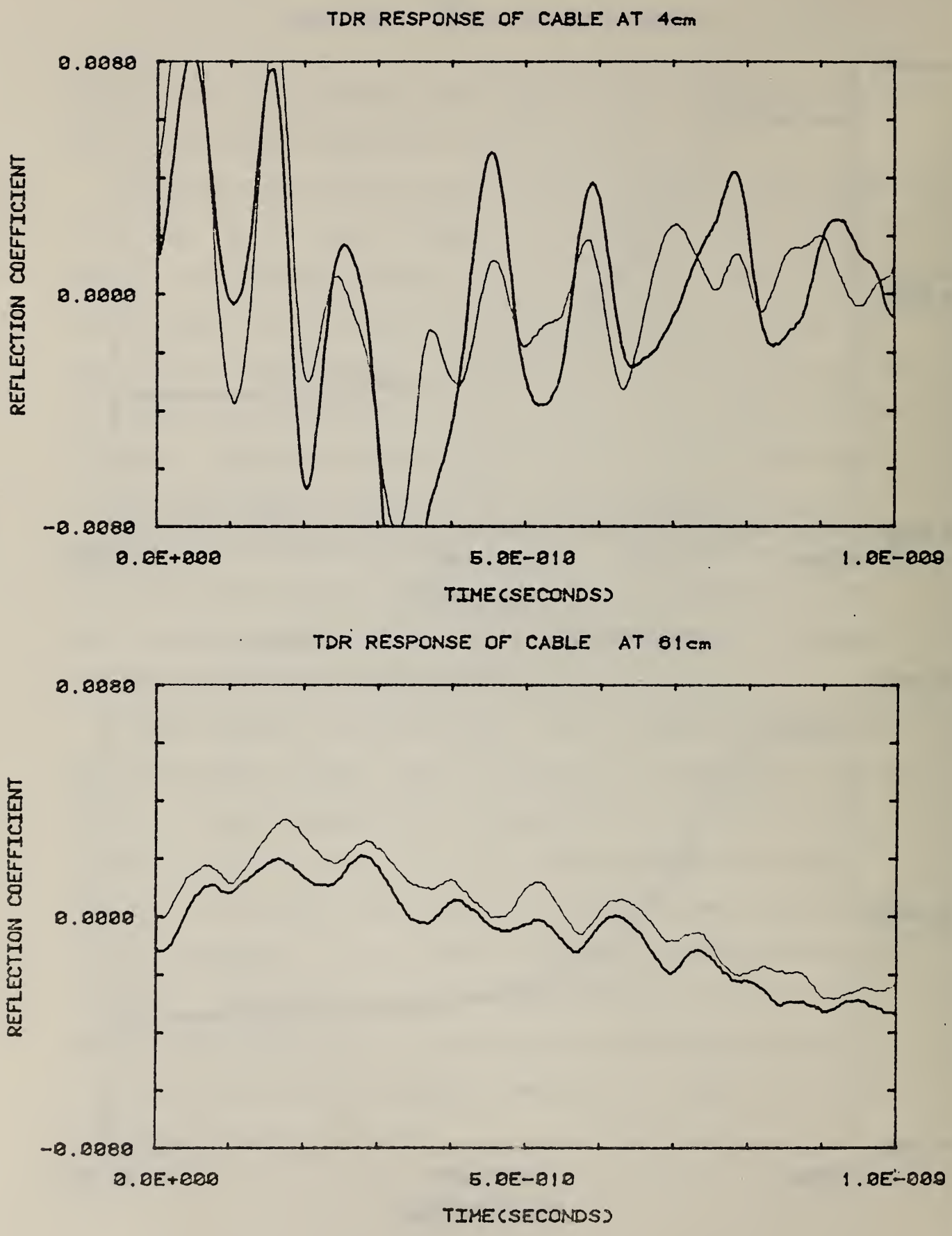

Figure 20. TDR response of power cable (using transition section) with (lighter) and without (darker) a hole drilled through dielectric. Distance of 1.3 mm diameter hole from cable end is 4 cm (upper) and 61 cm (lower).

The results indicate that incipient fault detection schemes based on high frequency sounding may not be practical for plastic-insulated cables although it is possible that such techniques may be of value for compressed-gas (spacer failure), superconducting, and other cable types. It is also possible that our results obtained on a 15 kV extruded polyethylene distribution cable may not fully apply to higher voltage transmission cables of similar design. High frequency sounding could still be useful for fault location and, if a sufficiently large damage site is available, incipient fault location.

II.3 Software Development

In addition to the software presented in Appendix A which was developed for data transfer between the digital processing oscilloscope and the intelligent terminal, other software needed to be developed. Experiments in the coming year will be initiated with the objective of determining the signal velocity and attenuation in cables at rf frequencies. Initial measurements will be in the time-domain. Step-like voltage waveforms will be applied to the cable and the output waveform digitized and transmitted to the smart terminal. A Fourier transform will then yield the transfer function in the frequency domain. Problems arise, however, because instead of a Fourier transform of continuous data we have a Fourier transform of discretely sampled data or a discrete Fourier transform (DFT). A DFT of an impulse-like waveform (a waveform which ends at the same amplitude it begins) is straightforward and a fast algorithm exists for its solution (FFT).[6] Step-like waveforms, however, will produce a serious truncation error[7] if they are treated by conventional DFT (and FFT) techniques.

We have found two different (but related) methods to overcome this problem. The first is the sin x/x expansion presented by Samulon.[8]

The measured curve is sampled at time intervals, τ, such that:

$$\tau \leq 1/2f_c \quad , \tag{3}$$

where f_c is the highest frequency component present. This restraint is necessary to avoid "aliasing" problems[7,9]. Using a sin x/x expansion the given time function, F(t), can be expressed

$$F(t) = \sum_{n=o}^{\infty} \frac{A_n \sin f_c(t-n\tau)2\pi}{f_c(t-n\tau)2\pi} \quad , \tag{4}$$

where A_n is the amplitude of the nth sampled point. The Fourier transform of the nth term of Eq. (4) is given by

$$\phi_n(\omega) = \int_{-\infty}^{\infty} \frac{A_n \sin[2\pi f_c(t-n\tau)]}{2\pi f_c(t-n\tau)} e^{-j\omega t} dt \quad , \tag{5}$$

or

$$\phi_n(\omega) = \frac{A_n}{2\pi f_c} \int_{-\infty}^{\infty} \frac{\sin[2\pi f_c(t-n\tau)]}{t-n\tau} \{\cos \omega t - j \sin \omega t\} dt \quad . \tag{6}$$

Subsituting t' for $t-n\tau$ and using

$$\int_{-\infty}^{\infty} \frac{\sin mx \cos nx}{x} dx = \pi \text{ for } m>n\geq o \tag{7}$$

We obtain

$$\phi_n(\omega) = \frac{A_n e^{-jn\omega\tau}}{2f_c}, \tag{8}$$

or

$$\Phi(\omega) = \sum_{n=o}^{\infty} \frac{A_n e^{-jn\omega\tau}}{2f_c} \quad ; \tau \leq 1/2f_c \quad . \tag{9}$$

Software based on Eq. (9) has been written and is incorporated in Appendix B. However, this is not the most useful form of the sin x/x expansion. If A_n does not equal zero for some n greater than an arbitrary m, Eq. (9) does not converge and cannot be used. If A_n does not converge and the summation is arbitrarily terminated at some point, ripples will occur obscuring the results.

A modified form of Eq. (9) can be used which does not have such limitations. Let $B_n \equiv A_n - A_{n-1}$ and replace the sequence $\{A_o, A_1, A_2 \ldots\}$ by $\{A_o, A_1 e^{-\tau/\delta}, A_2 e^{-2\tau/\delta}, \ldots\}$. The value of δ can be made arbitrarily large so as not to affect our transient unless τ is very large or in the frequency domain ω is very small. Using the relation

$$A_n = \sum_{m=o}^{n} B_m \tag{10}$$

Eq. (9) becomes

$$\Phi(\omega) = \frac{1}{2f_c} \sum_{n=o}^{\infty} \left(\sum_{m=o}^{n} B_m \right) e^{-jn\omega\tau - n\tau/\delta} \quad . \tag{11}$$

If we let $n\varepsilon = jn\omega\tau + n\tau/\delta$, we obtain

$$2f_c \, \Phi(\omega) = \sum_{n=o}^{\infty} \left(\sum_{m=o}^{n} B_m \right) e^{-n\varepsilon} \quad , \tag{12}$$

or equivalently

$$2f_c \, \Phi(\omega) = \left(\sum_{n=o}^{\infty} e^{-n\varepsilon} \right) \left(\sum_{m=o}^{\infty} B_m e^{-m\varepsilon} \right) \quad . \tag{13}$$

The series $\Sigma e^{-n\varepsilon}$ is absolutely convergent if

$$\sum_{o}^{\infty} \left| e^{-jn\omega\tau - n\omega/\delta} \right| \tag{14}$$

converges. But

$$\left| e^{-jn\omega\tau - n\tau/\delta} \right| = e^{-n\tau/\delta} \tag{15}$$

and (14) is seen to be a geometric progression, convergent for $e^{-\tau/\delta} < 1$. Using the formula for the sum of an infinite geometric progression:

$$\sum_{n=o}^{\infty} e^{-n\varepsilon} = 1/(1 - e^{-\varepsilon}) \quad , \tag{16}$$

or

$$\sum_{n=o}^{\infty} e^{-n\varepsilon} = 1/(1 - e^{-\tau/\delta}e^{-j\omega\tau}) \quad . \tag{17}$$

The factor $e^{-\tau/\delta}$ can be made arbitrarily close to unity yielding

$$\sum_{n=o}^{\infty} e^{-n\varepsilon} = 1/(1 - e^{-j\omega\tau}) \quad . \tag{18}$$

From Eq. (13), we obtain

$$\Phi(\omega) = [1/(2f_c(1 - e^{-j\omega\tau})] \sum_{n=o}^{\infty} B_n e^{-jn\omega\tau} \quad . \tag{19}$$

Appendix C contains the software utilizing Eq. (19). This program is good for waveforms of arbitrary shape and can always be used assuming $\tau \leq 1/2f_c$ and that, for n greater than some m, B_n approaches some constant (not necessarily zero). The only difficulty with Eq. (19) is that the processing can take several seconds per frequency point making it impractical for some experiments.

The second method used a modified FFT. As mentioned above a conventional FFT yields incorrect results due to truncation error. A modified FFT has recently been presented[10] which overcomes this problem.

From Eq. (19) and the definition of B_n we obtain

$$\Phi(\omega) = [1/(2f_c(1 - e^{-j\omega\tau}))] \sum_{n=o}^{\infty} (A_n - A_{n-1})e^{-jn\omega\tau} \quad . \tag{20}$$

We assume the waveform becomes a constant at $T = N\tau$ (i.e., $A_i = A_{i-1}$ for $i \geq N$). It is further assumed that A_o is equal to zero (i.e., the dc offset of the waveform is zero. A_{-1} is defined to be zero. Substituting ν_r for ν

($\nu = \omega/2n$) such that

$$\nu_\kappa = \kappa\nu_o = \kappa(1/T) = \kappa/N\tau, \quad \kappa = 1,2, --, N - 1 \quad . \tag{21}$$

Eq. (20) becomes

$$\Phi_\kappa = [\tau/(1 - e^{-j\kappa 2\pi/N})] \sum_{n=o}^{N-1} (A_n - A_{n-1})e^{-jn\kappa 2\pi/N} \quad . \tag{22}$$

In Eq. (22), τ has been set equal to $1/2f_c$ satisfying the sampling theorem. In order to be consistent with FFT conventional formalism the factor τ will be removed from Eq. (22). Separating the sum into two parts, we obtain

$$\Phi_\kappa = 1/(1 - e^{-j\kappa 2\pi/N}) \quad \{ \sum_{n=o}^{N-1} A_n e^{-jn\kappa 2\pi/N} - \sum_{n=o}^{N-1} A_{n-1} e^{-jn\kappa 2\pi/N} \} \quad . \tag{23}$$

Defining S_κ,

$$S_\kappa = \sum_{n=o}^{N-1} A_n e^{-jn\kappa 2\pi/N} \quad , \tag{24}$$

to be the FFT acting on the data set $\{A_n\}$, Eq. (23) becomes

$$\Phi_\kappa = 1/(1 - e^{-j\kappa 2\pi/N}) \{S_\kappa - \sum_{n=o}^{N-1} A_{n-1} e^{-jn\kappa 2\pi/N}\} \quad , \tag{25}$$

or

$$\Phi_\kappa = (1 - e^{-j\kappa 2\pi/N})^{-1} \{S_\kappa - e^{-j\kappa 2\pi/N} \sum_{\ell=o}^{N-2} A_\ell e^{-j\ell\kappa 2\pi/N}\} \quad . \tag{26}$$

This is equivalent to

$$\Phi_K = (1 - e^{-jK2\pi/N})^{-1} \{S_K - e^{-jK2\pi/N} (S_K - A_{N-1}e^{-j(N-1)K2\pi/N})\} \quad (27)$$

and, since $e^{-jK2\pi} = 1$,

$$\Phi_K = S_K + A_{N-1}/(1 - e^{-jK2\pi/N}) \quad K = 1, \ldots, N - 1 \quad . \quad (28)$$

This is a very important result in that it permits considerable saving in computational time. Using an FFT read-only-memory pack our intelligent terminal can compute for 256 frequency points, Φ_K in under a minute compared to over an hour if Eq. (19) were used. Appendix D contains the software utilizing Eq. (28). Appendix E contains the results of using the sin x/x approach Eq. (19) and the modified FFT approach Eq. (28) on the same data. The results are identical.

Both approaches are sensitive to dc offset. Assuming the zero frequency result is not of interest the waveform should be shifted so as to make the amplitude zero at time equal to zero. Equivalently, using Eq. (19), B_0 can be set to zero in software or using the modified FFT approach replacing Eq. (28) by

$$\Phi_K = S_K + (A_{N-1} - A_0)/(1 - e^{-jK2\pi/N}), \quad K = 1, \ldots, N - 1 \quad . \quad (29)$$

If the software is modified in such a way both methods are insensitive, as they should be, to dc offset.

The software development will be invaluable in future measurements. The sin x/x approach has the advantage of allowing the user to choose the points to be calculated. The modified FFT approach is considerably faster.

III. Conclusion

A measurement program has been initiated at NBS that will contribute to the development, testing, and utilization of incipient fault detection/location instrumentation. The measurement system, centered on an intelligent terminal, permits the digitizing of transient and continuous waveforms and subsequent processing.

The system was initially configured in such a way as to permit time-domain reflectometry studies on a 15 kV distribution cable. The results were significant in that they showed that TDR techniques would have very limited use for detection of incipient faults. The difficulty is that the high frequency attenuation in the extruded polyethylene insulated distribution cable prevents the spatial resolution of the anticipated incipient faults.

Measurements in the future will determine the rf properties of high voltage transmission cables. These results will be important in the design of incipient-fault intrumentation. These measurements will be made in the time domain requiring mathematical transformation to the desired frequency domain. Extensive software has been written and tested using two different methods.

IV. References

1. Certain commercial equipment, instruments, or materials are identified in this report in order to adequately specify the experimental procedure. In no case does such identification imply recommendation or endorsement by the National Bureau of Standards, nor does it imply that the material or equipment identified is necessarily the best available for the purpose.

2. The Tektronix General Purpose Interface Bus (GPIB) is compatible with the Hewlett Packard HP-IB and both are compatible with the IEEE-488-1975 interface specifications.

3. T. P. Lanctoe, J. H. Lawson, W. L. McVey, "Investigation of Insulation Deterioration in 15 kV and 22 kV Polyethylene Cables Removed from Service - III," IEEE Power Engineering Society Summer Meeting, Los Angeles, CA, pp. 759-763 (1978).

4. E. F. Kelley and R. E. Hebner, "The Electric Field Distribution Associated with Prebreakdown Phenomena in Nitrobenzene," Journal of Applied Physics (submitted).

5. H. H. Skilling, "Electric Transmission Lines," First Edition, McGraw-Hill, pp. 353-355 (1951).

6. J. W. Cooley and J. W. Tukey, "An algorithm for the machine calculation of complex Fourier series," Math. Comput., Vol. 19, pp. 297-301 (1965).

7. E. Oran Brigham, The Fast Fourier Transform, Englewood Cliffs, NJ: Prentice Hall (1974).

8. H. A. Samulon, "Spectrum Analysis of Transient Response Curves," Proc. of I.R.E., Vol. 39, pp. 175-186 (1951).

9. C. Shannon, "Communications in the presence of noise," Proc. I.R.E., Vol. 37, pp. 10-22 (1949).

10. J. Waldmeyer, "Fast Fourier transform for step-like functions: the synethesis of three apparently different methods," IEEE Trans. Inst. Meas. Vol. IM-29, No. 1, pp. 36-39 (1980).

APPENDIX A

This software permits the collection of data from the digital processing oscilloscope DPO. The data can first be averaged up to 4096 times by the DPO. The data are plotted on the terminal screen. Portions may be expanded. The data can be filtered (adjacent points averaged). The data can be output to a plotter for quality graphics.

```
1 INIT
2 PS=8
3 GO TO 9994
4 REM PROGRAM "DOE/DPO/VERSION3"   9-30-80
5 REM DATA COLLECT
6 SET NOKEY
7 GO TO 100
8 REM EXPAND
9 SET NOKEY
10 GO TO 790
12 REM REPLOT ORIGINAL
13 SET NOKEY
14 GO TO 480
16 REM FILTER
17 SET NOKEY
18 GO TO 3000
20 REM REPLOT EXPANDED
21 SET NOKEY
22 GO TO 953
24 REM PLOTTER
25 SET NOKEY
26 GO TO 2002
28 REM HIGH SPEED AVERAGE
29 SET NOKEY
30 GO TO 4000
32 REM HIGH SPEED AVERAGE-POINT
33 SET NOKEY
34 GO TO 4010
36 REM ACCESS DISC DATA
37 SET NOKEY
38 GO TO 5000
52 REM TITLE FOR PLOTS
53 SET NOKEY
54 PS=1
```

```
55 RETURN
76 REM REPLOT DISC DATA
77 SET NOKEY
78 GO TO 5105
100 PRINT @3:"STO ";"B"
120 FOR I=1 TO 30
130 NEXT I
140 PRINT @3:"HOL ";"B"
150 PRINT @3:"DPB?"
160 INPUT @3:W
170 W=W-512
180 PRINT @3:"CHL ";"B1"
190 PRINT @3:"SCL?"
200 INPUT @3:S$
210 V=VAL(S$)
220 M=1
230 V=V*10↑(-3*M)
240 GO TO 370
250 POLL M,M3;3
260 IF M3=83 THEN 280
270 GO TO 360
280 PRINT @3:"FPI?"
290 INPUT @3:F
300 IF F>9 THEN 330
310 GOSUB F OF 4,8,12,16,20,24,28,32,36
320 GO TO 350
330 F=F-9
340 GOSUB F OF 40,44,48,52,56,60
350 PRINT @3:"CLI "
360 RETURN
370 W=W*(V/102.3)
380 PRINT @3:"CHL ";"B2"
390 PRINT @3:"SCL?"
400 INPUT @3:S$
410 %=VAL(S$)
```

```
428 M=POS(S$,"S",1)
438 T$=SEG(S$,M-1,1)
448 M=POS("MUNP",T$,1)
458 X=X*10↑(-3*M)
480 E=0
482 O=10*X
484 A=-4*V
486 B=-A
488 F=W(1)
490 D=1
492 Z=512
493 T=1
495 C=W
500 GOSUB 2000
510 RETURN
790 HOME
800 W$="R"
810 PRINT "PLACE ARROW AT LEFT ,PRESS R"
820 POINTER E,F,W$
830 HOME
840 PRINT "JJPLACE ARROW AT RIGHT, PRESS R"
850 POINTER O,P,W$
855 IF O-E<=0 THEN 810
856 O1=O
857 E1=E
870 D=E*51.2/X
880 D=INT(D)
885 D1=D MAX 1
890 Z=O*51.2/X
900 Z=INT(Z)
910 A=W(D1)
915 B=W(D1)
917 Z1=Z MIN 512
920 FOR I=D1+1 TO Z1
930 A=A MIN W(I)
```

```
940 B=B MAX W(I)
945 NEXT I
946 A1=A
947 B1=B
951 T=2
952 GO TO 960
953 E=E1
954 O=O1
955 A=A1
956 B=B1
957 Z=Z1
958 D=D1
960 FOR I=D TO Z
965 C(I)=W(I)
970 NEXT I
980 GOSUB 2000
990 RETURN
2000 G=32
2001 GO TO 2005
2002 G=17
2003 VIEWPORT 25,125,15,85
2004 GO TO 2013
2005 PAGE
2010 VIEWPORT 20,110,15,85
2013 WINDOW E,O,A,B
2014 IF P5=1 THEN 2500
2015 AXIS @G:ABS(O-E)/10,0,E,B
2020 AXIS @G:ABS(O-E)/10,(B-A)/8,E,A
2030 AXIS @G:0,(B-A)/8,O,A
2040 MOVE @G:E,F
2050 FOR I=D TO Z
2060 DRAW @G:X*I/51.2,C(I)
2070 NEXT I
2080 MOVE @G:X*D/51.2,A
2090 PRINT @G:"JJHHHH";
```

```
2100 PRINT @G: USING "E":E
2110 MOVE @G:(O+E)/2,A
2120 PRINT @G:"JJHHHHH";
2130 PRINT @G: USING "E":(O+E)/2
2140 MOVE @G:O,A
2150 PRINT @G:"JJHHHHH";
2160 PRINT @G: USING "E":O
2170 MOVE @G:(O+E)/2,A
2180 PRINT @G:"JJJJHHHHHH";
2190 PRINT @G:"TIME(SECONDS)";
2195 IF G=17 THEN 2400
2200 MOVE E-0.18*ABS(O-E),(B+A)/2
2210 PRINT "KKKKKKKKKK";
2220 PRINT "RHJEHJFHJLHJEHJCHJTHJIHJOHJNHJ";
2230 PRINT "JJCHJOHJEHJFHJFHJIHJCHJIHJEHJNHJTHJ"
2235 IF ABS(A-B)=4 THEN 2300
2240 MOVE @G:E-0.15*ABS(O-E),A-0.015*ABS(A-B)
2250 PRINT @G: USING "-D.4D":A
2260 MOVE @G:E-0.15*ABS(O-E),(A+B)/2-0.015*ABS(A-B)
2270 PRINT @G: USING "-D.4D":(A+B)/2
2280 MOVE @G:E-0.15*ABS(O-E),B-0.015*ABS(A-B)
2290 PRINT @G: USING "-D.4D":B
2295 GO TO 2380
2300 MOVE @G:-0.05*O,-0.05
2302 PRINT @G:"O"
2305 FOR M=1 TO 4
2310 MOVE @G:-0.13*O,M*0.5-0.05
2320 PRINT @G:M*0.5
2330 MOVE @G:-0.13*O,-M*0.5-0.05
2340 PRINT @G:"H";
2350 PRINT @G:-M*0.5
2360 IF M*0.5=>1 THEN 2380
2370 NEXT M
2375 HOME @G:
2380 IF P5=1 THEN 2540
```

```
2385 HOME
2390 RETURN
2400 MOVE @17:E-0.18*ABS(O-E),(B+A)/2
2405 MOVE @17:E-0.18*ABS(O-E),(B+A)/2
2406 PRINT @17,25:90
2410 PRINT @17:"ННННННННННН";
2415 PRINT @17:"REFLECTION COEFFICIENT"
2418 PRINT @17,25:0
2420 GO TO 2235
2500 PRINT "TITLE?"
2510 INPUT H$
2520 P4=INT(LEN(H$)/2+1)
2523 IF G=17 THEN 2530
2525 PAGE
2530 GO TO 2015
2540 MOVE @G:(O+E)/2,B
2550 PRINT @G:"КК";
2560 FOR I=1 TO P4
2570 PRINT @G:"Н";
2580 NEXT I
2585 PRINT " ";
2590 PRINT @G:H$
2600 GO TO 2385
3000 HOME
3005 PRINT "DEG OF FILTERING?"
3010 INPUT S
3015 S=ABS(INT(S))
3017 IF S=0 THEN 3005
3020 IF S>15 THEN 3030
3025 GO TO 3040
3030 S=15
3040 IF S/2=INT(S/2) THEN 3050
3045 GO TO 3090
3050 S=S+1
3060 IF S=>Z-D THEN 3280
```

```
3090 J=1
3095 I=C(D)
3096 U(D)=C(D)
3100 IF S<2*J THEN 3210
3110 IF D+J>Z THEN 3150
3120 U(D)=U(D)+I+C(D+J)
3130 GO TO 3160
3150 C(D)=C(D)+C(Z)+I
3160 J=J+1
3170 GO TO 3100
3210 FOR I=D+1 TO Z
3215 IF I-(S-1)/2-1<D THEN 3240
3220 IF I+(S-1)/2>Z THEN 3250
3230 U(I)=U(I-1)-C(I-(S-1)/2-1)+C(I+(S-1)/2)
3235 GO TO 3260
3240 U(I)=U(I-1)-C(D)+C(I+(S-1)/2)
3245 GO TO 3260
3250 U(I)=U(I-1)-C(I-(S-1)/2-1)+C(Z)
3260 NEXT I
3270 C=U/S
3280 GOSUB 2000
3290 RETURN
4000 Z$=" S"
4003 X2=12
4005 GO TO 4020
4010 Z$=" P"
4015 X2=7
4020 PRINT "# OF AVERAGES (2-";2↑X2;")?";
4030 INPUT N1
4035 FOR I=1 TO 30
4036 PRINT @3:"STO ";"B"
4037 NEXT I
4038 PRINT @3:"HOL ";"B"
4039 PRINT @3:"STO ";"A"
4040 IF N1<1 THEN 4020
```

```
4050 M1=INT(LOG(M1)/LOG(2)) MIN X2
4060 PRINT "JPERFORMING "¡2↑M1¡" AVERAGES"
4070 PRINT @3:"HAV "¡"A/B "¡M1¡Z$
4080 GO TO 150
5000 PRINT "FILE #? "¡
5001 PRINT "FILE #? "¡
5002 G$="@TDRDATA/ARRAY/DF"
5010 INPUT N9
5012 P$=STR(N9)
5014 P$=REP("",1,1)
5016 F$=G$&P$
5045 UNIT 2
5050 OPEN F$;4,"R",W$
5060 READ #4:H
5063 CLOSE 4
5065 PRINT @3:"CHL ";"B1"
5070 PRINT @3:"SCL?"
5075 INPUT @3:S$
5080 V6=VAL(S$)
5090 M=1
5091 PRINT "TIME BETWEEN PTS?"
5092 INPUT T7
5093 PRINT "STARTING PT,ENDING PT?"
5094 INPUT D,Z
5095 D=D+2
5096 Z=Z+2
5097 D6=INT(D/2) MAX 1
5098 Z6=INT(Z/2)
5100 V6=V6*10↑(-3*M)
5105 Q5=V6
5106 D=D6
5107 Z=Z6
5110 FOR I=D TO Z
5120 W(I)=(H(2*I)+H(2*I-1))*Q5
5125 C(I+1-D)=W(I)
```

```
5130 NEXT I
5135 C=C-0.149425
5136 W=0
5137 Z=Z-D+1
5138 D=1
5140 PRINT @3:"CHL ";"B2"
5150 PRINT @3:"SCL?"
5160 INPUT @3:S$
5170 X=VAL(S$)
5180 M=POS(S$,"S",1)
5190 T$=SEG(S$,M-1,1)
5200 M=POS("munp",T$,1)
5210 X=X*10↑(-3*M)
5215 T7=T7*X/2.0E-9
5220 A=C(D)
5230 B=A
5240 FOR I=D+1 TO Z
5250 A=A MIN C(I)
5260 B=B MAX C(I)
5270 NEXT I
5290 E=0
5293 W=C
5295 F=C(D)
5300 O=(Z-1)*T7*2
5305 X=51.2*O/Z
5310 GOSUB 2000
5320 RETURN
9994 F7=0
9995 DIM W(512),C(512),U(512),H(1024)
9996 C=0
9997 U=0
9998 ON SRQ THEN 250
9999 SET KEY
10000 GO TO 9998
```

APPENDIX B

This software, using the sin x/x approach described in the text, Eq. (9), can be used for a discrete Fourier transform of time-domain results. It is essential that the last digitized point of the waveform equal zero or truncation errors will result.

```
1 REM PROGRAM "@DOE/DPO/ARRAYDFT/ANMINF" 9-30-80
2 POLL N,M;3
4 DELETE V,W
5 REM DPO DATA COLLECT
6 GO TO 100
8 REM PLOT DPO DATA
9 GO TO 330
12 REM ARRAY SQUASH
13 GO TO 1000
16 REM PLOT SQUASHED ARRAY
17 GO TO 2000
20 REM DFT ROUTINE
21 GO TO 3000
24 REM ATTEN. PLOT
25 GO TO 3300
28 REM DFT MAGNITUDE PLOT
29 GO TO 4000
44 REM ARRAY VERTICAL SHIFT ROUTINE
45 GO TO 600
48 REM TAPE FILE READING ROUTINE
49 X2=0
50 GO TO 1500
52 REM TAPE FILE WRITING ROUTINE
53 GO TO 6000
100 PAGE
102 GOSUB 9000
104 PRINT "DPO DATA COLLECTION CYCLE"
108 PRINT @3:"STO ";"B"
110 DIM W(512)
120 FOR I=1 TO 30
130 NEXT I
140 PRINT @3:"HOL ";"B"
141 PRINT @3:"STO ";"A"
145 PRINT @3:"HAV ";"A/B ";9;" S"
```

```
150 PRINT @3:"DPB?"
160 INPUT @3:W
170 W=W-512
180 PRINT @3:"CHL ";"B1"
190 PRINT @3:"SCL?"
200 INPUT @3:S$
205 DELETE M,V1,X1
210 V1=VAL(S$)
220 M=1
230 V1=V1*10↑(-3*M)
240 W=W*(V1/102.3)
250 PRINT @3:"CHL ";"B2"
260 PRINT @3:"SCL?"
270 INPUT @3:S$
280 X1=VAL(S$)
290 M=POS(S$,"S",1)
300 T$=SEG(S$,M-1,1)
310 M=POS("mump",T$,1)
320 X1=X1*10↑(-3*M)
321 T=X1*10/512
322 X2=0
323 HOME
325 END
330 V2=65
332 V3=130
334 V4=50
336 V5=80
340 CALL "MIN",W,M1,I1
346 CALL "MAX",W,M2,I1
350 WINDOW 1,512,M1,M2
354 VIEWPORT V2,V3,V4,V5
355 IF X2=1 THEN 370
356 PAGE
357 PRINT "ENTER TEST CONDITIONS; MAX OF ONE LINE:"
358 INPUT A$
```

```
360 PAGE
370 CALL "DISP",W
375 AXIS 512/10,V1
377 IF X2=1 THEN 440
380 HOME
381 GOSUB 9000
382 A$="TEST COND.:"&A$
384 PRINT A$;"J"
390 PRINT "TIME BASE SETTING: ";X1;" s/DIV"
400 PRINT "VERT. SENS. SETTING: ";V1;" RHO/DIV";"J"
430 END
440 RETURN
600 REM ARRAY 'W' SHIFT ROUTINE
602 PAGE
605 GOSUB 9000
610 PRINT "ARRAY 'W' SHIFT PROCEDURE"
620 X2=1
622 V2=5
624 V3=65
626 V4=5
628 V5=35
630 GOSUB 340
640 HOME
650 PRINT "JJ";"PLACE POINTER TO LEFT LOCATION"
652 PRINT "  RETURN A 'Z' IF ZERO LEFT POSITION IS DESIRED, OR"
654 PRINT "  RETURN A 'L' FOR THE LEFT POSITION SELECTED."
660 POINTER X5,Y5,C$
670 IF C$="L" THEN 692
672 IF C$="Z" THEN 690
674 GO TO 650
690 X5=1
692 HOME
694 PRINT "JJJJJJ";
700 PRINT "PLACE POINTER TO THE DESIRED RIGHT POSITION"
710 PRINT "  RETURN A 'R' FOR THE RIGHT POSITION SELECTED, OR"
720 PRINT "  RETURN A 'E' FOR THE MAXIMUM RIGHT POSI
```

```
720 PRINT "  RETURN A 'F' FOR THE MAXIMUM RIGHT POSITION."
725 MOVE 512,0
730 POINTER X6,Y6,D$
740 IF D$="R" THEN 762
742 IF D$="F" THEN 760
744 GO TO 700
760 X6=512
762 S=0
764 X5=INT(X5)
766 X6=INT(X6)
770 FOR I=X5 TO X6
780 S=S+W(I)
790 NEXT I
800 A1=S/(X6-X5)
802 HOME
804 PRINT "JJJJJJJJJJ";
810 PRINT "ENTER VALUE TO WHICH ARRAY 'W' IS TO BE SHIFTED: ";
820 INPUT Y1
830 Y2=Y1-A1
840 W=W+Y2
842 HOME
844 PRINT "JJJJJJJJJJJJ"
850 PRINT "ARRAY 'W' HAS BEEN SHIFTED BY RHO = ";Y2;"."
860 V2=70
862 V3=125
864 V4=5
866 V5=35
870 GOSUB 340
880 HOME
890 PRINT "JJJJJJJJJJJJJJ"
900 PRINT "TIME BASE SETTING: ";X1;" s/DIV"
910 PRINT "VERT. SENS. SETTING: ";V1;" RHO/DIV";"J"
915 X2=0
920 END
999 REM  ARRAY SQUASH SUBROUTINE
```

```
1000 HOME
1001 PRINT "JJJJJJJJJJJJJJJJJJ"
1002 PRINT "REDUCTION FACTOR; 2,4,8,16,32,64? ";
1004 INPUT A9
1005 DELETE V
1008 D9=512/A9
1010 DIM V(D9)
1015 Q2=0
1020 FOR Q1=1 TO 512 STEP A9
1030 Q2=Q2+1
1040 V(Q2)=W(Q1)
1050 NEXT Q1
1052 T1=T*A9
1060 END
1500 REM TAPE READING ROUTINE
1505 PAGE
1510 PRINT "TAPE READING ROUTINE"
1520 PRINT "J";"ENTER TAPE FILE TO BE READ: ";
1530 INPUT F
1540 FIND F
1542 DELETE W,X1,T,V1
1544 DIM W(512)
1546 INPUT @33:T,X1,V1
1550 INPUT @33:W
1560 PRINT "TAPE FILE READING COMPLETE."
1570 END
2000 REM PLOT ARRAY V (SQUASHED ARRAY)
2010 CALL "MAX",W,M2,I1
2020 CALL "MIN",W,M1,I1
2030 WINDOW 1,Q2,M1,M2
2035 VIEWPORT 65,130,10,40
2040 CALL "DISP",V
2050 AXIS (Q2-1)/10,V1
2055 HOME
2056 PRINT
2060 END
```

```
2060 END
2091 WINDOW 1,Q2,M1,M2
3000 REM BEGIN DFT ROUTINE
3002 DELETE X,Y,M,P,R,C,D
3010 PAGE
3012 CALL "TIME",T$
3014 PRINT T$
3016 PRINT A$
3020 W1=D9
3021 F1=1/(2*T1)
3022 PRINT "THE MAXIMUM ANALYSIS FREQUENCY IS ";F1/1000000;" MHz"
3023 PRINT "ENTER THE LOWER CALCULATION FREQUENCY (IN MHz): ";
3024 INPUT F5
3025 F5=F5*1000000
3026 IF F5<0 THEN 3023
3084 PRINT "ENTER THE UPPER CALCULATION FREQUENCY (IN MHz): ";
3086 INPUT F9
3088 F9=F9*1000000
3090 PRINT "ENTER DESIRED FREQ. RESOLUTION (IN MHz): ";
3091 INPUT F2
3092 F2=F2*1000000
3094 R=(F9-F5)/F2
3095 IF R<1 THEN 3023
3100 IF R<>INT(R) THEN 3023
3106 R=R+1
3107 DIM X(W1),Y(W1),M(R),P(R),D(R),C(W1)
3108 R=R-1
3109 PRINT "A SET OF ";R+1;" FREQUENCY POINTS WILL BE CALCULATED";"↵"
3110 REM *** BEGIN CALCULATION***
3120 ON SIZE THEN 3360
3140 PRINT "FREQ.","MAGNITUDE","PHASE,DEG","ATTEN,dB RE M(1)"
3150 PRINT
3155 PRINT @32,26:3
3160 L=0
3165 P9=PI*2*T1
```

```
3170 FOR J=F5 TO F9 STEP F2
3172 S=0
3174 U=0
3180 FOR N=1 TO W1
3190 X(N)=V(N)*COS((N-1)*P9*J)
3200 Y(N)=-V(N)*SIN((N-1)*P9*J)
3250 S=S+X(N)
3260 U=U+Y(N)
3270 NEXT N
3280 L=L+1
3290 M(L)=SQR(S↑2+U↑2)/(2*F1)
3300 P(L)=180/PI*ATN(U/S)
3310 D(L)=20*LGT(M(L)/M(1))
3320 PRINT J/1000000,M(L),P(L),D(L)
3330 IF J=F1 THEN 9999
3340 NEXT J
3342 PRINT @32,26:0
3344 COPY
3346 PRINT "GGGGGG"
3350 END
3360 PRINT J/1000000,"***SIZE ERROR***",N
3370 RETURN
3380 REM BEGIN OF ATTENUATION PLOT; +-45 Db
3385 VIEWPORT 25,120,5,65
3390 WINDOW 1,L,-45,45
3400 PAGE
3410 AXIS 8,5
3420 MOVE 1,D(1)
3430 FOR I=2 TO L
3440 DRAW I,D(I)
3450 NEXT I
3460 HOME
3470 END
4000 REM BEGIN OF MAGNITUDE PLOT
4005 PAGE
```

```
4012 CALL "MAX",M,M3,I1
4013 PRINT " THE MAXIMUM VALUE IS "¡M3¡" AT LOCATION "¡I1¡"⌟"
4020 PRINT "ENTER THE MIN AND MAX AMPLITUDE LIMITS FOR PLOT: ";
4030 INPUT W3,W4
4040 VIEWPORT 25,120,5,65
4050 WINDOW 1,L,W3,W4
4060 AXIS (L-1)/10,W4/10
4070 MOVE 1,M(1)
4080 FOR I=2 TO L
4090 DRAW I,M(I)
4100 NEXT I
4110 HOME
4120 END
6000 PAGE
6001 REM TAPE WRITING ROUTINE
6010 PRINT "TAPE WRITING ROUTINE"
6015 PRINT "⌟";"ENTER TAPE FILE TO BE WRITTEN: ";
6020 INPUT F
6025 FIND F
6030 PRINT @33:T,X1,V1
6035 PRINT @33:W
6040 PRINT "TAPE FILE WRITING COMPLETE"
6045 END
9000 CALL "TIME",B$
9010 PRINT B$
9030 RETURN
9999 END
```

APPENDIX C

This software using a modified sin x/x approach, Eq. (19), results in a discrete Fourier transform of time-domain data. The final point of the digitized waveform need not equal zero but the waveform is required to approach some constant value.

```
1 REM  PROGRAM "@DOE/DPO/ARRAYDFT/BN"  9-30-80
2 REM  BN DIFFERENCE VERSION BY ANDERSON 9-22-90
3 POLL N,M;3
4 DELETE V,W
5 REM DPO DATA COLLECT
6 GO TO 100
8 REM PLOT DPO DATA
9 GO TO 330
12 REM ARRAY SQUASH
13 GO TO 1000
16 REM PLOT SQUASHED ARRAY
17 GO TO 2000
20 REM DFT ROUTINE
21 GO TO 3000
24 REM ATTEN. PLOT
25 GO TO 3380
28 REM DFT MAGNITUDE PLOT
29 GO TO 4000
48 REM TAPE FILE READING ROUTINE
50 GO TO 1500
52 REM TAPE FILE WRITING ROUTINE
53 GO TO 6000
100 PAGE
102 GOSUB 9000
104 PRINT "DPO DATA COLLECTION CYCLE"
108 PRINT @3:"STO ";"B"
110 DIM W(512)
120 FOR I=1 TO 30
130 NEXT I
140 PRINT @3:"HOL ";"B"
141 PRINT @3:"STO ";"A"
145 PRINT @3:"HAV ";"A/B ";8;" S"
150 PRINT @3:"DPB?"
160 INPUT @3:W
```

```
170 W=W-512
180 PRINT @3:"CHL ";"B1"
190 PRINT @3:"SCL?"
200 INPUT @3:S$
205 DELETE M,V1,X1
210 V1=VAL(S$)
220 M=1
230 V1=V1*10↑(-3*M)
240 W=W*(V1/102.3)
250 PRINT @3:"CHL ";"B2"
260 PRINT @3:"SCL?"
270 INPUT @3:S$
280 X1=VAL(S$)
290 M=POS(S$,"S",1)
300 T$=SEG(S$,M-1,1)
310 M=POS("mump",T$,1)
320 X1=X1*10↑(-3*M)
321 T=X1*10/512
323 HOME
325 END
330 V2=65
332 V3=130
334 V4=50
336 V5=80
340 CALL "MIN",W,M1,I1
346 CALL "MAX",W,M2,I1
350 WINDOW 1,512,M1,M2
354 VIEWPORT V2,V3,V4,V5
356 PAGE
357 PRINT "ENTER TEST CONDITIONS; MAX OF ONE LINE:"
358 INPUT A$
360 PAGE
370 CALL "DISP",W
375 AXIS 512/10,V1
380 HOME
381 GOSUB 9000
```

```
381 GOSUB 9000
382 A$="TEST COND.:"&A$
384 PRINT A$;"␣"
390 PRINT "TIME BASE SETTING: ";X1;" s/DIV"
400 PRINT "VERT. SENS. SETTING: ";V1;" RHO/DIV";"␣"
430 END
440 RETURN
999 REM  ARRAY SQUASH SUBROUTNE
1000 HOME
1001 PRINT "␣␣␣␣␣␣␣␣␣␣␣␣␣␣␣␣␣␣␣␣"
1002 PRINT "REDUCTION FACTOR; 1,2,4,8,16,32,64? ";
1004 INPUT A9
1005 DELETE V
1008 D9=512/A9
1010 DIM V(D9)
1015 Q2=1
1016 V(1)=W(1)
1018 A8=1+A9
1020 FOR Q1=A8 TO 512 STEP A9
1030 Q2=Q2+1
1040 V(Q2)=W(Q1)-W(Q1-A9)
1050 NEXT Q1
1052 T1=T*A9
1060 END
1500 PAGE
1505 REM TAPE READING ROUTINE
1510 PRINT "TAPE READING ROUTINE"
1520 PRINT "␣";"ENTER TAPE FILE TO BE READ: ";
1530 INPUT F
1540 FIND F
1542 DELETE W,X1,T,V1
1544 DIM W(512)
1546 INPUT @33:T,X1,V1
1550 INPUT @33:W
1560 PRINT "TAPE FILE READING COMPLETE."
```

```
1570 END
2000 V6=V(1)
2001 REM PLOT ARRAY V (SQUASHED ARRAY)
2006 V(1)=0
2010 CALL "MAX",V,M2,I1
2020 CALL "MIN",V,M1,I1
2030 WINDOW 1,Q2,M1,M2
2035 VIEWPORT 65,130,10,40
2040 CALL "DISP",V
2050 AXIS (Q2-1)/10,V1
2052 V(1)=V6
2055 HOME
2056 PRINT
2060 END
2091 WINDOW 1,Q2,M1,M2
3000 DELETE X,Y,M,P,R,C,D
3001 REM BEGIN DFT ROUTINE
3010 PAGE
3012 CALL "TIME",T$
3014 PRINT T$
3016 PRINT A$
3021 F1=1/(2*T1)
3022 PRINT "THE MAXIMUM ANALYSIS FREQUENCY IS ";F1/1000000;" MHz"
3023 PRINT "ENTER THE LOWEST CALCULATED FREQUENCY (IN MHz): ";
3024 INPUT F5
3025 F5=F5*1000000
3026 IF F5<0 THEN 3023
3084 PRINT "ENTER THE UPPER CALCULATED FREQUENCY (IN MHz): ";
3086 INPUT F9
3088 F9=F9*1000000
3090 PRINT "ENTER DESIRED FREQ. RESOLUTION (IN MHz): ";
3091 INPUT F2
3092 F2=F2*1000000
3094 R=(F9-F5)/F2
3095 IF R<1 THEN 3023
```

```
3100 IF R<>INT(R) THEN 3023
3106 R=R+1
3107 DIM M(R),P(R),D(R)
3108 R=R-1
3109 PRINT "A SET OF ";R+1;" FREQUENCY POINTS WILL BE CALCULATED";"J"
3110 REM *** BEGIN CALCULATION***
3120 ON SIZE THEN 3360
3140 PRINT "FREQ.","MAGNITUDE","PHASE,DEG","ATTEN,dB RE M(1)"
3150 PRINT
3155 PRINT @32,26:3
3160 L=0
3165 P9=PI*2*T1
3170 FOR J=F5 TO F9 STEP F2
3171 IF J>F1 THEN 9999
3172 S=0
3174 U=0
3180 FOR N=1 TO D9
3190 S=S+V(N)*COS((N-1)*P9*J)
3200 U=U+V(N)*SIN((N-1)*P9*J)
3270 NEXT N
3280 L=L+1
3285 H5=COS(P9*J/2)
3286 H6=SIN(P9*J/2)
3290 M(L)=SQR(S↑2+U↑2)/(4*F1*H6)
3300 P(L)=180/PI*ATN((H5*S+H6*U)/(H5*U-H6*S))
3310 D(L)=20*LGT(M(L)/M(1))
3320 PRINT J/1000000,M(L),P(L),D(L)
3340 NEXT J
3342 PRINT @32,26:0
3344 COPY
3346 PRINT "GGGGGG"
3350 END
3360 PRINT J/1000000,"***SIZE ERROR***",N
3370 RETURN
3380 REM BEGIN OF ATTENUATION PLOT; +-45 Db
```

```
3385 VIEWPORT 25,120,5,65
3390 WINDOW 1,L,-45,45
3400 PAGE
3410 AXIS 8,5
3420 MOVE 1,D(1)
3430 FOR I=2 TO L
3440 DRAW I,D(I)
3450 NEXT I
3460 HOME
3470 END
4000 PAGE
4001 REM BEGIN OF MAGNITUDE PLOT
4012 CALL "MAX",M,M3,I1
4013 PRINT " THE MAXIMUM VALUE IS ";M3;" AT LOCATION ";I1;"J"
4020 PRINT "ENTER THE MIN AND MAX AMPLITUDE LIMITS FOR PLOT: ";
4030 INPUT W3,W4
4040 VIEWPORT 25,120,5,65
4050 WINDOW 1,L,W3,W4
4060 AXIS (L-1)/10,W4/10
4070 MOVE 1,M(1)
4080 FOR I=2 TO L
4090 DRAW I,M(I)
4100 NEXT I
4110 HOME
4120 END
6000 PAGE
6001 REM TAPE WRITING ROUTINE
6010 PRINT "TAPE WRITING ROUTINE"
6015 PRINT "J";"ENTER TAPE FILE TO BE WRITTEN: ";
6020 INPUT F
6025 FIND F
6030 PRINT @33:T,X1,V1
6035 PRINT @33:W
6040 PRINT "TAPE FILE WRITING COMPLETE"
6045 END
```

```
6100 DELETE 1,2
6101 DELETE 999
6102 DELETE 1505
6103 DELETE 2001
6104 DELETE 3001
6105 DELETE 3110
6106 DELETE 4001
6107 DELETE 6001
6108 DELETE 5
6109 DELETE 6100,6109
9000 CALL "TIME",B$
9010 PRINT B$
9030 RETURN
9999 END
```

APPENDIX D

This software performs a fast Fourier transform of time domain data. The technique is a modified Eq. (28) Cooley-Tukey technique that can successfully transform waveforms that do not have the same beginning and ending values. The waveform must begin at an amplitude of zero.

```
1 REM  PROGRAM "@DOE/DPO/ARRAYFFT"   9-30-80
2 REM  FFT VERSION BY ANDERSON 9-22-80
3 POLL N,M;3
4 DELETE V,W
5 REM DPO DATA COLLECT
6 GO TO 100
8 REM PLOT DPO DATA
9 GO TO 330
12 REM ARRAY SQUASH
13 GO TO 1000
16 REM PLOT SQUASHED ARRAY
17 GO TO 2000
20 REM DFT ROUTINE
21 GO TO 3000
24 REM ATTEN. PLOT
25 GO TO 3380
28 REM DFT MAGNITUDE PLOT
29 GO TO 4000
48 REM TAPE FILE READING ROUTINE
50 GO TO 1500
52 REM TAPE FILE WRITING ROUTINE
53 GO TO 6000
56 REM DISC INPUT WRITING ROUTINE
57 GO TO 7000
60 REM DISC OUTPUT WRITING ROUTINE
61 OPEN E$;1,"U",F$
62 GO TO 7050
100 PAGE
102 GOSUB 9000
104 PRINT "DPO DATA COLLECTION CYCLE"
108 PRINT @3:"STO ";"B"
110 DIM W(512)
120 FOR I=1 TO 30
130 NEXT I
```

```
140 PRINT @3:"HOL ";"B"
141 PRINT @3:"STO ";"A"
145 PRINT @3:"HAV ";"A/B ";8;" S"
150 PRINT @3:"DPB?"
160 INPUT @3:W
170 W=W-512
180 PRINT @3:"CHL ";"B1"
190 PRINT @3:"SCL?"
200 INPUT @3:S$
205 DELETE M,V1,X1
210 V1=VAL(S$)
220 M=1
230 V1=V1*10↑(-3*M)
240 W=W*(V1/102.3)
250 PRINT @3:"CHL ";"B2"
260 PRINT @3:"SCL?"
270 INPUT @3:S$
280 X1=VAL(S$)
290 M=POS(S$,"S",1)
300 T$=SEG(S$,M-1,1)
310 M=POS("mump",T$,1)
320 X1=X1*10↑(-3*M)
321 T=X1*10/512
323 HOME
325 END
330 V2=65
332 V3=130
334 V4=50
336 V5=80
340 CALL "MIN",W,M1,I1
346 CALL "MAX",W,M2,I1
350 WINDOW 1,512,M1,M2
354 VIEWPORT V2,V3,V4,V5
356 PAGE
357 PRINT "ENTER TEST CONDITIONS; MAX OF ONE LINE:"
```

```
358 INPUT A$
360 PAGE
370 CALL "DISP",W
375 AXIS 512/10,V1
380 HOME
381 GOSUB 9000
382 A$="TEST COND.:"&A$
384 PRINT A$;"␊"
390 PRINT "TIME BASE SETTING: ";X1;" s/DIV"
400 PRINT "VERT. SENS. SETTING: ";V1;" RHO/DIV";"␊"
430 END
440 RETURN
999 REM  ARRAY SQUASH SUBROUTNE
1000 HOME
1001 PRINT "␊␊␊␊␊␊␊␊␊␊␊␊␊␊␊␊␊␊␊␊"
1002 PRINT "REDUCTION FACTOR; 1,2,4,8,16,32? ";
1004 INPUT A9
1005 DELETE V
1008 D9=512/A9
1010 DIM V(D9)
1015 Q2=0
1020 FOR Q1=1 TO 512 STEP A9
1030 Q2=Q2+1
1040 V(Q2)=W(Q1)
1050 NEXT Q1
1052 T1=T*A9
1060 END
1500 PAGE
1505 REM TAPE READING ROUTINE
1510 PRINT "TAPE READING ROUTINE"
1520 PRINT "␊";"ENTER TAPE FILE TO BE READ: ";
1530 INPUT F
1540 FIND F
1542 DELETE W,X1,T,V1
1544 DIM W(512)
```

```
1546 INPUT @33:T,X1,V1
1550 INPUT @33:W
1560 PRINT "TAPE FILE READING COMPLETE."
1570 END
2000 V6=V(1)
2001 REM PLOT ARRAY V (SQUASHED ARRAY)
2006 V(1)=0
2010 CALL "MAX",V,M2,I1
2020 CALL "MIN",V,M1,I1
2030 WINDOW 1,Q2,M1,M2
2035 VIEWPORT 65,130,10,40
2040 CALL "DISP",V
2050 AXIS (Q2-1)/10,V1
2052 V(1)=V6
2055 HOME
2056 PRINT
2060 END
3000 DELETE X,Y,M,P,R,C,D
3001 REM BEGIN FFT ROUTINE
3010 PAGE
3012 CALL "TIME",T$
3014 PRINT T$
3016 PRINT A$
3021 F1=1/(2*T1)
3022 PRINT "THE MAXIMUM ANALYSIS FREQUENCY IS ";F1/1000000;" MHz"
3106 D8=D9/2+1
3107 DIM X(D8),Y(D8),M(D8),P(D8),D(D8)
3109 PRINT "A SET OF ";D9/2;" FREQUENCY POINTS WILL BE CALCULATED";"␣"
3110 REM *** BEGIN CALCULATION***
3111 M=0
3112 P=0
3113 D=0
3115 F9=F1*2/D9
3120 CALL "FFT",V
3130 CALL "UNLEAV",V,X,Y
```

```
3132 PRINT "FREQ.","MAGNITUDE","PHASE,DEG","ATTEN,dB RE M(1)"
3134 PRINT
3135 P9=2*PI/D9
3136 PRINT @32,26:3
3140 FOR K=2 TO D8
3150 X(K)=X(K)+W(512)/2
3155 PRINT @32,26:3
3160 Y(K)=Y(K)-W(512)*SIN(P9*(K-1))/(2-2*COS(P9*(K-1)))
3170 M(K)=SQR(X(K)↑2+Y(K)↑2)/(2*F1)
3180 P(K)=180/PI*ATN(Y(K)/X(K))
3190 D(K)=20*LGT(M(K)/M(2))
3200 PRINT (K-1)*F9/1000000,M(K),P(K),D(K)
3210 NEXT K
3342 PRINT @32,26:0
3344 COPY
3346 PRINT "GGGGGG"
3350 END
3380 REM BEGIN OF ATTENUATION PLOT; +-45 Db
3385 VIEWPORT 25,120,5,65
3390 WINDOW 2,D8,-45,45
3400 PAGE
3410 AXIS 8,5
3420 MOVE 2,D(2)
3430 FOR I=2 TO D8
3440 DRAW I,D(I)
3450 NEXT I
3460 HOME
3470 END
4000 PAGE
4001 REM BEGIN OF MAGNITUDE PLOT
4012 CALL "MAX",M,M3,I1
4013 PRINT " THE MAXIMUM VALUE IS ";M3;" AT LOCATION ";I1;"␣"
4020 PRINT "ENTER THE MIN AND MAX AMPLITUDE LIMITS FOR PLOT: ";
4030 INPUT W3,W4
4040 VIEWPORT 25,120,5,65
```

```
4850 WINDOW 2,D8,W3,W4
4860 AXIS (D8-2)/10,W4/10
4870 MOVE 2,M(2)
4880 FOR I=2 TO D8
4890 DRAW I,M(I)
4100 NEXT I
4110 HOME
4120 END
6000 PAGE
6001 REM TAPE WRITING ROUTINE
6010 PRINT "TAPE WRITING ROUTINE"
6015 PRINT "J";"ENTER TAPE FILE TO BE WRITTEN: ";
6020 INPUT F
6025 FIND F
6030 PRINT @33:T,X1,V1
6035 PRINT @33:W
6040 PRINT "TAPE FILE WRITING COMPLETE"
6045 END
6100 DELETE 1,2
6101 DELETE 999
6102 DELETE 1505
6103 DELETE 2001
6104 DELETE 3001
6105 DELETE 3110
6106 DELETE 4001
6107 DELETE 6001
6108 DELETE 5
6109 DELETE 6100,6109
7000 REM DISC WRITING ROUTINE
7010 PRINT "DISC WRITING ROUTINE"
7015 PRINT "UNIT?"
7016 INPUT Z
7017 CALL "UNIT",Z
7020 PRINT "DISC FILE NAME(e.g. DP0/WAVE1)"
7030 INPUT E$
```

```
7035 CREATE E$;2500,0
7040 OPEN E$;1,"F",F$
7050 WRITE #1:A$,D8,F1,M
7060 CLOSE 1
7070 END
9000 CALL "TIME",B$
9010 PRINT B$
9030 RETURN
9999 END
```

APPENDIX E

Five different sets of data are included. The first two show the results of using the software contained in Appendices B and C on the same data. The results are identical because the waveform ends at zero amplitude.

The other three sets of data illustrate the performance of the different software approaches, Appendices B, C, and D, to the rising step (starting at zero, ending above zero). Only the software contained in Appendices C and D handle the data correctly.

The following three pages demonstrate the results of applying the software contained in Appendix B to a step with endpoint equal to zero.

The first page shows the waveform as acquired from the DPO and a reduced form of the waveform which includes only every fourth data point. The sin x/x software yields the frequency spectrum of the reduced waveform on the second page and a plot of this spectrum is on the third page.

This software correctly transforms waveforms of this type.

31-OCT-80 13:29:49
TEST COND.:AN

TIME BASE SETTING: 2.0E-9 s/DIV
VERT. SENS. SETTING: 0.5 RHO/DIV

REDUCTION FACTOR; 2,4,8,16,32,64? 4

```
31-OCT-80 13:30:10
TEST COND.:AN
THE MAXIMUM ANALYSIS FREQUENCY IS 3200 MHz
ENTER THE LOWER CALCULATION FREQUENCY (IN MHz): 150
ENTER THE UPPER CALCULATION FREQUENCY (IN MHz): 3000
ENTER DESIRED FREQ. RESOLUTION (IN MHz): 150
A SET OF 20 FREQUENCY POINTS WILL BE CALCULATED
```

FREQ.	MAGNITUDE	PHASE,DEG	ATTEN,dB RE M(1)
150	9.403280294E-10	30.8443594468	0
300	8.162139125E-10	63.2153915003	-1.22950777299
450	6.185697282E-10	87.3021506336	-3.63781438515
600	4.116128118E-10	-70.5697571092	-7.17580995417
750	2.714364157E-10	-55.9985017431	-10.7922253979
900	1.748521652E-10	-55.2828537557	-14.612167345
1050	1.472801418E-10	-60.7495231143	-16.1027037638
1200	1.471688233E-10	-62.6495909554	-16.1092712871
1350	1.405788124E-10	-54.6883591389	-16.5071902337
1500	1.326882026E-10	-48.0236269054	-17.0089414108
1650	1.138968307E-10	-39.6893372692	-18.3353548481
1800	1.009091662E-10	-37.5544163954	-19.386975279
1950	1.00036363E-10	-37.1316665676	-19.4624297607
2100	9.936822032E-11	-30.6550098654	-19.5206374018
2250	9.138340855E-11	-26.2726635551	-20.2482405764
2400	8.917032725E-11	-22.2855258176	-20.4611804264
2550	8.808599587E-11	-18.2831081161	-20.5674502619
2700	8.773892032E-11	-13.5219329882	-20.6017419186
2850	8.708184882E-11	-7.56362502862	-20.6670348173
3000	8.311337098E-11	-5.36980499065	-21.0721696931

THE MAXIMUM VALUE IS 9.403280294E-10 AT LOCATION 1

ENTER THE MIN AND MAX AMPLITUDE LIMITS FOR PLOT: 0,9.41E-10

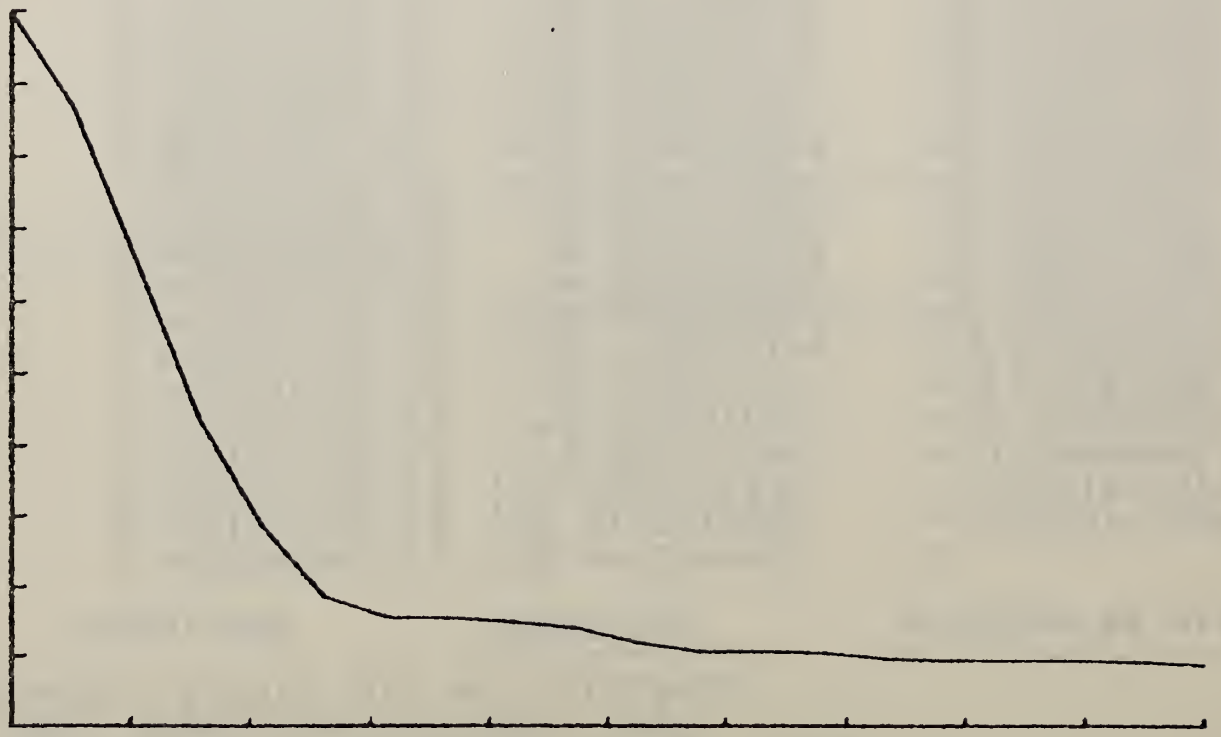

The following three pages demonstrate the results of applying the software contained in Appendix C to a step with endpoint equal to zero.

The first page shows the waveform as acquired from the DPO and a waveform showing the difference between every fourth data point. The modified sin x/x software yields the frequency spectrum of the reduced waveform on the second page and a plot of this spectrum is on the third page.

This software correctly transforms waveforms of this type.

31-OCT-80 13:41:12
TEST COND.:8N

TIME BASE SETTING: 2.0E-9 s/DIV
VERT. SENS. SETTING: 0.5 RHO/DIV

REDUCTION FACTOR; 1,2,4,8,16,32,64? 4

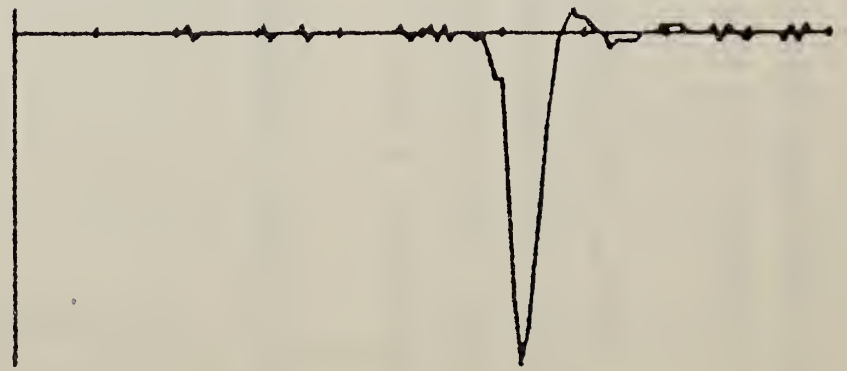

```
31-OCT-80 13:41:49
TEST COND.:BN
THE MAXIMUM ANALYSIS FREQUENCY IS 3200 MHz
ENTER THE LOWEST CALCULATED FREQUENCY (IN MHz): 150
ENTER THE UPPER CALCULATED FREQUENCY (IN MHz): 3000
ENTER DESIRED FREQ. RESOLUTION (IN MHz): 150
A SET OF 20 FREQUENCY POINTS WILL BE CALCULATED
```

FREQ.	MAGNITUDE	PHASE,DEG	ATTEN,dB RE M(1)
150	9.403280294E-10	30.8443594468	0
300	8.162139125E-10	63.2153915003	-1.22950777297
450	6.185697282E-10	87.3021506337	-3.63781438514
600	4.116128118E-10	-70.5697571091	-7.17580995419
750	2.714364157E-10	-55.9985017433	-10.7922253979
900	1.748521652E-10	-55.2828537554	-14.6121673449
1050	1.472801418E-10	-60.7495231138	-16.1027037638
1200	1.471688233E-10	-62.6495909551	-16.1092712872
1350	1.405788124E-10	-54.6883591393	-16.5071902336
1500	1.326882026E-10	-48.023626905	-17.0089414108
1650	1.138968307E-10	-39.6893372695	-18.3353548481
1800	1.009091662E-10	-37.5544163958	-19.386975279
1950	1.00036363E-10	-37.1316665676	-19.4624297606
2100	9.936822032E-11	-30.6550098662	-19.5206374018
2250	9.138340855E-11	-26.2726635553	-20.2482405762
2400	8.917032725E-11	-22.2855258176	-20.4611804264
2550	8.808599587E-11	-18.2831081167	-20.567450262
2700	8.773892032E-11	-13.5219329874	-20.6017419186
2850	8.708184882E-11	-7.56362502853	-20.6670348174
3000	8.311337098E-11	-5.36980498968	-21.072169693

THE MAXIMUM VALUE IS 9.403280294E-10 AT LOCATION 1

ENTER THE MIN AND MAX AMPLITUDE LIMITS FOR PLOT: 0,9.41E-10

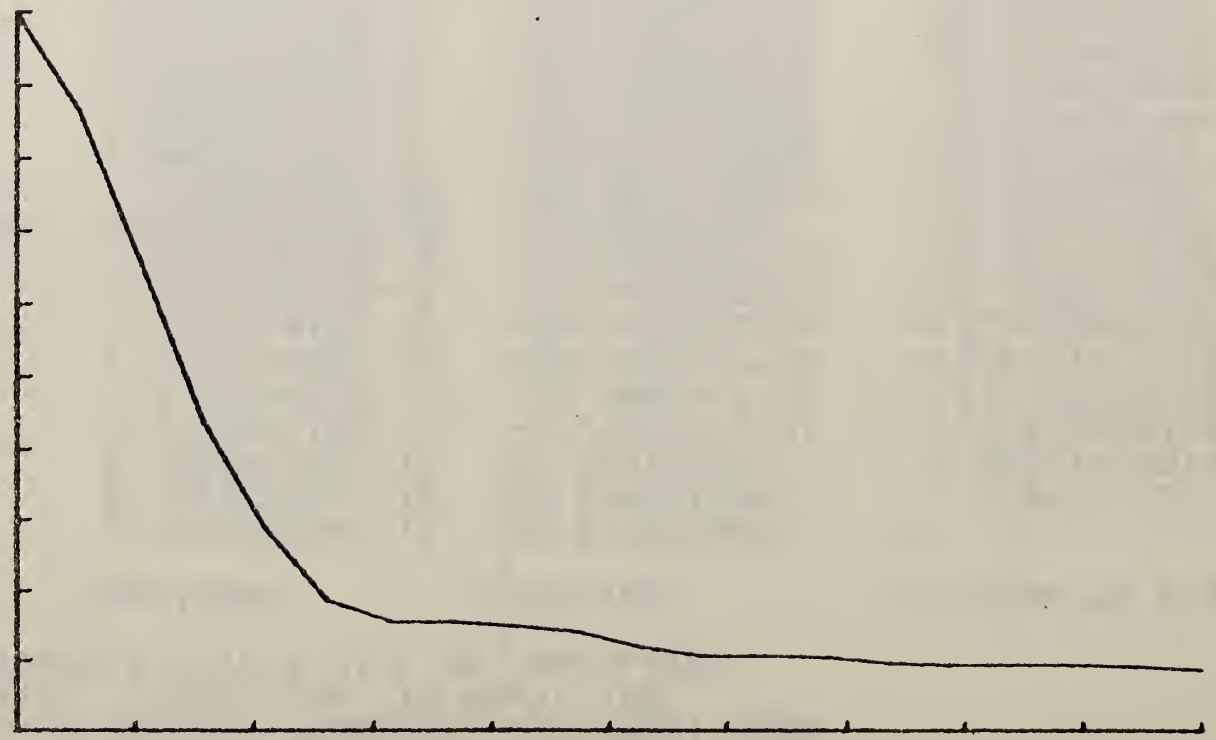

The following ten pages show the results of applying the software contained in Appendix B to a step-like waveform with endpoint not equal to zero.

The waveform, as acquired from the DPO, is on the first page. The transformed spectra is tabulated on the next eight pages and plotted on the last page.

From theoretical considerations in the text and results shown next in this appendix, this software is clearly not applicable to waveforms of this type.

31-OCT-80 15:39:31
TEST COND.:AN

TIME BASE SETTING: 2.0E-10 s/DIV
VERT. SENS. SETTING: 0.5 RHO/DIV

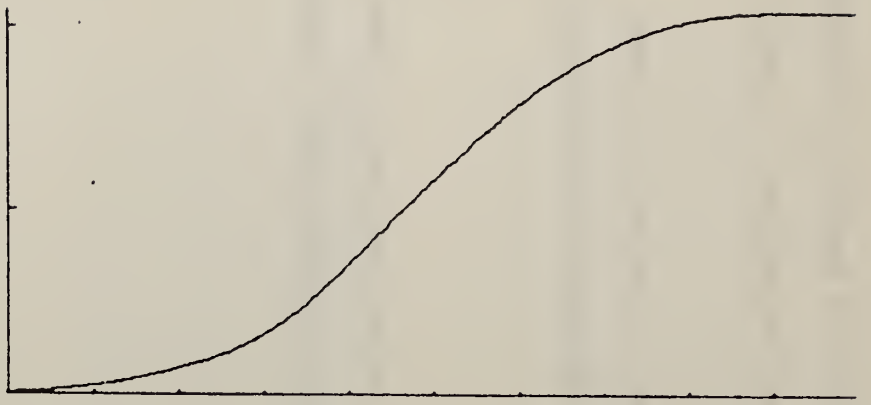

REDUCTION FACTOR; 2,4,8,16,32,64? 1

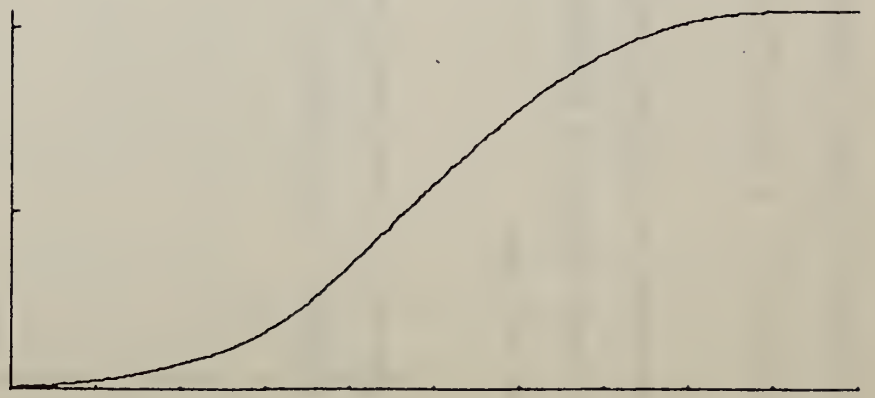

31-OCT-80 15:39:57
TEST COND.:AN
THE MAXIMUM ANALYSIS FREQUENCY IS 128000 MHz
ENTER THE LOWER CALCULATION FREQUENCY (IN MHz): 500
ENTER THE UPPER CALCULATION FREQUENCY (IN MHz): 128000
ENTER DESIRED FREQ. RESOLUTION (IN MHz): 500
A SET OF 256 FREQUENCY POINTS WILL BE CALCULATED

FREQ.	MAGNITUDE	PHASE,DEG	ATTEN,dB RE M(1)
500	5.114020372E-10	-87.2323387024	0
1000	1.559253235E-10	89.2860887371	-10.316916
1500	1.100192419E-10	-86.2001493872	-13.3458761174
2000	8.522098626E-11	-88.3706537006	-15.5643179562
2500	6.570052095E-11	-88.9499228853	-17.8238728121
3000	5 540946577E-11	-87.6353273999	-19.3035698159
3500	4.738809984E-11	-87.4390862808	-20.6618631798
4000	4.165203262E-11	-87.1361148781	-21.782525078
4500	3.692588463E-11	-86.4935354128	-22.8286309053
5000	3.328566432E-11	-86.8509368372	-23.7301044938
5500	3.003099551E-11	-86.0573605755	-24.6238544955
6000	2.773087322E-11	-85.7232102534	-25.3159781695
6500	2.567194502E-11	-85.5456634356	-25.9860735967
7000	2.364064475E-11	-85.1745602517	-26.7020627386
7500	2.22662243E-11	-83.9823986047	-27.2223174809
8000	2.075405319E-11	-84.2019247604	-27.8331905655
8500	1.94960712E-11	-83.233136445	-28.3763070325
9000	1.84214732E-11	-83.5346108238	-28.8687619021
9500	1.751325674E-11	-83.4252738671	-29.3079107883
10000	1.6484308E-11	-82.8450637986	-29.8338346633
10500	1.591948167E-11	-82.1659365175	-30.1366706129
11000	1.510702714E-11	-82.4782992032	-30.5916688853
11500	1.47792016E-11	-80.9256223103	-30.7822304533
12000	1.381455295E-11	-80.9899396811	-31.3685123659
12500	1.334392581E-11	-80.7428608879	-31.6695767012

13000	1.273012832E-11	-79.2807556775	-32.0785934484
13500	1.247399411E-11	-80.9364628037	-32.2551383836
14000	1.206102137E-11	-78.8039786571	-32.5475673395
14500	1.136260992E-11	-80.5800356482	-33.0656871245
15000	1.141019976E-11	-80.2072740414	-33.0293841194
15500	1.080957689E-11	-77.4922007025	-33.4990751749
16000	1.075757717E-11	-78.3651585161	-33.5409596676
16500	9.981262713E-12	-78.4434378915	-34.1915393422
17000	1.006726744E-11	-76.9108537158	-34.1170169533
17500	9.481127398E-12	-77.7974983869	-34.6380494305
18000	9.36329411E-12	-77.1046507041	-34.7466757708
18500	8.992684535E-12	-79.1843638396	-35.097461904
19000	8.853972124E-12	-75.3869759956	-35.2324860694
19500	8.714315926E-12	-76.4648269274	-35.3705830619
20000	8.410785366E-12	-75.1665005813	-35.6785180668
20500	8.199814077E-12	-73.4576659585	-35.8991689696
21000	7.905156523E-12	-76.6141884201	-36.2170396062
21500	7.968156277E-12	-72.9971356854	-36.1480922119
22000	7.745715385E-12	-74.1502864992	-36.3940183783
22500	7.409517834E-12	-74.8100146759	-36.7794501215
23000	7.490668652E-12	-72.5326440812	-36.6848373433
23500	7.20662307E-12	-72.7523892088	-37.0206129229
24000	7.26540764E-12	-73.9738174854	-36.9500493499
24500	6.877243258E-12	-72.1971010473	-37.4269613503
25000	6.87527111E-12	-72.6433253453	-37.4294525115
25500	6.718763136E-12	-72.9485114467	-37.6294624616
26000	6.606857106E-12	-71.4445744797	-37.7753507964
26500	6.316835335E-12	-72.1508862639	-38.1652579547
27000	6.154705032E-12	-70.0976365619	-38.3911041966
27500	6.056808047E-12	-70.8095610178	-38.530372872
28000	6.126156749E-12	-70.3527927163	-38.4314869788
28500	5.968972361E-12	-69.0435158336	-38.6572577161
29000	6.04780512E-12	-69.4738491909	-38.543293309
29500	5.976879759E-12	-67.6960376979	-38.6457586962
30000	5.645433313E-12	-69.6182948505	-39.1413034419

30500	5.644570445E-12	-67.6718733453	-39.1426311266
31000	5.505626207E-12	-70.0914425355	-39.3591146237
31500	5.360873454E-12	-68.6213825813	-39.5905379624
32000	5.265043511E-12	-68.1883119107	-39.7472097837
32500	5.276623027E-12	-66.7503327503	-39.7281277074
33000	5.32022687E-12	-66.4157038758	-39.6566460291
33500	5.116761138E-12	-64.9221363794	-39.9953462032
34000	4.96670833E-12	-64.9609750698	-40.2538759397
34500	5.12243572E-12	-66.4249366388	-39.985718729
35000	4.867008844E-12	-65.1801595289	-40.4300063669
35500	4.9471896E-12	-66.0133083795	-40.2880779774
36000	4.881872936E-12	-65.6370966671	-40.4035196453
36500	4.714263174E-12	-64:5940476157	-40.7069726078
37000	4.523261985E-12	-62.7249237741	-41.0662142232
37500	4.529892458E-12	-66.1936682896	-41.0534912402
38000	4.605280549E-12	-62.9717144064	-40.9101272322
38500	4.562114286E-12	-60.010457695	-40.9919258621
39000	4.589077607E-12	-63.8142924138	-40.940741031
39500	4.269967616E-12	-62.6553007687	-41.5667574489
40000	4.30066351E-12	-60.9763248804	-41.5045397944
40500	4.229976859E-12	-63.9726928124	-41.6484892464
41000	4 230539569E-12	-60.2333153021	-41.6473338458
41500	4.18822375E-12	-60.4822809781	-41.7346515712
42000	4.219347141E-12	-60.6393320442	-41.6703439175
42500	4.131601709E-12	-58.2066310817	-41.8528801077
43000	4.112805129E-12	-59.70173459	-41.8924864261
43500	3.954997549E-12	-61.4340820915	-42.2323247004
44000	4.034731709E-12	-58.8937504024	-42.0589558466
44500	3.838041916E-12	-59.1525136165	-42.4930548073
45000	3.899732277E-12	-56.6638003208	-42.3545532158
45500	3.800137859E-12	-58.9446806095	-42.5792620353
46000	3.840577945E-12	-57.8892168072	-42.4873174025
46500	3.774722479E-12	-57 2751772474	-42.6375485269
47000	3.886008271E-12	-57.1255749941	-42.3851746621
47500	3.70690156E-12	-55.382492263	-42.7950280131

48000	3.583120765E-12	-56.9235531244	-43.0900201596
48500	3.492929899E-12	-52.7818897255	-43.3114516825
49000	3.591425504E-12	-58.1520866803	-43.0699118259
49500	3.688060085E-12	-54.8184431317	-42.8392893172
50000	3.712731752E-12	-53.1910046048	-42.7813776303
50500	3.514297146E-12	-54.6976620561	-43.2584794791
51000	3.466404531E-12	-54.6302543956	-43.3776642005
51500	3.37094154E-12	-56.7319368093	-43.6202246583
52000	3.32464899E-12	-51.7350566066	-43.7403330727
52500	3.354219171E-12	-51.9687518075	-43.6634203395
53000	3.526770335E-12	-49.8872779864	-43.2277054922
53500	3.279945708E-12	-53.4058042794	-43.857915976 1
54000	3.400112711E-12	-53.2795315907	-43.5453827987
54500	3.096520926E-12	-50.6059131579	-44.3577686887
55000	3.303416426E-12	-52.1936585659	-43.7959825961
55500	3.27028408E-12	-46.5591524061	-43.8835394725
56000	3.328626153E-12	-50.0089702067	-43.7299486528
56500	3.226986159E-12	-51.2423032325	-43.9993070233
57000	3.261795574E-12	-49.8019368069	-43.9061142933
57500	3.063314929E-12	-49.5263144575	-44.4514161269
58000	3.171250636E-12	-48.4246719365	-44.1506377281
58500	2.976600571E-12	-49.5589769526	-44.7008378592
59000	3.158630321E-12	-49.7400085425	-44.185273076
59500	3.020910326E-12	-47.1161851006	-44.5724924003
60000	3.099064002E-12	-48.4574173084	-44.3506381663
60500	3.060662405E-12	-43.9741605433	-44.4589404939
61000	2.853491395E-12	-46.2378506869	-45.06771773
61500	2.923775705E-12	-44.0810797363	-44.8563680141
62000	3.175699844E-12	-46.7746267769	-44.1384601199
62500	3.075411399E-12	-48.8992971619	-44.4171846804
63000	2.85212391E-12	-43.9028769813	-45.0718812862
63500	2.768067465E-12	-46.1746755637	-45.3317156599
64000	2.877089754E-12	-43.1177175569	-44.9961808662
64500	3.031227236E-12	-44.4098581392	-44.542879185
65000	2.844770261E-12	-42.7957536996	-45.0943050894

65500	2.781360643E-12	-41.6408720295	-45.2901029745
66000	2.756613374E-12	-42.9360234697	-45.3677318988
66500	3.047907799E-12	-43.1620907496	-44.49521257
67000	2.809319429E-12	-43.6297627739	-45.2032266214
67500	2.861017531E-12	-41.9530719631	-45.0448386962
68000	2.509549141E-12	-42.6131251218	-46.1833349907
68500	2.892133536E-12	-41.5984338155	-44.9508822486
69000	2.806833041E-12	-39.2271456864	-45.2109174688
69500	2.803452278E-12	-42.4632135199	-45.22138572
70000	2.650183207E-12	-40.388185318	-45.7097311197
70500	2.601599755E-12	-40.2131207403	-45.8704394149
71000	2.742969488E-12	-39.8292852498	-45.4108295409
71500	2.637348236E-12	-37.9155093719	-45.7518995181
72000	2.679163055E-12	-38.6892408196	-45.6152661592
72500	2.678963557E-12	-42.7010168277	-45.6159129598
73000	2.589794834E-12	-36.1023026927	-45.9099418706
73500	2.612459698E-12	-35.3505424528	-45.8342570866
74000	2.651295569E-12	-38.4117738111	-45.7060861559
74500	2.656400625E-12	-35.0637590782	-45.6893775992
75000	2.529616829E-12	-38.2085388103	-46.1141542385
75500	2.612517986E-12	-37.0212360097	-45.8340632926
76000	2.635485915E-12	-33.8521487375	-45.7580350846
76500	2.563605864E-12	-37.9613584474	-45.9982239494
77000	2.60671931E-12	-36.9043060399	-45.8533636929
77500	2.538843902E-12	-35.9148000132	-46.0825290842
78000	2.556876024E-12	-35.0388722835	-46.0210556613
78500	2.483663739E-12	-34.5148418608	-46.2733931393
79000	2.504042723E-12	-34.4214246676	-46.2024143873
79500	2.300512696E-12	-34.7759198786	-46.9387563879
80000	2.572615487E-12	-33.2042368585	-45.9677514793
80500	2.534465912E-12	-34.4412134038	-46.0975199874
81000	2.302016305E-12	-32.9949628591	-46.9330811667
81500	2.524407267E-12	-29.7462619181	-46.1320606425
82000	2.474616676E-12	-32.5521284016	-46.3050903715
82500	2.402118681E-12	-32.6481952811	-46.5633598601

83000	2.457769592E-12	-29.7265507238	-46.3644257402
83500	2.286929894E-12	-30.7762928077	-46.9901920461
84000	2.570964051E-12	-32.8918297773	-45.9733289935
84500	2.500733778E-12	-28.8835520749	-46.2138998686
85000	2.285083205E-12	-30.5679768016	-46.9972087072
85500	2.243963281E-12	-29.9828546352	-47.1549341541
86000	2.483738859E-12	-31.9641371102	-46.2731304356
86500	2.380757379E-12	-25.8488508477	-46.6409462934
87000	2.42399684E-12	-32.2601793634	-46.4846080876
87500	2.316492448E-12	-24.986782226	-46.8786313021
88000	2.439389466E-12	-28.2762011855	-46.4296261938
88500	2.164402758E-12	-30.024172212	-47.4684875017
89000	2.34597689E-12	-28.0045259685	-46.7687744838
89500	2.265444454E-12	-30.0787814192	-47.0721807107
90000	2.383073368E-12	-24.8809399132	-46.6325008111
90500	2.311574061E-12	-26.1089675055	-46.8970928277
91000	2.252179371E-12	-24.8772480855	-47.1231895517
91500	2.135192242E-12	-29.7270561248	-47.5865094204
92000	2.320790707E-12	-23.6517386598	-46.8625295382
92500	2.286575159E-12	-21.6235289208	-46.9915394555
93000	2.098805221E-12	-23.8490125325	-47.7358063588
93500	2.36862663E-12	-23.4142166886	-46.6853169213
94000	2.391401091E-12	-23.0455257246	-46.6022006157
94500	2.223813008E-12	-25.2744326897	-47.2332837488
95000	2.397174166E-12	-24.3246047852	-46.5812573018
95500	2.040192332E-12	-23.0317248184	-47.9818268581
96000	2.283463398E-12	-23.675970834	-47.0033679826
96500	2.25257483E-12	-20.6920335555	-47.1216645351
97000	2.186576673E-12	-21.5791570069	-47.3799548622
97500	2.166865035E-12	-25.3941970566	-47.458611841
98000	2.191688727E-12	-17.1894664445	-47.3596715999
98500	2.249403348E-12	-24.0325872368	-47.1339023301
99000	2.242403169E-12	-20.0446638171	-47.1609751053
99500	2.012830993E-12	-20.5930834091	-48.0991028575
100000	2.183667216E-12	-20.4596187129	-47.391519997

100500	2.156725241E-12	-18.9159597746	-47.499352654
101000	2.161920374E-12	-15.1809807174	-47.4784551862
101500	2.077326309E-12	-17.8084761467	-47.8251546457
102000	2.265063988E-12	-18.0181473567	-47.0736395692
102500	2.166910037E-12	-15.9870688175	-47.4584314486
103000	2.13258774E-12	-20.7350356695	-47.5971109105
103500	2.228944818E-12	-15.0365940074	-47.2132627408
104000	2.116961696E-12	-16.5275883107	-47.6609890732
104500	2.246089081E-12	-17.4978761308	-47.1467095439
105000	2.056190734E-12	-14.7062684352	-47.9139811209
105500	2.284260574E-12	-16.6460172626	-47.000336194
106000	1.952897897E-12	-15.9477995084	-48.3616583195
106500	2.175976939E-12	-15.950529947	-47.4221633056
107000	2.131092612E-12	-12.6318288736	-47.6032026049
107500	2.104804839E-12	-16.1989289638	-47.7110124039
108000	2.054871341E-12	-17.0003213219	-47.9195563735
108500	2.311848134E-12	-10.7113590604	-46.89606304
109000	1.998179261E-12	-12.0298169971	-48.1625601332
109500	1.974567529E-12	-12.6920165039	-48.2658092551
110000	2.05468625E-12	-16.5122490677	-47.9203387803
110500	2.324711569E-12	-6.60669033039	-46.8478675361
111000	1.947223031E-12	-14.2497861046	-48.3869351209
111500	2.142882168E-12	-10.3715751615	-47.5552832578
112000	2.098951958E-12	-12.8277301226	-47.735199107
112500	1.972352898E-12	-8.37609862052	-48.2755566221
113000	2.173829285E-12	-6.08350975781	-47.4307403711
113500	2.231544474E-12	-10.3566087516	-47.2031381416
114000	2.131120652E-12	-11.5850997822	-47.6030883196
114500	1.969896797E-12	-5.45692385916	-48.2863795921
115000	2.371247915E-12	-13.3364460116	-46.6757098353
115500	1.894401224E-12	-10.6488912788	-48.6258097608
116000	2.094400103E-12	-2.96605284654	-47.7540560624
116500	2.135755322E-12	-10.325429445	-47.5842191319
117000	2.117287642E-12	-10.9563760363	-47.6596518214
117500	2.031893693E-12	-9.67216261854	-48.0172294305

118000	2.05447613E-12	-2.32632859909	-47.9212270796
118500	2.043353314E-12	-8.07225328002	-47.9683797464
119000	2.047131399E-12	-5.70457043996	-47.9523346819
119500	1.970481084E-12	-4.01975807837	-48.2838036727
120000	2.05417178E-12	-3.12334217924	-47.9225139017
120500	2.088659143E-12	-7.03026527176	-47.7778976483
121000	2.200165264E-12	-2.92341764337	-47.3261429988
121500	2.139396559E-12	-2,93184233115	-47.5694232157
122000	2.084947039E-12	-2.78147633007	-47.7933485218
122500	1.98786092E-12	-7.74864732169	-48.2075291561
123000	2.118614273E-12	-2.03031451905	-47.6542112012
123500	2.049184525E-12	-0.258181804145	-47.9436277235
124000	2.211677738E-12	-4.85085066966	-47.2808121466
124500	2.086800567E-12	-4.12903334876	-47.7856301543
125000	1.867820276E-12	0.488034726311	-48.7485473631
125500	2.263805912E-12	-4.04324907955	-47.0784652794
126000	2.120928079E-12	-0.193637303132	-47.6447302382
126500	1.962386066E-12	-3.27526943207	-48.3195600449
127000	2.144370647E-12	-2.12808258099	-47.5492519984
127500	1.93806288E-12	1.56676474759	-48.4278918034
128000	2.11922654E-12	3.115921935E-9	-47.6517013932

THE MAXIMUM VALUE IS 5.114020372E-10 AT LOCATION 1

ENTER THE MIN AND MAX AMPLITUDE LIMITS FOR PLOT: 0,5.12E-10

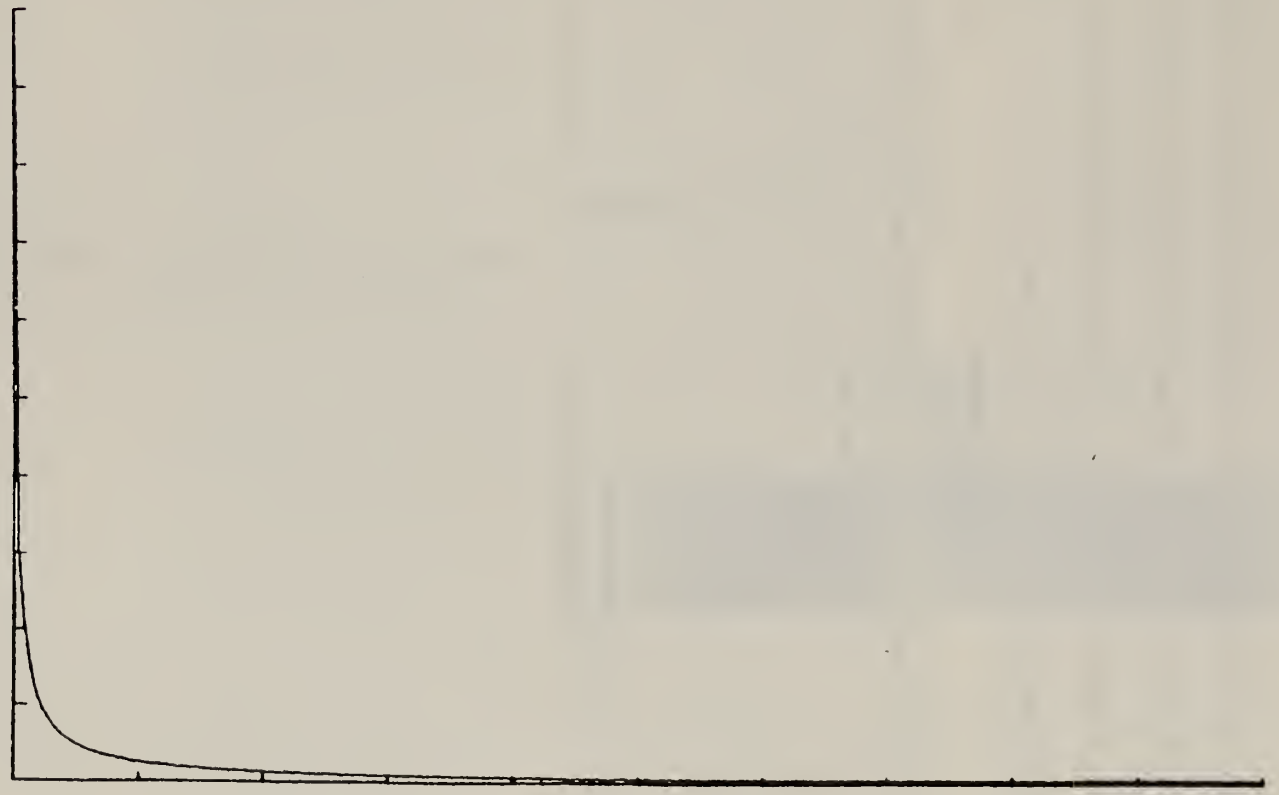

The following ten pages show the results of applying the software contained in Appendix C to a step-like waveform with endpoint not equal to zero.

The first page shows the waveform as acquired from the DPO and the difference waveform obtained by subtracting successive points of the original waveform. The frequency spectrum of this difference waveform is tabulated on the next eight pages and plotted on the last.

This software correctly transforms waveforms of this type.

31-OCT-80 14:45:36
TEST COND.:BN

TIME BASE SETTING: 2.0E-10 s/DIV
VERT. SENS. SETTING: 0.5 RHO/DIV

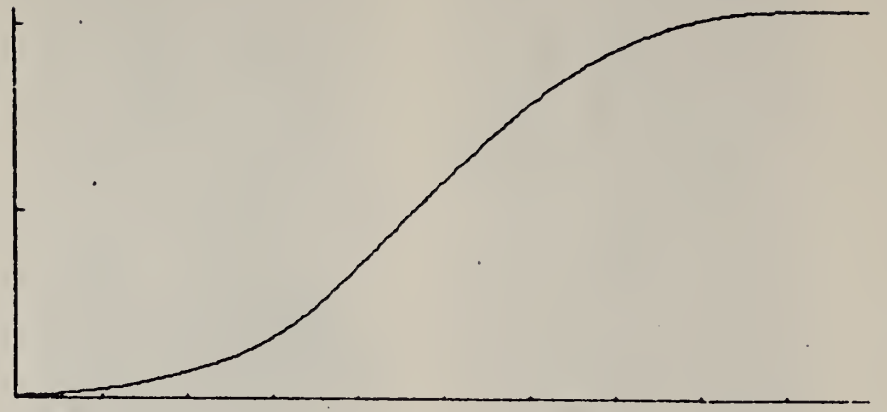

REDUCTION FACTOR: 1,2,4,8,16,32,64? 1

31-OCT-80 14:46:51
TEST COND.:8N
THE MAXIMUM ANALYSIS FREQUENCY IS 128000 MHz
ENTER THE LOWEST CALCULATED FREQUENCY (IN MHz): 500
ENTER THE UPPER CALCULATED FREQUENCY (IN MHz): 128000
ENTER DESIRED FREQ. RESOLUTION (IN MHz): 500
A SET OF 256 FREQUENCY POINTS WILL BE CALCULATED

FREQ.	MAGNITUDE	PHASE,DEG	ATTEN,dB RE M(1)
500	1.777675774E-10	-82.6827138426	0
1000	1.200745944E-11	-70.5656567653	-23.4080285079
1500	5.509697494E-12	18.0443589165	-30.1744959788
2000	1.623746855E-12	-76.8016865012	-40.7866846165
2500	1.459402321E-12	-54.457605419	-41.7135504268
3000	4.299446126E-13	57.0628864097	-52.3288008475
3500	4.191703057E-13	81.0837993027	-52.5492408894
4000	1.799329379E-13	80.8303963122	-59.8948376565
4500	3.404198217E-13	52.7559887162	-54.3567542782
5000	2.820875703E-13	-37.4669059483	-55.9893720725
5500	4.022486492E-13	88.2250005901	-52.9071591881
6000	1.708243245E-13	84.753843927	-60.3460568363
6500	9.996956749E-14	-54.1108794184	-64.999694813
7000	2.837353912E-13	-77.0166358169	-55.9387808741
7500	2.967338282E-13	18.2222803998	-55.5497098872
8000	1.95597194E-13	76.9307667942	-59.1697986717
8500	3.457849746E-13	44.9285342561	-54.2209287169
9000	2.040142995E-13	83.8351085523	-58.8038389084
9500	1.353033167E-13	-69.6037901314	-62.3708822218
10000	2.845094866E-13	89.8461341333	-55.9151160359
10500	1.362222416E-13	30.3996338071	-62.3120906284
11000	1.54007154E-13	-60.9129747413	-61.2462331678
11500	3.153391184E-13	-27.9645581209	-55.0214940943
12000	2.21887842E-13	59.9642316006	-58.0743809468
12500	1.40558542E-13	47.9331576315	-62.0399062034

13000	4.009892699E-13	38.1452407292	-52.9343960471
13500	9.751224304E-14	26.3506612231	-65.2158681468
14000	2.894565499E-13	-0.630967271017	-55.7653834493
14500	2.797094438E-13	-46.4577239989	-56.0629084824
15000	2.471858348E-13	63.1333387143	-57.1365794858
15500	3.076804463E-13	20.2553932868	-55.2350531386
16000	2 478254761E-13	-61.7987641913	-57.1141320924
16500	2.245300671E-13	-76.3975830173	-57.9715609531
17000	2.530944781E-13	-25.990727531	-56.9313976746
17500	1.505521306E-13	-71.2464797655	-61.4433129576
18000	3.929493997E-14	18.7408877124	-73.1103184834
18500	3.685445692E-13	-8.02841402707	-53.667250759
19000	1.961421231E-13	22.3876295737	-59.1456336372
19500	6.133657117E-14	77.872539409	-69.2426611877
20000	1.190002001E-13	32.0621572052	-63.4860972399
20500	3.087273971E-13	23.8898516093	-55.2055476499
21000	2.42367143E-13	-23.4764209986	-57.3075762072
21500	2.785411425E-13	-4.6093304504	-56.0992640225
22000	7 203064344E-14	-28.8886263349	-67.8467051909
22500	1.445176914E-13	-39.8446044268	-61.7986307673
23000	2.07431427E-13	-19.099408768	-58.6595599755
23500	9.167222949E-14	23.019915878	-65.7522952043
24000	2.221150016E-13	77.8905960277	-58.0654932438
24500	8.737123487E-14	54.8765293597	-66.1696815986
25000	8.364677167E-14	89.0552948423	-66.5480673944
25500	1.14945586E-13	44.3078760502	-63.7872051003
26000	7.12315647E-14	-45.3695792981	-67.9436013901
26500	1.379286939E-13	-32.5815156148	-62.2039586028
27000	1.838339555E-13	76.5464132087	-59.7085364398
27500	1.426687667E-13	-64.4750995596	-61.910472936
28000	3.421650418E-14	-77.5457452779	-74.3123383449
28500	9.793850516E-14	32.6619875542	-65.1779816552
29000	1.578120686E-13	-64.4085080529	-61.034246825
29500	2.424593716E-13	-27.0471781238	-57.3042715731
30000	9.089241778E-14	-18.384298255	-65.8264979562

30500	9.209643178E-14	2.23487928	-65.7121949954
31000	1.830950611E-13	14.0362013214	-59.7435184848
31500	1.103072332E-13	-27.0865836853	-64.144971247
32000	1.170810072E-13	-34.8016323533	-63.6273220767
32500	3.763665013E-14	35.9128972155	-73.4848318389
33000	1.163695157E-13	-49.089957138	-63.6802665365
33500	1.376039217E-13	32.2833682876	-62.2244348454
34000	1.39370043E-13	69.115654807	-62.1136623939
34500	1.404400005E-13	88.4964262934	-62.0472346306
35000	6.414038454E-14	-81.5752043077	-68.8544198902
35500	1.181446248E-13	69.5644524334	-63.5487717294
36000	1.143973843E-13	70.3016744918	-63.8287291854
36500	3.259058795E-14	-23.6711596646	-74.7352071676
37000	1.85917355E-13	83.6882687246	-59.6106524319
37500	2.239645251E-13	1.01657682141	-57.9934664037
38000	4.742302805E-14	-31.6379491299	-71.4772654548
38500	2.368974502E-13	15.8133981313	-57.5058433502
39000	1.645863491E-13	80.4427908717	-60.6691748431
39500	1.384130229E-13	-48.8799648391	-62.1735120013
40000	8.62452413E-14	66.671694291	-66.282348244
40500	1.970486157E-13	5.02089800445	-59.1055833111
41000	7.419306087E-14	49.7590639963	-67.5897853065
41500	3.273770596E-14	70.1745550112	-74.696086203
42000	5.678403165E-14	-73.2495898545	-69.9125265955
42500	1.380997314E-13	25.7740615948	-62.1931943969
43000	3.712343013E-14	-52.6692503725	-73.6040891289
43500	1.612491267E-13	0.41768592282l	-60.8471036525
44000	4.413791224E-14	-43.4440877672	-72.1008153394
44500	1.176754895E-13	-44.1527212784	-63.5833308057
45000	1.162811874E-13	38.7414043537	-63.6868619185
45500	9.683074666E-14	-18.0901594405	-65.2767854626
46000	1.618648078E-14	47.6020813935	-80.8140023559
46500	2.48958344E-14	-61.7836110006	-77.0745173476
47000	1.229136662E-13	-62.4135152949	-63.205047619
47500	8.200540806E-14	49.3060238202	-66.7202011957

48000	1.190566251E-13	-35.5306184195	-63.4819797275
48500	2.568330305E-13	76.4217363297	-56.8040335523
49000	1.681117478E-13	20.6317861594	-60.4850898068
49500	9.533463702E-14	-40.453971633	-65.4120367289
50000	1.817042465E-13	-18.7349425258	-59.8097495368
50500	2.3129343E-14	-21.474969067	-77.7137851452
51000	4.765249773E-14	-15.7052383363	-71.4353376894
51500	2.038303613E-13	4.32095397807	-58.8116735904
52000	1.571167783E-13	87.6118593422	-61.0725997727
52500	9.121113254E-14	81.1067634887	-65.796094111
53000	2.198712112E-13	0.0843346470123	-58.1536837004
53500	1.016304213E-13	-17.1994617635	-64.8565765601
54000	9.744693436E-14	78.4941960233	-65.2216874574
54500	2.217728605E-13	-66.8480296294	-58.0788831128
55000	5.320400888E-14	58.9674808043	-70.4781639312
55500	2.518854516E-13	38.8156849694	-56.9729893922
56000	9.984446761E-14	-29.6208179487	-65.0105709648
56500	5.665644304E-14	55.3414543484	-69.932064966
57000	7.430608175E-14	-44.6495443341	-67.5765638551
57500	1.014911964E-13	-50.8984268114	-64.8684836311
58000	5.251228132E-14	7.60004527774	-70.5918333573
58500	1.481143695E-13	-34.8247228442	-61.5851071935
59000	9.000649479E-14	82.9051418878	-65.911574099
59500	7.913788926E-14	87.5612546605	-67.0293618224
60000	5.512824095E-14	-87.0654264954	-70.1695683738
60500	1.871430608E-13	36.6158631659	-59.5535765107
61000	1.681141103E-13	-62.0711171316	-60.4849677429
61500	1.559095546E-13	72.1045987733	-61.1395964606
62000	2.001974649E-13	-52.2598885348	-58.9678796002
62500	1.905873451E-13	80.7375637071	-59.3951698695
63000	1.256618338E-13	88.8155042851	-63.0129832101
63500	1.578224452E-13	-30.7580981318	-61.0336757194
64000	9.828275961E-14	60.9453959282	-65.1475042319
64500	1.468537499E-13	-39.7178209285	-61.6593502635
65000	7.82221789E-14	63.3939644497	-67.1304528927

65500	1.327066162E-13	78.6247324309	-62.5391995638
66000	8.363113591E-14	-65.8267381536	-66.5496911647
66500	2.30505071E-13	-42.183029311	-57.7434413931
67000	3.706155691E-14	59.193613062	-73.6185778861
67500	8.084665226E-14	-21.3205834552	-66.8438102542
68000	2.611451365E-13	-38.0938889846	-56.6594122365
68500	1.379395025E-13	-36.8499973687	-62.2032779713
69000	1.282234027E-13	18.0760793702	-62.8377051247
69500	1.013885531E-13	-81.0728380597	-64.8772725675
70000	6.304372608E-14	-57.5425169595	-69.0042136085
70500	9.519405127E-14	-46.3588978383	-65.4248548781
71000	6.180785755E-14	-28.9653633117	-69.1761772789
71500	8.947507539E-14	71.5972329479	-65.9630096161
72000	3.998767897E-14	13.935395061	-72.958527139
72500	1.747188183E-13	61.4035744038	-60.1502574018
73000	1.233383549E-13	71.0454011698	-63.1750880467
73500	1.3553277E-13	54.663052066	-62.35616479
74000	5.199875023E-14	-61.1875973265	-70.6771929625
74500	1.339251627E-13	24.4707485349	-62.4598074255
75000	6.479293375E-14	2.71106662401	-68.7664981813
75500	4.578507129E-14	-43.0411018106	-71.7825731805
76000	1.46638963E-13	21.6349864322	-61.6720634604
76500	8.050414048E-14	67.2042515964	-66.8806867255
77000	8.785500334E-14	-68.6171765287	-66.121721084
77500	2.513710231E-14	-81.3499786873	-76.9907468223
78000	4.683887889E-14	-28.735319826	-71.5849212474
78500	2.02956674E-14	-73.0521067343	-78.8489843344
79000	1.510442704E-14	-29.1903802422	-81.414965964
79500	1.803052294E-13	-25.4649727465	-59.8768846209
80000	1.069388285E-13	-20.5031338699	-64.414342634
80500	8.862245169E-14	-64.7615271048	-66.0461758688
81000	1.465124775E-13	-33.8625503296	-61.679558829
81500	1.53724311E-13	24.9616125391	-61.262199971
82000	4.618414254E-14	-43.580857995	-71.7071933785
82500	3.2859989!9E-14	24.8281353546	-74.6637027519

83000	9.392962731E-14	29.2820701453	-65.5409990926
83500	1.166848784E-13	-41.3910601692	-63.6567595202
84000	1.971960947E-13	-57.3365093809	-59.0990848773
84500	1.373440716E-13	2.16000043293	-62.2408527128
85000	9.147062515E-14	-21.8708434321	-65.771418131
85500	1.232242601E-13	-28.0606988104	-63.1831266969
86000	1.617381924E-13	-70.2141226353	-60.8207993743
86500	1.407498675E-13	50.1698512793	-62.0280911851
87000	1.642335524E-13	89.095575298	-60.687813337
87500	1.428217725E-13	70.6693068091	-61.9011627029
88000	1.123690171E-13	-31.4091811443	-63.9841194332
88500	1.784453717E-13	0.67360401215	-59.9669453128
89000	4.12496632E-14	-62.75560128	-72.6886429384
89500	1.26295645E-13	43.222917303	-62.9692835714
90000	1.13638521E-13	15.544326984	-63.8865396208
90500	2.329411773E-14	0.19867617937	-77.6521257543
91000	5.505484665E-14	-80.3784129335	-70.18113993
91500	2.110879042E-13	20.1180480247	-58.5077841151
92000	8.347057988E-14	28.3749180455	-66.5663824645
92500	1.344413638E-13	56.983802476	-62.4263928868
93000	1.612561981E-13	-34.5553409398	-60.8467227477
93500	1.222794589E-13	-7.68741411893	-63.2499809136
94000	1.504786319E-13	-10.0947942452	-61.4475543929
94500	6.866321977E-14	52.8461425704	-68.2625677848
95000	1.702814258E-13	-39.1968965153	-60.373705519
95500	1.871364421E-13	-20.8870215091	-59.5538837129
96000	7.730167426E-14	-59.8185258071	-67.23327307
96500	6.759330483E-14	35.739381897	-68.3989774593
97000	2.528039051E-14	-40.9845541691	-76.9413755123
97500	1.553926491E-13	52.357069074	-61.1684416644
98000	1.498148925E-13	73.9628885989	-61.4859513384
98500	1.38831544E-13	-89.1715023849	-62.1472880035
99000	5.446510549E-14	-5.99606650618	-70.2746840942
99500	1.730266365E-13	-13.5805300987	-60.2347917666
100000	2.965063636E-14	77.3659887427	-75.5563707029

100500	2.42784101E-14	-59.9635383385	-77.292646214
101000	1.440223364E-13	76.3152315222	-61.8284540339
101500	9.371206855E-14	-37.2301821109	-65.5611405893
102000	1.040623538E-13	-12.5448914093	-64.6511781783
102500	7.394511958E-14	65.4712636814	-67.6188607644
103000	1.197870138E-13	61.0683185536	-63.428856309
103500	1.158451561E-13	30.1011939321	-63.7194934918
104000	3.065102122E-14	-41.6326638809	-75.268152102
104500	1.11687089E-13	-36.5226327344	-64.0369916417
105000	9.694851127E-14	-49.023299582	-65.2662281869
105500	1.543670332E-13	-28.1328795758	-61.2259599276
106000	1.774676523E-13	-10.189766526	-60.0146669931
106500	5.89816475E-14	-47.5673466491	-69.58271309
107000	7.966598539E-14	70.1078967197	-66.9715924299
107500	6.732536207E-14	62.4281001122	-68.4334771226
108000	1.230522376E-13	44.7934262907	-63.1952607712
108500	2.303926825E-13	17.9630440847	-57.7476774484
109000	1.210745703E-13	-35.8750934952	-63.3359923465
109500	1.323676908E-13	-17.7239333393	-62.5614112281
110000	1.481643317E-13	56.1851119243	-61.5821777483
110500	3.137780787E-13	35.0515689703	-55.0645990875
111000	1.710669653E-13	15.1858160629	-60.3337280518
111500	6.589146878E-14	32.6727026054	-68.6204673068
112000	5.805590266E-14	84.2289446603	-69.7201234377
112500	1.478269746E-13	-46.8556026221	-61.6019772997
113000	1.869465077E-13	54.2651716883	-59.5627039443
113500	1.463392658E-13	-12.655690619	-61.6898336389
114000	8.005558542E-14	-63.8356305563	-66.9292183222
114500	1.80678943E-13	-59.5980668086	-59.8589002518
115000	3.345860324E-13	-40.3744312892	-54.5068949375
115500	1.934190528E-13	9.74497546812	-59.2670660341
116000	1.999504444E-13	78.6968504811	-58.9786036009
116500	1.034394909E-13	-61.8731841939	-64.7033235889
117000	1.264287036E-13	-77.998141388	-62.9601373821
117500	9.017537323E-14	56.78739075	-65.8952921061

118000	1.697472069E-13	89.8721247008	-60.4009983357
118500	5.501611856E-14	57.8246292826	-70.1872521318
119000	2.862643419E-14	-57.4291731675	-75.8617059926
119500	1.158340209E-13	-41.4880888517	-63.7203284328
120000	9.023048647E-14	-89.1848577338	-65.8899850997
120500	6.931909116E-14	-72.7536574215	-68.1799938753
121000	1.586181509E-13	24.0062272589	-60.9899934223
121500	1.003666507E-13	32.9815107047	-64.9652624447
122000	5.854146701E-14	59.0735590677	-69.6477790486
122500	1.534657119E-13	57.3949849152	-61.2768239113
123000	8.254602086E-14	38.1878616935	-66.6631282189
123500	1.042724144E-13	-88.2191946912	-64.6336624821
124000	1.741757038E-13	-29.6618893741	-60.1772995935
124500	6.848174409E-14	-64.9645428722	-68.2855548287
125000	2.060805528E-13	-26.3607123754	-58.7163108626
125500	2.273283656E-13	-25.155795561	-57.863978486
126000	8.100298598E-14	32.2428319058	-66.8270305088
126500	1.19230738E-13	38.567504402	-63.4692864328
127000	1.056016973E-13	-31.0323247802	-64.52363311
127500	1.324437494E-13	-29.6817076671	-62.5564217403
128000	6.682245847E-14	8.925431851E-11	-68.4986020815

THE MAXIMUM VALUE IS 1.777675774E-10 AT LOCATION 1

ENTER THE MIN AND MAX AMPLITUDE LIMITS FOR PLOT: 0,1.78E-10

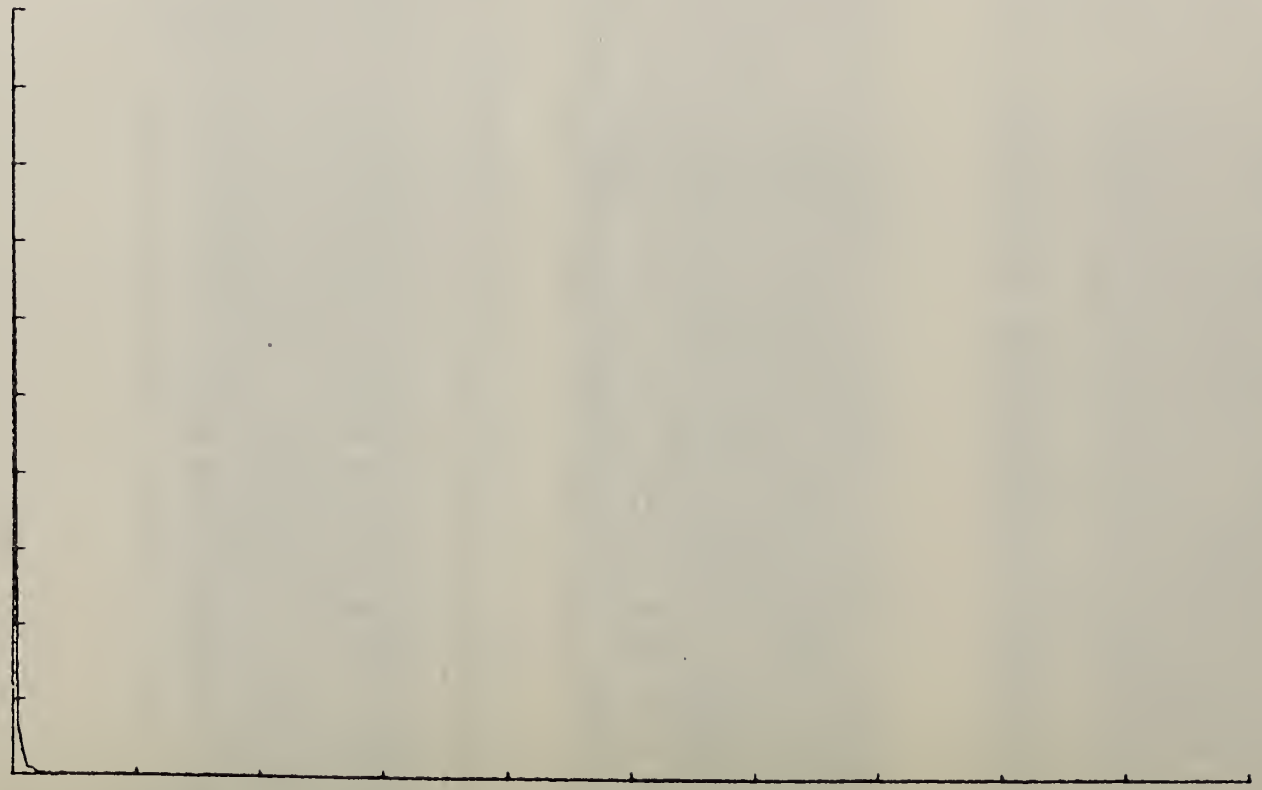

The following ten pages show the results of applying the software contained in Appendix D to a step-like waveform that begins at zero and ends at some nonzero value.

The waveform, as acquired by the DPO, is shown on the first page. The transformed spectrum is tabulated on the next eight pages and plotted on the last.

This software correctly transforms waveforms of this type.

31-OCT-80 14:35:11
TEST COND.:FFT MODIFIED

TIME BASE SETTING: 2.0E-10 s/DIV
VERT. SENS. SETTING: 0.5 RHO/DIV

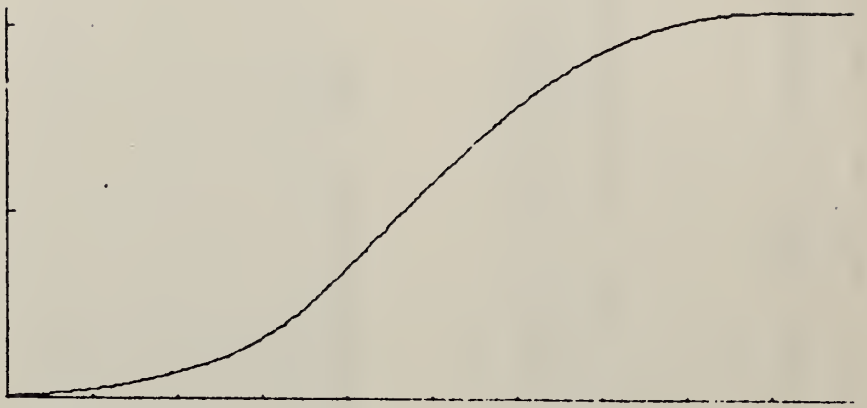

REDUCTION FACTOR; 1,2,4,8,16,32? 1

31-OCT-80 14:38:28
TEST COND.:FFT MODIFIED
THE MAXIMUM ANALYSIS FREQUENCY IS 128000 MHz
A SET OF 256 FREQUENCY POINTS WILL BE CALCULATED

FREQ.	MAGNITUDE	PHASE,DEG	ATTEN,dB RE M(1)
500	1.777675774E-10	-82.6827138445	0
1000	1.200745944E-11	-70.5656567578	-23.4080285133
1500	5.509697493E-12	18.0443588997	-30.1744959818
2000	1.623746856E-12	-76.8016865051	-40.7866846162
2500	1.45940232E-12	-54.4576054149	-41.7135504298
3000	4.299446125E-13	57.0628864001	-52.3288008519
3500	4.191703056E-13	81.0837993004	-52.5492408938
4000	1.799329378E-13	80.8303963103	-59.8948376604
4500	3.404198217E-13	52.7559887122	-54.3567542811
5000	2.820875703E-13	-37.4669059418	-55.9893720754
5500	4.022486492E-13	88.22500059	-52.9071591908
6000	1.708243245E-13	84.7538439261	-60.3460568398
6500	9.996956747E-14	-54.1108794115	-64.9996948166
7000	2.837353912E-13	-77.0166358165	-55.9387808764
7500	2.967338282E-13	18.2222803983	-55.5497098895
8000	1.95597194E-13	76.9307667938	-59.1697986741
8500	3.457849746E-13	44.9285342556	-54.2209287191
9000	2.040142995E-13	83.835108552	-58.8038389108
9500	1.353033167E-13	-69.6037901312	-62.370882224
10000	2.845094866E-13	89.8461341333	-55.9151160383
10500	1.362222416E-13	30.3996338061	-62.3120906307
11000	1.54007154E-13	-60.9129747413	-61.24623317
11500	3.153391184E-13	-27.9645581212	-55.0214940965
12000	2.21887842E-13	59.9642316006	-58.074380949
12500	1.40558542E-13	47.9331576308	-62.0399062057
13000	4.009892699E-13	38.1452407288	-52.9343960493
13500	9.751224304E-14	26.3506612233	-65.2158681489
14000	2.894565499E-13	-0.630967271216	-55.7653834515

14500	2.797094438E-13	-46.457723999	-56.0629084846
15000	2.471858348E-13	63.1333387143	-57.1365794879
15500	3.076804463E-13	20.2553932868	-55.2350531408
16000	2.478254761E-13	-61.7987641916	-57.1141320945
16500	2.245300671E-13	-76.3975830173	-57.9715609553
17000	2.530944781E-13	-25.9907275312	-56.9313976768
17500	1.505521306E-13	-71.2464797654	-61.4433129598
18000	3.929493997E-14	18.7408877107	-73.1103184855
18500	3.685445692E-13	-8.02841402731	-53.6672507612
19000	1.961421231E-13	22.3876295735	-59.1456336394
19500	6.133657117E-14	77.872539409	-69.2426611899
20000	1.190002001E-13	32.062157205	-63.4860972421
20500	3.087273971E-13	23.8898516092	-55.205547652
21000	2.42367143E-13	-23.4764209988	-57.3075762094
21500	2.785411425E-13	-4.60933045046	-56.0992640247
22000	7.203064344E-14	-28.8886263348	-67.846705193
22500	1.445176914E-13	-39.8446044272	-61.7986307695
23000	2.07431427E-13	-19.0994087681	-58.6595599777
23500	9.167222949E-14	23.0199158779	-65.7522952065
24000	2.221150016E-13	77.8905960276	-58.0654932459
24500	8.737123487E-14	54.8765293593	-66.1696816008
25000	8.364677167E-14	89.0552948418	-66.5480673966
25500	1.14945586E-13	44.30787605	-63.7872051025
26000	7.12315647E-14	-45.3695792988	-67.9436013923
26500	1.379286939E-13	-32.5815156149	-62.203958605
27000	1.838339555E-13	76.5464132085	-59.708536442
27500	1.426687667E-13	-64.4750995599	-61.9104729381
28000	3.421650418E-14	-77.5457452789	-74.3123383472
28500	9.793850516E-14	32.6619875544	-65.1779816574
29000	1.578120686E-13	-64.408508053	-61.0342468272
29500	2.424593716E-13	-27.047178124	-57.3042715753
30000	9.089241778E-14	-18.3842982553	-65.8264979584
30500	9.209643178E-14	2.23487927982	-65.7121949976
31000	1.830950611E-13	14.036201321	-59.743518487
31500	1.103072332E-13	-27.0865836858	-64.1449712492

32000	1.170810072E-13	-34.8016323532	-63.6273220788
32500	3.763665013E-14	35.9128972159	-73.4848318413
33000	1.163695157E-13	-49.0899571382	-63.6802665387
33500	1.376039217E-13	32.2833682871	-62.2244348476
34000	1.39370043E-13	69.1156548067	-62.113662396
34500	1.404400005E-13	88.4964262931	-62.0472346328
35000	6.414038454E-14	-81.5752043086	-68.8544198924
35500	1.181446248E-13	69.5644524329	-63.5487717316
36000	1.143973843E-13	70.3016744918	-63.8287291874
36500	3.259058795E-14	-23.6711596644	-74.7352071698
37000	1.85917355E-13	83.6882687242	-59 6106524341
37500	2.239645251E-13	1.01657682071	-57.9934664059
38000	4.742302805E-14	-31.637949131	-71.4772654572
38500	2.368974502E-13	15.8133981311	-57.5058433523
39000	1.645863491E-13	80.4427908715	-60.6691748453
39500	1.384130229E-13	-48.8799648394	-62.1735120035
40000	8.62452413E-14	66.6716942904	-66.2823482462
40500	1.970486157E-13	5.02089800395	-59.1055833133
41000	7.419306087E-14	49.7590639963	-67.5897853087
41500	3.273770596E-14	70.1745550107	-74.6960862051
42000	5.678403165E-14	-73.2495898551	-69.9125265977
42500	1.380997314E-13	25.7740615944	-62.1931943991
43000	3.712343013E-14	-52.6692503723	-73.6040891311
43500	1.612491267E-13	0.417685922352	-60.8471036547
44000	4.413791224E-14	-43.4440877683	-72.1008153416
44500	1.176754895E-13	-44.1527212785	-63.5833308079
45000	1.162811874E-13	38.7414043532	-63.6868619207
45500	9.683074666E-14	-18.0901594412	-65.2767854648
46000	1.618648078E-14	47.6020813922	-80.8140023579
46500	2.48958344E-14	-61.7836110004	-77.0745173496
47000	1.229136662E-13	-62.4135152954	-63.2050476211
47500	8.200540806E-14	49.3060238198	-66.7202011979
48000	1.190566251E-13	-35.5306184195	-63.4819797297
48500	2.568330305E-13	76.4217363294	-56.8040335545
49000	1.681117478E-13	20.6317861589	-60.485089809

49500	9.533463702E-14	-40.4539716337	-65.4120367311
50000	1.817042465E-13	-18.7349425262	-59.809749539
50500	2.3129343E-14	-21.4749690671	-77.7137851477
51000	4.765249773E-14	-15.705238337	-71.4353376916
51500	2.038303613E-13	4.32095397773	-58.8116735926
52000	1.571167783E-13	87.6118593421	-61.0725997749
52500	9.121113254E-14	81.1067634891	-65.7960941132
53000	2.198712112E-13	0.0843346466492	-58.1536837026
53500	1.016304213E-13	-17.1994617641	-64.8565765623
54000	9.744693436E-14	78.4941960229	-65.2216874596
54500	2.217728605E-13	-66.8480296297	-58.078883115
55000	5.320400888E-14	58.9674808027	-70.4781639334
55500	2.518854516E-13	38.8156849691	-56.9729893944
56000	9.984446761E-14	-29.6208179485	-65.010570967
56500	5.665644304E-14	55.3414543483	-69.9320649679
57000	7.430608175E-14	-44.6495443347	-67.5765638573
57500	1.014911964E-13	-50.8984268117	-64.8684836333
58000	5.251228132E-14	7.60004527743	-70.5918333594
58500	1.481143695E-13	-34.8247228448	-61.5851071957
59000	9.000649479E-14	82.905141887	-65.9115741012
59500	7.913788926E-14	87.5612546604	-67.0293618246
60000	5.512824095E-14	-87.0654264963	-70.169568376
60500	1.871430608E-13	36.6158631652	-59.5535765129
61000	1.681141103E-13	-62.0711171321	-60.4849677451
61500	1.559095546E-13	72.104598773!	-61.1395964627
62000	2.001974649E-13	-52.2598885352	-58.9678796025
62500	1.905873451E-13	80.7375637069	-59.3951698716
63000	1.2566!8338E-13	88.8155042845	-63.0129832124
63500	1.578224452E-13	-30.7580981325	-61.0336757216
64000	9.828275961E-14	60.9453959281	-65.147504234
64500	1.468537499E-13	-39.7178209307	-61.6593502657
65000	7.82221789E-14	63.3939644493	-67.1304528949
65500	1.327066162E-13	78.6247324306	-62.539199566
66000	8.363113591E-14	-65.8267381539	-66.5496911668
66500	2.30505071E-13	-42.1830293116	-57.7434413953

67000	3.706155691E-14	59.1936130616	-73.6185778883
67500	8.084665226E-14	-21.320583456	-66.8438102564
68000	2.611451365E-13	-38.0938889851	-56.6594122386
68500	1.379395025E-13	-36.8499973695	-62.2032779735
69000	1.282234027E-13	18.0760793697	-62.8377051269
69500	1.013885531E-13	-81.0728380598	-64.8772725697
70000	6.304372608E-14	-57.5425169602	-69.0042136108
70500	9.519405127E-14	-46.3588978389	-65.4248548802
71000	6.180785755E-14	-28.9653633124	-69.1761772812
71500	8.947507539E-14	71.5972329478	-65.9630096182
72000	3.998767897E-14	13.9353950607	-72.9585271411
72500	1.747188183E-13	61.403574403	-60.1502574039
73000	1.233383549E-13	71.0454011693	-63.1750880489
73500	1.3553277E-13	54.6630520657	-62.3561647922
74000	5.199875023E-14	-61.1875973277	-70.6771929649
74500	1.339251627E-13	24.4707485346	-62.4598074276
75000	6.479293375E-14	2.71106662243	-68.7664981835
75500	4.578507129E-14	-43.0411018113	-71.7825731829
76000	1.46638963E-13	21.6349864317	-61.6720634625
76500	8.050414048E-14	67.2042515957	-66.8806867277
77000	8.785500334E-14	-68.6171765292	-66.1217210862
77500	2.513710231E-14	-81.349978688	-76.9907468244
78000	4.683887889E-14	-28.7353198266	-71.5849212496
78500	2.02956674E-14	-73.0521067353	-78.8489843365
79000	1.510442704E-14	-29.1903802418	-81.4149659659
79500	1.803052294E-13	-25.4649727473	-59.8768846231
80000	1.069388285E-13	-20.5031338701	-64.4143426363
80500	8.862245169E-14	-64.7615271064	-66.0461758709
81000	1.465124775E-13	-33.8625503301	-61.6795588312
81500	1.53724311E-13	24.9616125386	-61.2621999732
82000	4.618414254E-14	-43.5808579949	-71.7071933807
82500	3.285998919E-14	24.8281353529	-74.6637027541
83000	9.392962732E-14	29.2820701445	-65.5409990947
83500	1.166848784E-13	-41.3910601703	-63.6567595223
84000	1.971960947E-13	-57.3365093816	-59.0990848795

84500	1.3734407 16E-13	2.16000043219	-62.240852715
85000	9.147062515E-14	-21.8708434329	-65.7714181333
85500	1.232242601E-13	-28.0606988114	-63.1831266991
86000	1.617381924E-13	-70.2141226361	-60.8207993765
86500	1.407498675E-13	50.1698512786	-62.0280911873
87000	1.642335524E-13	89 0955752972	-60.6878133392
87500	1.428217725E-13	70.6693068084	-61.901162705i
88000	1 123690171E-13	-31.4091811446	-63.9841194353
88500	1.7844537:7E-13	0.673604011475	-59.966945315
89000	4.12496632E-14	-62.755601281	-72.6886429406
89500	1.26295645E-13	43.2229173022	-62 9692835735
90000	1.13638521E-13	15.5443269829	-63.886539623
90500	2.329411773E-14	0.198676178584	-77.6521257563
91000	5.505484665E-14	-80.378412935	-70.1811399322
91500	2.110879042E-13	20.1180480241	-58.5077841173
92000	8.347057988E-14	28.3749180444	-66.5663824668
92500	1.344413638E-13	56.9838024752	-62.426392889
93000	1.612561981E-13	-34.5553409407	-60.8467227499
93500	1.222794589E-13	-7.68741411936	-63.2499809159
94000	1.5047863:9E-13	-10.0947942456	-61.4475543951
94500	6.866321977E-14	52.8461425698	-68.2625677871
95000	1.702814258E-13	-39.1968965161	-60.3737055212
95500	1.871364421E-13	-20.88702151	-59.5538837151
96000	7.730167426E-14	-59.8185258087	-67 2332730722
96500	6.759330483E-14	35.7393818953	-68.3989774618
97000	2 528039051E-14	-40.984554:686	-76.9413755143
97500	1.553926491E-13	52.3570690731	-61.1684416665
98000	1.498148925E-13	73.9628885983	-61.4859513406
98500	1.38831544E-13	-89.17:5023859	-62.1472880057
99000	5.446510549E-:4	-5.99606650765	-70.2746840963
99500	1.730266365E-13	-13.5805300995	-60.2347917687
100000	2.965063637E-14	77.3659887409	-75.5563707049
100500	2.42784101E-14	-59.9635383379	-77.2926462164
101000	1.440223364E-:3	76.3:52315215	-61.8284540361
101500	9.371206855E-:4	-37.230182112	-65.5611405914

102000	1.040623538E-13	-12.5448914099	-64.6511781806
102500	7.394511958E-14	65.4712636806	-67.6188607666
103000	1.197870138E-13	61.0683185523	-63.4288563112
103500	1.158451561E-13	30.1011939314	-63.719493494
104000	3.065102122E-14	-41.632663883	-75.2681521041
104500	1.11687089E-13	-36.522632735	-64.036991644
105000	9.694851126E-14	-49.0232995833	-65.2662281892
105500	1.543670332E-13	-28.1328795766	-61.2259599298
106000	1.774676523E-13	-10.189766527	-60.0146669953
106500	5.89816475E-14	-47.5673466498	-69.5827130922
107000	7.966598539E-14	70.107896719	-66.9715924321
107500	6.732536207E-14	62.4281001113	-68.4334771248
108000	1.230522376E-13	44.7934262897	-63.1952607734
108500	2.303926825E-13	17.9630440836	-57.7476774506
109000	1.210745703E-13	-35.8750934966	-63.3359923488
109500	1.323676908E-13	-17.7239333402	-62.5614112302
110000	1.481643317E-13	56.1851119229	-61.5821777504
110500	3.137780787E-13	35.0515689693	-55.0645990897
111000	1.710669653E-13	15.1858160618	-60.333728054
111500	6.589146878E-14	32.6727026052	-68.620467309
112000	5.805590266E-14	84.2289446588	-69.7201234398
112500	1.478269746E-13	-46.8556026221	-61.6019773018
113000	1.869465077E-13	54.2651716879	-59.5627039465
113500	1.463392658E-13	-12.6556906194	-61.6898336411
114000	8.005558542E-14	-63.8356305569	-66.9292183244
114500	1.80678943E-13	-59.5980668097	-59.8589002539
115000	3.345860324E-13	-40.3744312901	-54.5068949397
115500	1.934190528E-13	9.74497546745	-59.2670660364
116000	1.999504444E-13	78.6968504804	-58.9786036031
116500	1.034394909E-13	-61.8731841949	-64.7033235912
117000	1.264287036E-13	-77.998141389	-62.9601373842
117500	9.017537323E-14	56.7873907497	-65.8952921081
118000	1.697472069E-13	89.8721246998	-60.4009983379
118500	5.501611856E-14	57.8246292808	-70.1872521339
119000	2.862643419E-14	-57.4291731669	-75.861705995

119500	1.158340209E-13	-41.4880888529	-63.720328435
120000	9.023048647E-14	-89.1848577337	-65.8899851018
120500	6.931909116E-14	-72.7536574245	-68.1799938776
121000	1.586181509E-13	24.0062272581	-60.9899934245
121500	1.003666507E-13	32.9815107039	-64.9652624468
122000	5.854146702E-14	59.0735590664	-69.6477790504
122500	1.534657119E-13	57.3949849141	-61.2768239135
123000	8.254602086E-14	38.1878616925	-66.6631282211
123500	1.042724144E-13	-88.2191946922	-64.6336624842
124000	1.741757038E-13	-29.6618893748	-60.1772995957
124500	6.848174409E-14	-64.9645428727	-68.2855548308
125000	2.060805528E-13	-26.3607123767	-58.7163108648
125500	2.273283656E-13	-25.1557955618	-57.8639784882
126000	8.100298598E-14	32.2428319036	-66.8270305108
126500	1.19230738E-13	38.5675044005	-63.4692864351
127000	1.056016973E-13	-31.0323247812	-64.523633112
127500	1.324437494E-13	-29.6817076717	-62.556421743
128000	6.682245847E-14	1.964143133E-11	-68.4986020835

THE MAXIMUM VALUE IS 1.777675774E-10 AT LOCATION 2

ENTER THE MIN AND MAX AMPLITUDE LIMITS FOR PLOT: 0,1.78E-10

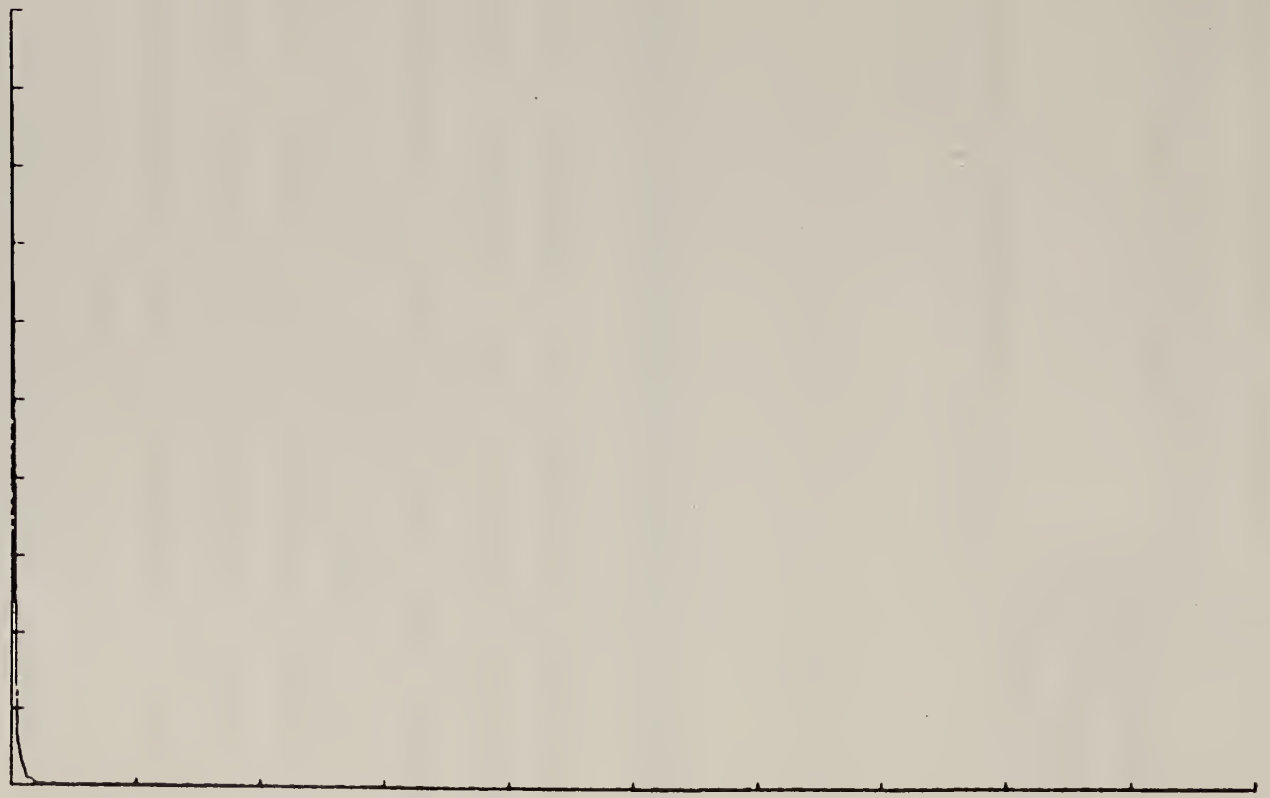

NBS-114A (REV. 2-8C)

U.S. DEPT. OF COMM. BIBLIOGRAPHIC DATA SHEET (See instructions)	1. PUBLICATION OR REPORT NO. 81-2235	2. Performing Organ. Report No.	3. Publication Date

4. TITLE AND SUBTITLE

1980 Annual Report: Technical Contributions to the Development of Incipient Fault Detection/Location Instrumentation

5. AUTHOR(S)

W. E. Anderson and J. D. Ramboz

6. PERFORMING ORGANIZATION (If joint or other than NBS, see instructions)

NATIONAL BUREAU OF STANDARDS
DEPARTMENT OF COMMERCE
WASHINGTON, D.C. 20234

7. Contract/Grant No.
EA-77-01-6010
A063-EES

8. Type of Report & Period Covered
Oct. 1, 1979 -
September 30, 1980

9. SPONSORING ORGANIZATION NAME AND COMPLETE ADDRESS (Street, City, State, ZIP)

Department of Energy
Office of Electric Energy Systems
Washington, D.C. 20461

10. SUPPLEMENTARY NOTES

☐ Document describes a computer program; SF-185, FIPS Software Summary, is attached.

11. ABSTRACT (A 200-word or less factual summary of most significant information. If document includes a significant bibliography or literature survey, mention it here)

Technical barriers exist in the development of instrumentation to detect and locate incipient faults in underground transmission cables. Knowledge is required of the physical, chemical, and electromagnetic properties of cables which precede breakdown, of the manner in which characteristic rf signals propagate in cables, and of appropriate methods of coupling detection systems to operating transmission cables. A measurement program has been initiated that will provide data on the rf properties of cables and on the characteristics of some forms of incipient faults. Preliminary measurements demonstrate the limitations of frequency- or time-domain-reflectometry techniques in the detection of incipient faults. Software is presented which permits the Fourier transform of step-like waveforms.

12. KEY WORDS (Six to twelve entries; alphabetical order; capitalize only proper names; and separate key words by semicolons)

aging; cables; dielectrics; electric insulation fault location; time-domain-reflectometry; underground transmission.

13. AVAILABILITY

☒ Unlimited
☐ For Official Distribution. Do Not Release to NTIS
☐ Order From Superintendent of Documents, U.S. Government Printing Office, Washington, D.C. 20402.
☐ Order From National Technical Information Service (NTIS), Springfield, VA. 22161

14. NO. OF PRINTED PAGES
130

15. Price
$12.50

NBS-114A (REV. 2-8C)

U.S. DEPT. OF COMM. BIBLIOGRAPHIC DATA SHEET (See instructions)	1. PUBLICATION OR REPORT NO. 81-2235	2. Performing Organ. Report No.	3. Publication Date

4. TITLE AND SUBTITLE

1980 Annual Report: Technical Contributions to the Development of Incipient Fault Detection/Location Instrumentation

5. AUTHOR(S)

W. E. Anderson and J. D. Ramboz

6. PERFORMING ORGANIZATION (If joint or other than NBS, see instructions)

NATIONAL BUREAU OF STANDARDS
DEPARTMENT OF COMMERCE
WASHINGTON, D.C. 20234

7. Contract/Grant No.
EA-77-01-6010
A063-EES

8. Type of Report & Period Covered
Oct. 1, 1979 -
September 30, 1980

9. SPONSORING ORGANIZATION NAME AND COMPLETE ADDRESS (Street, City, State, ZIP)

Department of Energy
Office of Electric Energy Systems
Washington, D.C. 20461

10. SUPPLEMENTARY NOTES

☐ Document describes a computer program; SF-185, FIPS Software Summary, is attached.

11. ABSTRACT (A 200-word or less factual summary of most significant information. If document includes a significant bibliography or literature survey, mention it here)

Technical barriers exist in the development of instrumentation to detect and locate incipient faults in underground transmission cables. Knowledge is required of the physical, chemical, and electromagnetic properties of cables which precede breakdown, of the manner in which characteristic rf signals propagate in cables, and of appropriate methods of coupling detection systems to operating transmission cables. A measurement program has been initiated that will provide data on the rf properties of cables and on the characteristics of some forms of incipient faults. Preliminary measurements demonstrate the limitations of frequency- or time-domain-reflectometry techniques in the detection of incipient faults. Software is presented which permits the Fourier transform of step-like waveforms.

12. KEY WORDS (Six to twelve entries; alphabetical order; capitalize only proper names; and separate key words by semicolons)

aging; cables; dielectrics; electric insulation fault location; time-domain-reflectometry; underground transmission.

13. AVAILABILITY

☒ Unlimited

☐ For Official Distribution. Do Not Release to NTIS

☐ Order From Superintendent of Documents, U.S. Government Printing Office, Washington, D.C. 20402.

☐ Order From National Technical Information Service (NTIS), Springfield, VA. 22161

14. NO. OF PRINTED PAGES
130

15. Price
$12.50